8-1-2018

Developing Peptide Therapeutics that Inhibit Bacterial Toxins Utilizing a Cholesterol Recognition Amino Acid Consensus (CRAC) Motif

Evan Koufos
Lehigh University, ekoufos17@gmail.com

Developing Peptide Therapeutics that Inhibit Bacterial Toxins Utilizing a Cholesterol Recognition Amino Acid Consensus (CRAC) Motif

by

Evan Koufos

Presented to the Graduate and Research Committee
of Lehigh University
in Candidacy for the Degree of
Doctor of Philosophy

in

Chemical Engineering

Lehigh University

August 2018

Copyright Permissions

Certificate of Approval

Approved and recommended for acceptance as a dissertation in partial fulfillment of the requirements for the degree of Doctor of Philosophy.

_____
Date

_____
Angela C. Brown, Ph.D.
Dissertation Advisor

_____
Accepted Date

Committee Members:

_____
Anand Jagota, Ph.D.

_____
Lesley Chow, Ph.D.

_____
Damien Thévenin, Ph.D.

Acknowledgements

Lehigh University was the last graduate school that I visited in late March of 2013, not because I had no interest in this program but because the graduate student coordinator had taken way too long to schedule my visit. By the time that I came to visit I thought I had already made up my mind on where I wanted to attend. It was not until my meeting with the department chair that afternoon that I considered coming to Lehigh. He informed me that Angela C. Brown, my soon to be advisor, had signed her letter of intent to join the department. When he explained to me the nature of her research, which focused on engineering alternative therapeutics to combat bacterial illnesses, I became so intrigued in her work that I emailed her that day inquiring if she would be taking any graduate students in the coming fall. After an exchange of emails, I was convinced that this is what I wanted to spend the next five years working on and a few days later I accepted the offer to pursue my doctorate of philosophy in chemical engineering at Lehigh University.

To begin my lengthy list of thanks, I want to first acknowledge and thank my advisor Angela C. Brown for this long and fulfilling journey which would not have been possible without her. I was her first graduate student and this allowed me to partake in the invaluable opportunity of helping her start her lab. During my first year, when I was learning the ropes of being a graduate student, her door was always open to me. The willingness she displayed to guide me and answer any questions that I had is the epitome of fantastic mentorship. I will never forgot all the words of wisdom she provided and I will try to resonate what she instilled in me onto others in the next chapters of my life.

Even though they will never be able to spell my last name right, smh, I want to give a special thanks to Leahbean Spangler and Christopher Currann who sat next to me for five

years in our office C-346. We shared many laughs and venting sessions with one another and I'll always cherish those memories. I also want to thank Zhou Yang, William Taifan, John Sakizadeh, Daniyal Kiani, and Bobert who spent some time and shared some laughs in C-346 with me as well.

Next, I want to thank my group members Elnaz Rasti Boroujeni, Eric Krueger, Shannon Collins, Tony Enhyung Chang, and Justin Nice for sitting through countless group meetings of me yapping on about CRAC peptides. Additionally, I want to thank the following undergraduate researchers of the Brown Lab that I had the pleasure to work with: Anxela Sinani, Josh Webb, Matthew Sheehan, Logan Hodges, Kirsten Leskowich, Michael Di Martino, Ben Dunmire, and Joanne Huang.

The next group of individuals I want to thank is the helpful staff of my department. They include Barbara Kessler, Janine Jekels, Tracey Lopez, Paul Bader, John Caffrey, and Greg Sado. I appreciate everything all of you have done along the way to make my journey just a little bit easier. I also want to thank the two faculty members in which I had the pleasure of being their teaching assistant in Introduction to Heat Transfer in the fall of 2014 and 2016, Steven McIntosh and Kelly Schultz respectively. Furthermore, I want to also thank my committee members Lesley Chow, Damien Thévenin, and Anand Jagota for the support and advice they provided me during my time Lehigh.

I want to give a very special thanks to my boys from home: Dan Schroen, Joe Carbaugh, Alex Parisi, Eric Frayman, and Michael Sica who shared this journey with me on the channels of our discord server BlaHat, you guys got me through some rough times and I'll always be thankful for that. Furthermore, I also want to thank my cat Heather and my girlfriend Sam who were there with me every step of the way.

Lastly, I want to thank my family who are the most important people in my life. They include my sister Elena, my three uncles Jimmy, Mario, and Andy, my grandparents Georgia and Kypros, and most importantly my parents Nick and Terry. I am forever grateful for the sacrifices my parents endured emigrating from Greece and Cyprus to America in the 1980's and the hardships they put up with to ensure that my sister and I would have a much better upbringing than what they had experienced growing up. Without them none of what I achieved would be possible and I love them more than they realize.

Table of Contents

List of Tables

List of Figures

Abstract

Treatment of bacterial illnesses has become increasingly difficult as the development of new antibiotics is being outpaced by the increasing number of antibiotic-resistant organisms. This has led us to search for alternative therapeutic approaches to help combat these illnesses. A viable approach in treating these illnesses is to focus on inhibiting protein toxins, which are one of the many virulence factors that bacteria secrete. Many toxins recognize and bind to cholesterol (Chol) on the host cell membrane as an initial step in their mechanism; however, a viable method of inhibiting this interaction has yet to be uncovered.

For our model toxin, which recognizes and binds to Chol, we have chosen the repeats-in-toxin (RTX) toxin leukotoxin A (LtxA) secreted by the Gram-negative bacterium *Aggregatibacter actinomycetemcomitans*. LtxA functions by resisting the host's immune response by binding to and killing white blood cells via Chol within their membrane. This association with Chol is regulated by a Chol recognition amino acid consensus (CRAC) motif, with a sequence of ^{334}LEEYSKR^{340}, in the N-terminal (hydrophobic) region of the toxin.

Here, we have demonstrated LtxA's requirement for Chol; removal of Chol from the plasma membrane of leukocytes inhibits the activity of the toxin. We have shown that a peptide designed from LtxA's CRAC motif (CRAC^{WT}) has a similar affinity for Chol and can inhibit LtxA cytotoxicity by binding to Chol and preventing subsequent LtxA binding and internalization. Utilizing biophysical techniques, we characterized the interaction between CRAC^{WT} and Chol and found that the hydroxyl group within Chol is key to this

interaction and that $CRAC^{WT}$ does not disrupt membrane packing, suggesting that $CRAC^{WT}$ primarily sits near the water-membrane interface.

To further improve upon the interaction between $CRAC^{WT}$ and Chol-containing membranes, we investigated the effect of altering the net charge of $CRAC^{WT}$ to create a peptide that binds to Chol with a stronger affinity. We synthesized four $CRAC^{WT}$ mutants that corresponded to an increase or decrease in the overall net charge of $CRAC^{WT}$. To measure the affinities of these mutants for Chol-containing membranes, as well as their ability to inhibit LtxA cytotoxicity, we employed localized surface plasmon resonance (LSPR) measurements and cell-based assays respectively. We found that neither decreasing nor increasing the net charge of $CRAC^{WT}$ led to an increase in the peptide's affinity for Chol-containing membranes, but mutants with high net charges were incapable of inhibiting LtxA cytotoxicity.

Next, to determine the significance that each residue within the CRAC motif has on the peptide's ability to bind to membrane Chol, we synthesized 10 CRAC peptide mutants. Each peptide mutant had one residue within the CRAC domain substituted with an alanine residue. We found that seven of the ten residues within the CRAC motif have a significant effect on the peptide's affinity for Chol-containing membranes, with the most prominent residues being the three highlighted in the CRAC domain definition, leucine (Leu), tyrosine (Tyr), and arginine (Arg).

Finally, to test the efficacy of $CRAC^{WT}$ *in vitro* against other Chol-binding pathogens we utilized two *Streptococcal* toxins, streptolysin O (SLO) and pneumolysin O (PLO), which are considered important virulence factors for this genus. We investigated the inhibitory effect of $CRAC^{WT}$ on the cytotoxic and hemolytic activity of SLO and PLO

and found that $CRAC^{WT}$ inhibited the cytotoxicity of SLO and PLO, as well as the hemolytic activity of PLO in a concentration-dependent fashion.

These results suggest that $CRAC^{WT}$ holds potential clinical applicability to treat not just bacterial illnesses but potentially other viruses that utilize Chol during pathogenesis since features of the CRAC motif have been implicated in the function of proteins relevant to the human immunodeficiency virus (HIV), the influenza virus (flu), and the herpes simplex virus.

Chapter 1

Introduction and Background

1.1 Introduction

Every year bacterial infections are becoming increasingly challenging to treat as bacteria quickly develop resistance due to the increased exposure they receive from the overuse and misuse of antibiotics, which results in more antibiotic-resistant organisms [1, 2]. Currently, out of the 18 drug-resistant threats that the United States Centers for Disease Control and Prevention (CDC) is monitoring, bacteria are responsible for 17 of them [3]. Furthermore, antibiotics that were once successful in treating such organisms are now rendered obsolete, and the rate of development for new antibiotics to treat these emerging pathogens has been declining since the 1980's [3, 4]. This has led to an estimated two million people developing antibiotic-resistant infections annually in the United States, with more than 23,000 of those infections resulting in fatalities, thus leading to costs estimated to be US$21-34 billion a year for the U.S. health care system [3, 5]. Furthermore, many large pharmaceutical companies have cut funding into the research and development of antibiotics due to the increased difficulty of discovering new antibiotics and the increased costs of clinical trials [5-7].

1.2 Antibiotic Alternatives

The decrease in effectiveness of antibiotics has led us and many others to search for alternative options that could be utilized in their place, or in combination [3, 8, 9].

Some of the current alternative treatments strategies which are highlighted below include antimicrobial peptides, antibacterial monoclonal antibodies, and vaccines [10-13].

1.2.1 Antimicrobial Peptides

The increasing rise of bacterial resistance to conventional antibiotics has led to many studies focusing on the use of antimicrobial peptides (AMPs) as an alternative treatment option for antibiotic-resistant bacteria due to their effectiveness against these organisms [14-19]. This is leading the global peptide drug market to experience a rapid growth that is projected to increase to US$25.4 billion in 2018, up from US$14.1 billion in 2011, thus making the exploration of peptide therapeutics worthwhile [20]. Furthermore, AMPs have many advantages over traditional therapeutics. They have a rapid onset of activity, low levels of induced resistance, and broad-spectrum capabilities allowing them to target and inhibit numerous infectious Gram-positive and Gram-negative bacteria and their virulence factors [21-25].

Although AMPs can offer various advantages over traditional treatments they come with numerous disadvantages as well .They are sensitive to environmental conditions making them vulnerable to hydrolysis, oxidation, and aggregation, which decreases the success of transferring an AMP effective treatment from *in vitro* to *in vivo* [10, 12, 25-29]. While their sensitivity to the environment can lead to limitations, several groups are focusing on improving their stability in these conditions with the use of D amino acids and structural modifications [30-32].

Currently there are several AMPs in development that show promise against a variety of microbial infections. These include PAC-113 that targets infections in HIV patients, LTX-109 that treats methicillin-resistant and vancomycin resistant

Staphylococcus aureus skin infections, and hLF1-11 that targets fatal bacterial and fungal infections for immunocompromised stem cell transplant patients [33-36].

1.2.2 Monoclonal Antibodies

Antibacterial monoclonal antibodies (AMAs) offer another potential avenue of treatment as they have demonstrated success against bacterial infections and cancer *in vitro in vivo* [37-39]. Due to their effectiveness against certain cancers their popularity has risen and paved the way for significant improvements in the manufacturing and production of AMAs thus driving down their cost and making them a cost-effective alternative therapeutic in the treatment of bacterial infections [37, 40].

AMAs provide numerous advantages over current antibiotics. They tend to have a lower risk of side effects, they can be synthesized into bispecific antibodies for increased potency and targetability, they do not harm the host's microbiome, they can be designed to incorporate multiple inhibitory mechanisms, and most importantly they induce less selective pressure for cross-resistance [41-45]. Even with advances to their production and manufacturing they are still very expensive to produce versus small-molecule therapeutics and only a very limited number of clinical studies have been performed supporting AMA treatments [40, 46]. Furthermore, their ability to target outer membrane proteins as potential epitopes in bacterial infections is reduced by the exopolysaccharides masking of those targets thus making them less effective in these situations [47-49].

Even with these limitations several AMAs have found success against bacteria. BiS4αPa is utilized against *Pseudomonas aeruginosa,* a multidrug resistant bacterium that is the leading cause of lung infections in patients suffering from cystic fibrosis and hospital-acquired pneumonia [50, 51]. BiS4αPa inhibits *P. aeruginosa* from successfully attaching

to epithelial cells and it increases the host's ability to clear the pathogen through phagocytosis [51, 52]. The AMA bezlotoxumab has also been utilized against the *Clostridium difficile* cytotoxin, Toxin B, which acts by binding to the toxin and inhibiting it from binding to the cell lining of the gut [53-55].

1.2.3 Vaccines

Vaccines have also been studied for their potential antibacterial effects [56]. Two major benefits of their applicability toward bacterial infections is the potential reduction of antibiotics use they will provide if rendered effective, which will result in decreased antibiotic-resistant bacteria and provide herd protection against their target bacterial disease [57]. While many of the most effective vaccines are live attenuated mutant vaccines, they are also the most harmful because they are unsafe for immunocompromised individuals [58, 59]. Other limitations also exist for combination vaccines such as DTaP which protect against diphtheria, tetanus, and acellular pertussis [60]. Furthermore, if there is an adverse reaction from a combination vaccine, it would lead to an uncertainty in the cause of the reaction and additionally these treatments are costly with a complex administration process [61]. Lastly, another vaccine limitation arises from the development of single antigen targeting vaccines since they tend to be less effective than the vaccines mentioned previously due to differences in the target's antigenic expression [57].

Currently, there are numerous vaccines in development or that have been developed against pathogenic bacteria. A live attenuated strain vaccine (ΔtrxA) for multi-drug resistant *Acinetobacter baumannii*, which causes nosocomial and combat related infections, has been has shown to be effective in treating this infection in murine models

[62]. MeNZB, an outer membrane vesicle meningococcal vaccine, has been developed to target *Neisseria gonorrhoeae,* the bacterium responsible for gonorrhea and potential infertility in females [63, 64]. Lastly, VLA84, a vaccine against the diarrhea causing *C. difficile* and SA4Ag, a vaccine against vancomycin resistant *S. aureus,* have also shown promise in the inhibition of their respective targets [55, 65-68].

1.2.4 Antivirulence Strategies

One potential pathway for treatments involves focusing on bacterial virulence factors instead of directly killing the bacterium [69, 70]. Virulence factors are molecules produced by bacteria that allow them to defend themselves and infect their host. These include effector molecules, enzymes, adhesins, and toxins [71].

A majority of antivirulence studies focus on targeting secreted protein toxins utilizing a variety of mechanisms. For example, the blocking of membrane pores formed by pore-forming toxins has found success as an alternative antivirulence strategy. Utilizing cyclodextrin derivatives, these molecules are able to bind to and block transmembrane pores formed by the lethal pore-forming bacterial toxins secreted by *Bacillus anthracis* and several *Staphylococcal* toxins, which include α-hemolysin and γ-hemolysin [72, 73].

Another potential avenue of inhibition is targeting the membrane environment of the target cell. In a separate study, we found that we could alter the properties of the cell membrane to inhibit toxin activity. Using the nuclear stain DRAQ5™, we demonstrated that the stain reduced the fluidity of the membrane which prevented leukotoxin A (LtxA) of *Aggregatibacter actinomycetemcomitans* from binding to the membrane, thus inhibiting the cytotoxicity of this toxin [74].

Antivirulence strategies that target the toxins directly after secretion from the cell have also been developed. Protein toxins released by the bacterial genera *Escherichia*, *Campylobacter*, *Salmonella*, *Shigella*, and *Vibrio* bind to intestinal cells and lead to diseases including cholera and travellers' diarrhea [75-77]. To inhibit toxin-cell interactions, carbohydrate-based scaffolds have been engineered to mimic the membrane glycolipid environment that the toxins utilize in their pathogenic mechanism. The scaffolds intercept the toxin before it reaches the cell, allowing the toxin to bind to the scaffold instead of the targeted cellular membrane leading to an inhibition of cytotoxicity.

In addition, several inhibitors have been found for the cholera toxin. These inhibitors, Geldanamycin, sodium 4-phenylbutyrate, and a group of polyphenolic compounds, act in targeting molecular chaperones, subunits of the cholera toxin, or the entire toxin respectively [78-80]. Geldanamycin, which is an anti-cancer agent, inhibits cholera toxin cytotoxicity by blocking the cytosolic chaperone Hsp90, thus preventing the A1 subunit of cholera toxin from passing into the cytosol [79]. Sodium 4-phenylbutyrate, a drug used to treat urea cycle deficiencies, has been found to prevent thermal unfolding of the A1 subunit of cholera toxin which inhibits cholera toxin cytotoxicity as well [78]. Lastly, a group of polyphenolic compounds (polyphenols) have been found to inhibit cholera toxin and other structurally similar toxins including a diphtheria toxin, and ricin in numerous ways [80]. Polyphenols can inhibit cholera toxin by preventing the toxin from binding to the cell membrane, stripping the toxin from the cell membrane, inhibiting the activity of the toxin's A1 subunit, or by blocking its cytosolic activity [80].

In this study we present a novel antivirulence strategy against a bacterial exotoxin. Utilizing a peptide derived from the protein LtxA in the repeats-in-toxin (RTX) toxin

family, we demonstrate that we can use this peptide to inhibit LtxA from binding to the membrane, thus preventing cytotoxicity.

1.3 RTX Toxins and LtxA

One class of toxins that are secreted by bacteria and used in pathogenesis are protein exotoxins. A specific class of protein exotoxins is the RTX family of toxins. RTX toxins are characterized by nonapeptide aspartate-rich and glycine-rich repeats, along with a common method of secretion across the bacterial membrane through the type 1 secretion system [81]. The family includes toxins secreted by *Escherichia coli*, *Bordetella pertussis*, and *Vibrio cholerae,* as well as three genera listed on the CDC's report of the biggest antimicrobial threats, *Streptococcus*, *Enterobacteriaceae*, and *Campylobacter* [3, 81].

To investigate a potential peptide therapeutic to treat these emerging threats, we use LtxA (sequence shown in Figure 1.3) as a model RTX toxin, which is secreted by the bacterium *A. actinomycetemcomitans*. *A. actinomycetemcomitans* is a Gram-negative pathogenic bacterium that has a significant role in localized juvenile periodontitis, as well as nonoral infections including endocarditis and pneumonia [82, 83].

A. actinomycetemcomitans expresses and secretes two protein toxins that allow it to avoid the host's immune system, cytolethal distending toxin (CDT) which kills host cells by blocking their proliferation and LtxA which kills host cells by disrupting their membrane environment [84-89]. Furthermore, it has been shown that the virulence of *A. actinomycetemcomitans* is correlated with the amount of LtxA secreted; strains with most LtxA secretion (JP2 strains) are correlated to the most severe cases of illness versus strains that produce the least amount of LtxA (652 strains) [90-96].

1.3.1 Mechanism and Structure of LtxA

Once LtxA is secreted it acts by specifically attacking the host's immune response, killing off any defending leukocytes of humans and Old-World primates [97-101]. This binding of LtxA to leukocytes is facilitated by its interaction with membrane Chol and it has been shown that removal of Chol or blocking of Chol inhibits the toxin's activity [17, 19, 102, 103]. Once bound to the cell, it has been suggested that LtxA utilizes the lymphocyte function-associated receptor 1 (LFA-1) of the cell membrane to orient itself into a conformation state that allows it to begin its cytotoxic mechanism as shown in Figure 1.1 [87, 104].

LtxA contains four unique regions. The N-terminal region (hydrophobic domain), consisting of residues 1–408 (green highlighted region in Figure 1.3), contains multiple hydrophobic and hydrophilic domains, as shown by the positive and negative peaks respectively in Figure 1.2 between the 0 to 408 position. Furthermore, it has been suggested that the hydrophobic region between residues 175-400 penetrate the membrane (Figure 1.1) and facilitate LtxA's cytotoxicity [87, 105, 106]. The central domain of LtxA (residues 409–729), as shown by the gray highlighted region in Figure 1.3, contains the fatty acid chains that are believed to be critical in the initial binding stages of LtxA to the cell membrane [107]. Located between residues 730-900 is the repeat domain (turquoise highlighted region in Figure 1.3) associated with all RTX toxins. This region contains multiple nonapeptide aspartate-rich and glycine-rich repeats and has been linked to the protein's interaction with LFA-1, as shown in Figure 1.1 [98, 101, 103, 105, 108]. Finally, the C-terminal domain (teal highlighted region in Figure 1.3) contains residues 730-900

and is only believed to play a role in the toxin's secretion from *A. actinomycetemcomitans* and not in the toxin's interaction with the cellular membrane [109].

A. actinomycetemcomitans, which secretes LtxA, is resistant to multiple antibiotics (amoxicillin, clindamycin, and doxycycline) which are commonly used to initially treat this infection; if such antibiotics fail the next course of treatment is usually surgery [110-114]. Since LtxA attacks hematopoietic cells from humans and Old-World primates and is associated with the severe illnesses caused by *A. actinomycetemcomitans*, LtxA make an excellent virulence factor to target therapeutically.

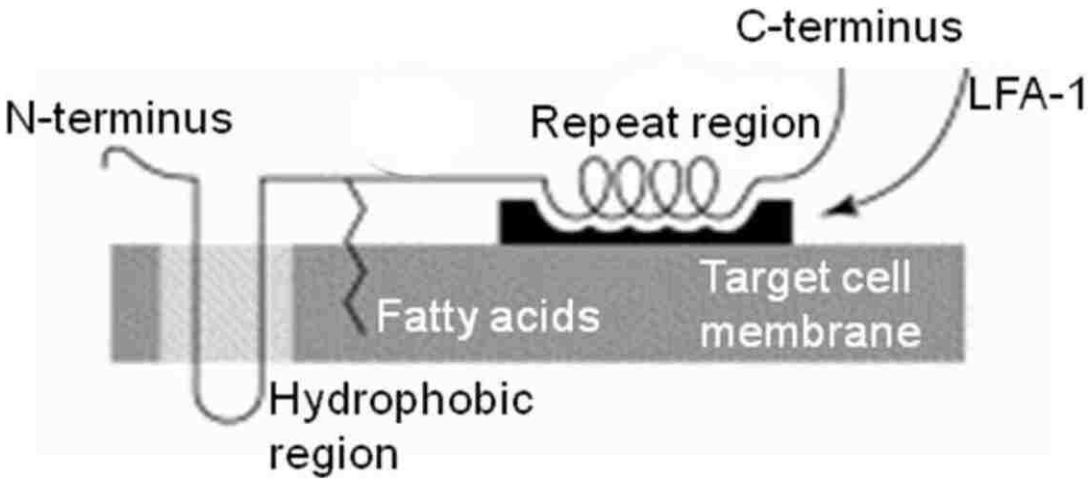

Figure 1.1 Interaction of LtxA with target cell membrane
The N-terminal region and the fatty acids in the central domain interact with the membrane to facilitate LtxA to the membrane and the repeat region interacts with LFA-1 [87, 115].

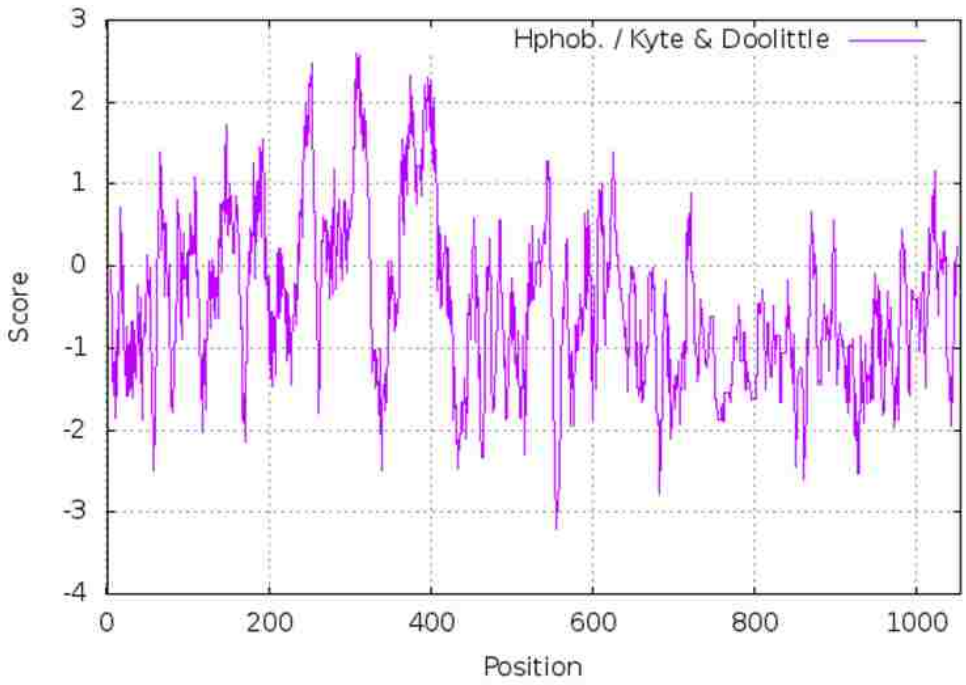

Figure 1.2 Hydrophobicity scale of LtxA

Positive values represent hydrophobic domains and negative values represent hydrophilic domains.

```
LtxA       1  MATTTLPNTKQQAAQFANSVADRAKENIDAAKEQLQKALDKLGKTGKKLTLYIPKNYKKG
LtxA      61  NGLTALIKAAQKLGIEVYHEGKDGPALTNGILNTGKKLLGLTERGLTLFAPELDKWIQGN
LtxA     121  KHLSNSVGSTGNLTKAIDKVQSVLGTLQAFLNTAFSGMDLDALIKARQNGKNVTDVQLAK
LtxA     181  ASLNLINELIGTISSITNNVDTFSKQLNKLGEALGQVKHFGSFGDKLKNLPKLGNLGKGL
LtxA     241  GALSGVLSAISAALLLANKDADTATKAAAAAELTNKVLGNIGKAITQYLIAQRAAAGLST
LtxA     301  TGPVAGLIASVVSLAISPLSFLGIAKQFDRARMLEEYSKRFKKFGYNGDSLLGQFYKNTG
LtxA     361  IADAAITTINTVLSAIAAGVGAASAGSLVGAPIGLLVSAITSLISGILDASKQAVFEHIA
LtxA     421  NQLADKIKAWENKYGKNYFENGYDARHSAFLEDSLKLFNELREKYKTENILSITQQGWDQ
LtxA     481  RIGELAGITRNGDRIQSGKAYVDYLKKGEELAKHSDKFTKQILDPIKGNIDLSGIKGSTT
LtxA     541  LTFLNPLLTAGKEERKTRQSGKYEFITELKVKGRTDWKVKGVPNSNGVYDFSNLIQHAVT
LtxA     601  RDNKVLEARLIANLGAKDDYVFVGSGSTIVNAGDGYDVVDYSKGRTGALTIDGRNATKAG
LtxA     661  QYKVERDLSGTQVLQETVSKQETKRGKVTDLLEYRNYKLDYYYTNKGFKAHDELNSVEEI
LtxA     721  IGSTLRDKFYGSKFNDVFHGHDGDDLIYGYDGDDRLYGDNGNDEIHGGQGNDKLYGGAGN
LtxA     781  DRLFGEYGNNYLDGGEGDDHLEGGNGSDILRGGSGNDKLFGNQGDDLLDGGEGDDQLAGG
LtxA     841  EGNDIYVYRKEYGHHTITEHSGDKDKLSLANINLKDVSFERNGNDLLLKTNNRTAVTFKG
LtxA     901  WFSKPNSSAGLDEYQRKLLEYAPEKDRARLKRQFELQRGKVDKSLNNKVEEIIGKDGERI
LtxA     961  TSQDIDNLFDKSGNKKTISPQELAGLIKNKGKSSSLMSSSRSSSMLTQKSGLSNDISRII
LtxA    1021  SATSGFGSSGKALSASPLQTNNNFNSYANSLATTA
```

Figure 1.3 Sequence of LtxA

The putative CRAC motif within LtxA is highlighted in yellow. The N-terminal region (residues 1-408) is highlighted in green, the central domain (residues 409–729) is highlighted in gray, the repeat region (residues 730-900) is highlighted in turquoise, and the C-terminal region (residues 901-1055) is highlighted in teal.

1.3.2 Interaction of LtxA and Chol

The toxicity of LtxA against host cells is critical on its ability to bind to Chol within the plasma membrane of the cell. The affinity of LtxA for Chol is regulated in part by a putative Chol recognition amino acid consensus (CRAC) motif within the protein's primary structure as shown by the yellow highlighted region in Figure 1.3 [102]. This work focuses on the interaction of this CRAC domain with Chol and its potential as an alternative therapeutic against Chol-dependent bacterial toxins.

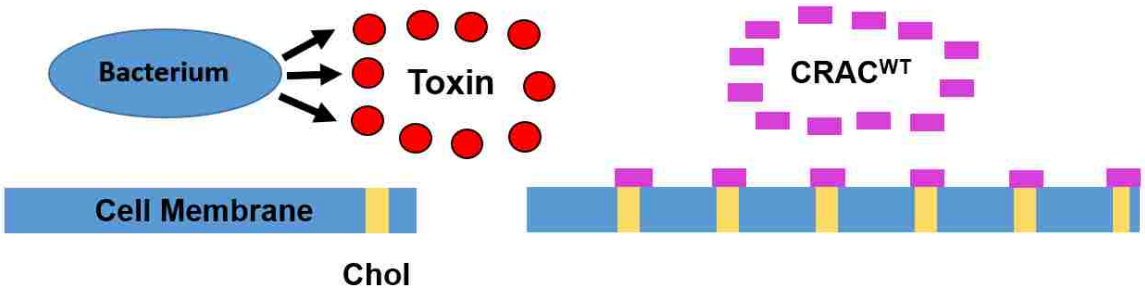

Figure 1.4 CRAC^{WT} blocks the recognition of Chol by the toxin.

1.4 Background of the CRAC Motif

1.4.1 Membrane Chol

A cell membrane's main function is to protect the interior of the cell from its surroundings with Chol being one of the membrane's primary components [116, 117]. Chol functions by maintaining membrane structure and dynamics, while also facilitating membrane protein function [116-120]. In the case of the membrane proteins known as G protein coupled receptors (GPCRs), which include the cannabinoid receptor, the opioid receptor, rhodopsin, and the β_2-adrenergic receptor, Chol regulates their functions,

dynamics, and oligomerization [121-123]. Many extracellular pathogenic proteins also utilize Chol as one of their key binding sites in the cell membrane or in Chol-rich domains known as lipid rafts [117-119, 124-129]. Many of these pathogenic proteins that bind to Chol include the gp41 protein of HIV-1, the influenza virus M2 protein, intermedilysin (ILY) of *Streptococcus intermedius*, and LtxA of *A. actinomycetemcomitans* [130-133].

A number of pathogens, such as the ones mentioned above, recognize Chol through a variety of different Chol-binding domains which include the sterol-sensing domain (SSD), the Chol recognition motif (CRM) of Chol-dependent cytolysins, and the CRAC motif [131, 134, 135]. The SSD is a domain with a unique interaction and affinity for Chol [134]. It is composed of approximately 180 amino acids which form five adjacent membrane spanning domains [134]. SSDs are implicated in the NPC1 protein which mediates Chol trafficking and is required in the production of HIV-1 and the cell entry of the Ebola virus [136, 137]. The CRM of Chol-dependent cytolysins is composed of a threonine and Leu pair which facilitates the binding of pathogens, such as ILY, perfringolysin O (PFO), pneumolysin O (PLO), and streptolysin O (SLO) to Chol [133, 135]. Lastly, the CRAC motif, which has been mentioned previously, is also a domain with an affinity for Chol [131]. Pathogenic proteins that contain an active CRAC motif include LtxA and CDT, as well as the viral protein gp41, which is critical in the pathogenesis of HIV-1 [102, 130, 138].

1.4.2 Discovery and History of the CRAC Motif

Utilizing computational methods to investigate protein-membrane interactions involving Chol led to the discovery of several potential Chol-binding domains within proteins, with one of these domains being the CRAC motif [131, 139-143]. An important

feature of this motif is the presence of three key amino acids, which are a central aromatic residue, a positively charged basic residue, and a hydrophobic residue [140].

The CRAC motif was first proposed in 1998 and was based on the active Chol binding site of 20 proteins, with a majority of those proteins being the translocator protein (formally known as the peripheral-type benzodiazepine receptor) and the Chol side-chain cleavage cytochrome P450scc of numerous species [131, 144]. It is defined as follows, the first residue needs to be a Leu or a Val, the next residue(s) (up to five residues) can be any amino acid, this is then followed by a key central Tyr residue that is required, then the next residue(s) (up to five residues) can be any amino acid, and finally the sequence is concluded with a Lys or an Arg [140, 142, 143, 145]. This CRAC definition is stylized as (L/V)-(X_{1-5})-Y-(X_{1-5})-(K/R).

Location of the CRAC motif varies between proteins but it is essential that the CRAC motif of any protein be found at the protein's membrane-interacting region. For this reason CRAC sequences are usually found adjacent to transmembrane helices as in the case of the HIV-1 fusion protein gp41, but have also been found to coexist between the transmembrane domain and the extracellular regions of the protein as in the nicotinic acetylcholine receptor protein [139, 145-147]. Furthermore, CRAC motifs are also found in non-transmembrane proteins. These amphipathic proteins contain CRAC regions that are exposed on the surface of the protein where they bind to Chol within the membrane; examples include the cytolethal distending toxin C (CdtC) and LtxA, both of *A. actinomycetemcomitans* [102, 138]. For example, when LtxA is interacting with a cell membrane, its CRAC domain (Figure 1.3) is believed to reside in the protein's extracellular and transmembrane regions as shown in Figure 1.1.

Based on the CRAC algorithm definition, a CRAC domain can range from five to 13 residues in length which leads to a possible 1.02×10^{13} CRAC sequences [143]. This leaves the biggest issue with this domain unaddressed; the algorithm is not well defined and is very inaccurate. It overpredicts Chol-binding domains to the point where many of these domains do not have an affinity for Chol, thus making these domains a difficult topic to study [102, 148-151]. For example, our model bacterial protein toxin, LtxA of *A. actinomycetemcomitans*, contains 12 putative CRAC motifs within its primary structure, but only one has demonstrated an affinity for Chol, while the neurotensin receptor 1, a transmembrane protein, contains two putative CRAC motifs with neither having an affinity for Chol [102, 152].

1.4.3 Prevalence of the CRAC Motif in Medically Relevant Pathogens

The CRAC motif has been identified and implicated in Chol binding of numerous medically relevant proteins, including gp41 protein of HIV-1, the influenza virus M2 protein, and the Herpes virus [130-132].

The CRAC motif of gp41 is found adjacent to its transmembrane domain [130]. Although the exact mechanism of the CRAC domain in gp41 is not known, it is believed that this CRAC domain plays a role in the fusogenic ability of the virus [153, 154]. Mutations to the CRAC domain of gp41 resulted in a decrease of fusogenic ability and studies performed with a peptide derivative of gp41's CRAC domain further supported these findings [153, 155].

The M2 protein of the influenza virus was also found to contain a putative CRAC motif. This motif is located immediately downstream of the transmembrane domain of M2 [156]. The CRAC domain of M2 is suggested to facilitate membrane targeting of the

protein; subsequent mutations to the central Tyr of the CRAC domain reduced the ability of the M2 protein mutant to bind to Chol-containing liposomes [132].

Through an *in silico* analysis another putative viral CRAC motif was discovered within the Herpes virus [157]. This CRAC domain is situated in the domain responsible for the refolding of critical viral proteins during the fusion step of virus internalization [157, 158].

CRAC motifs are also present in an important class of transmembrane proteins that has been shown to bind Chol, GPCRs. GPCRs that contain CRAC motifs include rhodopsin, the β_2-adrenergic receptor, and the serotonin$_{1A}$ receptor [159]. These proteins participate in critical bodily functions including visual transduction and serving as receptors for neurotransmitters and hormones [160-162]. Two proposed functions of CRAC motifs in GPCRs include inducing conformational changes that facilitate binding between a GPCR and Chol, or indirectly changing membrane properties of the surrounding GPCR environment to facilitate a more favorable conformational state for the protein [163-168]. Furthermore, the mechanism of how the CRAC motifs, of the mentioned GPCRs, interact with Chol is still undetermined [123, 169-171].

1.4.4 CRAC Domain's Interaction with Chol

Previously, other groups have tried to investigate certain characteristics that regulate the CRAC domain's affinity for Chol. One group performed several studies to investigate the significance that the primary structure of a CRAC peptide, derived from the gp41 protein of HIV-1, had on its ability to sequester Chol [143, 172, 173]. In this study, the initial, final, and central residues of the CRAC domain were determined to be critical to the peptide's ability to sequester Chol [143]. It was also found that their CRAC peptide

favors Lys over Arg due to the increased structural flexibility that it provides and the ability of Arg to bring the peptide closer to the membrane-water interface due to its more polar side chain [143]. Furthermore, the peptide's conformation was found to affect the peptide's ability to bind to Chol when it interacts with the membrane, additionally this study also found that the peptide's effectiveness is also dependent on small changes to the amino acid composition. A follow up study demonstrated an increase in their peptide's ability to sequester Chol when they substituted out X residues for glycine, which provides the greatest rotational freedom of any amino acid [173]. Lastly, they found that substituting the critical initial residue with an alanine decreased the peptide's ability to sequester Chol [172].

Studies performed on CRAC domain's in viruses that investigate mutations to the central Tyr residue or to the initial and final residue of the CRAC motif have found these changes to negatively affect virion structure organisation with the Chol-containing membranes [131, 157, 174-176]. In addition, studies involving full length proteins have found that the Tyr residue within the protein's CRAC motifs is critical in its ability to bind to Chol [17, 138, 177, 178]. Any changes to the CRAC domain's central Tyr was found to result in a decreased sensitivity for membrane Chol [173, 174, 177-179].

The importance of these residues for binding to Chol cannot be understated because they each play a unique role in driving a CRAC motif's interaction with Chol. For example, it is believed that the Leu or Val uses its branched side chains to associate with the β face of Chol (Figure 1.5) through van der Waals interactions and to accommodate the molecule's unique structure [140, 180, 181]. The central Tyr, the most essential residue in the recognition of Chol, has been found to bind to Chol by means of a CH-π stacking

interaction with the B ring of Chol (Figure 1.5), while the hydroxyl group of Tyr allows for electrostatic interactions with the sterol's hydroxyl group as well [140, 142, 181, 182]. Finally, Lys or Arg, with its lengthy apolar side chains, buries itself into the membrane bilayer with the charged group sitting at the membrane surface [140, 183, 184]. This distinctive trait allows Arg and Lys to attract water molecules and/or lipid headgroups to hydrogen bond with [184-186].

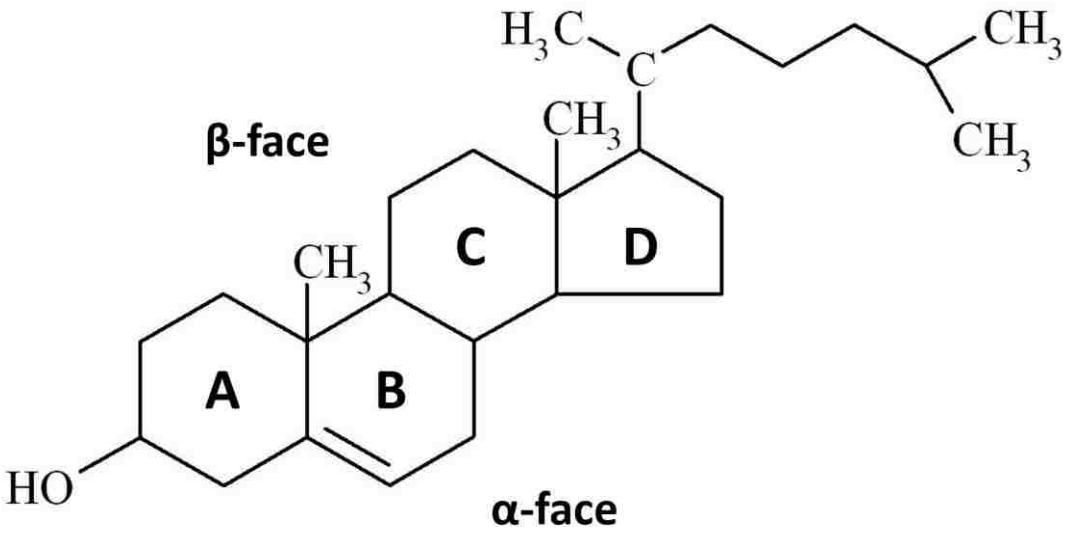

Figure 1.5 Structure of Chol

1.4.5 Structure of the CRAC Motif

A downside to the analysis of CRAC motifs is that there is a lack of high resolution structural information available for this Chol-binding motif. Furthermore, there is also a lack of structural information on proteins which contain CRAC domains that interact with Chol in lipid membranes [149]. This deficiency in structural information has been

suggested to reduce the chance to predict a successful binding CRAC motif [140]. The limited amount of structural data that is available comes from computational simulations and an experimental data set. For the case of the CRAC peptide from the protein LtxA of *A. actinomycetemcomitans*, its structure in solution is composed of β-sheets, α-helices, and random coils. Once the peptide interacts with Chol-containing membranes significant changes to its secondary structure occur. This results in a decreased α-helical structure and β-sheet propensity and leads to an increased coil conformation as it interacts with Chol in the membrane [182]. In addition, one circular dichroism (CD) study performed on a CRAC peptide derived from the gp41 protein of HIV-1 has found that as the CRAC peptide transitions from a solution environment to an environment composed of lipid and Chol the peptide's helical structure increased [187].

1.5 Use of the CRAC Motif as an Antivirulence Strategy

Many bacterial and viral pathogens recognize Chol as an initial step in their activity against host cells [17, 188, 189]. Demonstrating the effectiveness of this Chol-binding peptide to inhibit the interaction between a virulence factor and Chol introduces a novel strategy that has enormous potential for the treatment of not just illnesses caused by bacteria, but also those caused by viruses that utilize Chol, including HIV and the influenza virus [17, 188, 189].

With a Chol-binding peptide, we gain the ability to attack any Chol-dependent illnesses, as there are currently no viable approaches to inhibit this interaction. More importantly, $CRAC^{WT}$ exhibits no long-term toxicity to white blood cells or short-term toxicity to red blood cells, further bolstering its potential as an alternative therapeutic [19]. Furthermore, the use of these types of peptides has the potential to replace or supplement

the use of antibiotics, leading to a decrease in the increasingly rising number of antibiotic resistant bacteria.

Using this CRAC motif within LtxA as a model, we engineered a peptide ($CRAC^{WT}$) and demonstrated its inherently strong affinity for Chol-containing membranes [19]. $CRAC^{WT}$ functions by binding to Chol near the surface of the immune cell's membrane where it blocks the recognition of Chol by the toxin, thus inhibiting membrane binding and subsequent toxin internalization, as depicted in Figure 1.4 [19]. This renders the bacterial toxin ineffective and allows the immune cells to clear the infection.

Chapter 2

Materials & Methods

2.1 Chemicals

1,2-dipalmitoyl-*sn*-glycero-3-phosphocholine (DPPC), 1,2-ditetradecanoyl-*sn*-glycero-3-phosphocholine (DMPC), 1,2-dioleoyl-*sn*-glycero-3-phosphocholine (DOPC), and 1-palmitoyl-2-oleoyl-*sn*-glycero-3-phosphocholine (POPC) were purchased from Avanti Polar Lipids (Alabaster, AL). Cholesterol (Chol), desmosterol (Desmo), dihydrocholesterol (DHC), cholesteryl chloride (CC), 1-Octanol, poly-L-lysine, phorbol 12-myristate 13-acetate (PMA), methyl-β-cyclodextrin (MβCD), and methyl-β-cyclodextrin-cholesterol (MβCD-Chol) were purchased from Sigma-Aldrich (St. Louis, MO). Ergosterol (Ergo) was purchased from MP Biomedicals (Solon, OH). *N*-(7-Nitrobenz-2-Oxa-1,3-Diazol-4-yl)-1,2-Dihexadecanoyl-*sn*-Glycero-3-Phosphoethanolamine (NBD-PE) and 6-Dodecanoyl-2-Dimethylaminonaphthalene (Laurdan) were manufactured by Molecular Probes (Eugene, OR).

2.2 LtxA purification

A. actinomycetemcomitans strain JP2 was grown overnight in AAGM broth supplemented with 12.5 µg/ml vancomycin and 75 µg/ml bacitracin [190]. LtxA was purified as described previously [191]. The toxin was confirmed to be free of any impurities by SDS-PAGE, Coomassie staining, and western blot, as shown in Figure 2.1, and activity was confirmed using a cytotoxicity assay (data not shown).

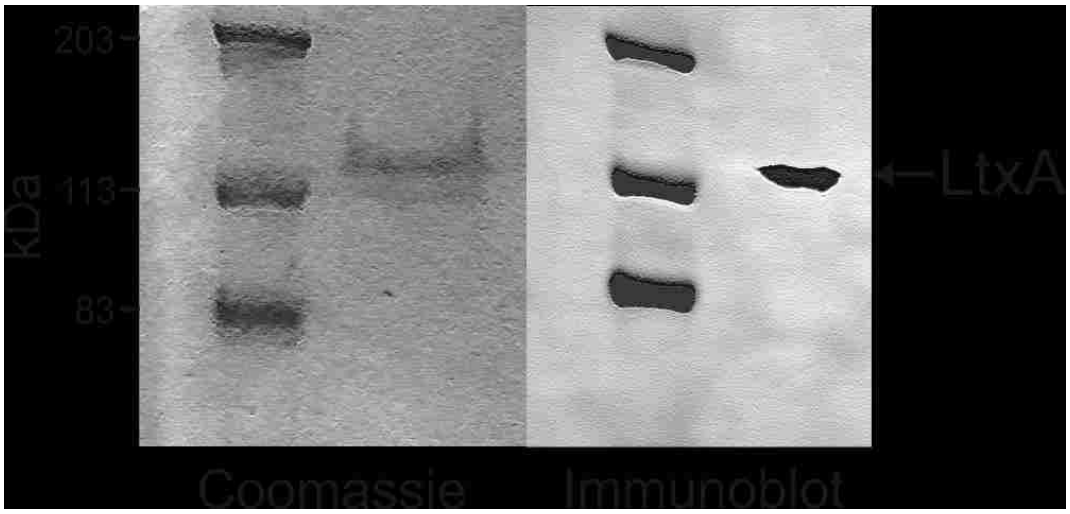

Figure 2.1 Coomassie stain and immunoblot (western blot) of purified LtxA.

2.3 Liposome Preparation

2.3.1 Large Unilamellar Vesicles

Liposomes were prepared using the lipid film technique. Stock solutions of lipids at 25 mg/mL were prepared in chloroform and then added to a glass vial in the required amounts [192]. The chloroform was evaporated under a stream of nitrogen, and the residual chloroform was removed under vacuum to create a thin lipid film on the glass surface. Multilamellar liposomes (MLVs) were created by hydrating the lipid film with buffer. The MLVs were then extruded through a 100-nm polycarbonate Whatman membrane (GE Healthcare Bio-Sciences, Pittsburgh, PA) with a LiposoFast® extruder (AVESTIN Inc., Ottawa, ON) to create large unilamellar vesicles (LUVs) [193].

2.3.1.1 Cell Cytotoxicity Experiments

Lipids used to create films for this experiment were POPC, Chol, and Ergo. Lipid films were hydrated with PBS (137 mM NaCl, 2.7 mM KCl, Na_2PO_4, KH_2PO_4, pH 7.4).

Liposomes composed of POPC and Ergo were formed using the rapid solvent exchange (RSE) technique [194]. Stock solutions of POPC and Ergo were added to a glass vial, PBS was added directly, and the chloroform was evaporated while the solution was vortexed.

2.3.1.2 ITC and CD Experiments

Lipids used to create films for this experiment were POPC and Chol. The lipid films were hydrated with a phosphate buffer (10 mM NaH_2PO_4, pH 6.5).

2.3.1.3 Laurdan experiments

Lipids used to create films for this experiment were POPC, DMPC, Chol, DHC, Desmo, and CC. The lipid films were hydrated with a liposome buffer (150 mM NaCl, 5 mM $CaCl_2$, 5 mM HEPES, and 3 mM NaN_3, pH 7.4).

2.3.2 Giant Unilamellar Vesicles

Giant unilamellar vesicles (GUVs), were formed from a mixture of DOPC/DPPC/Chol/NBD-PE (33/33/33/1 mol%) or POPC/Chol/NBD-PE (66/33/1 mole ratio) lipids dissolved in chloroform/acetonitrile (90/10 vol%) for a final lipid concentration of 4 mg/mL. The mixture was spin-coated onto indium tin oxide (ITO) coated glass slides (SPI, West Chester, PA) using a Laurell WS-650-23 spin coater [195]. To remove any remaining solvent, the lipid-coated slides were placed under vacuum for 30 min. A polydimethylsiloxane (PDMS) spacer was used to separate two slides and create a compartment that was filled with 18.2 MΩ/cm ultrapure water from a Milli-Q® Advantage A10 system (EMD Millipore, Billerica, MA), and sealed using binder clips. For 3 hr at 23 °C, an electric field was applied to form GUVs [196]. The GUVs were used within the same day.

2.4 Cell Culture

THP-1 cells obtained from ATCC were maintained in RPMI 1640 medium containing 10% FBS and 0.05 mM 2-mercaptoethanol at 37 °C under 5% CO_2.

2.5 Depletion and Replenishment of Plasma Membrane Chol

THP-1 cells, maintained in cell culture media, were depleted of Chol through incubation with 10 mM MβCD for 15 min at 37 °C and 5% CO_2. After the incubation, the cells were washed with cell culture media to remove any excess MβCD and were used in the cytotoxicity assay immediately. To replenish Chol, some of the MβCD-treated cells were subjected to an additional incubation with 1 mM MβCD-Chol for 1 hr at 37 °C and 5% CO_2. These Chol-replenished cells were then washed and used immediately. The concentration of Chol in the THP-1 cell membranes before depletion, after depletion, and after replenishment was measured with an Amplex® Red Cholesterol Assay Kit (Life Technologies™). Intensity measurements were performed with an Infinite 200 Pro plate reader (Tecan Group Ltd., Männedorf, Switzerland) with an excitation wavelength of 555 nm and an emission wavelength of 580 nm.

2.6 Cytotoxicity Assays

For the cytotoxicity tests, the cell membrane permeability was determined with a trypan blue assay using a Countess II automated cell counter (Thermo Fisher Scientific, Waltham, MA). Each experiment was performed three independent times. Untreated cells were used as a control. Cells were incubated at 37 °C under 5% CO_2. The percentage of cells alive after each treatment was calculated using the following equation:

$$Cell\ Viability\ \% = \frac{N_h}{N_0}$$

where N_0 is the number of cells before treatment, and N_h is the number of cells after h hrs of treatment.

2.6.1 LtxA Cell Cytotoxicity with Chol-Depleted Cells and Chol-Replenished Cells using MβCD

To determine the role of Chol in toxicity of LtxA, Chol-depleted and –replenished cells were incubated with 2 µg of LtxA for 3 hr. Untreated cells, as well as Chol-depleted and Chol-replenished cells that had not been treated with LtxA, were used as controls.

2.6.2 LtxA Cell Cytotoxicity with Chol-Containing Liposomes

To measure the protective effect of Chol-containing liposomes against LtxA, THP-1 cells were incubated with (i) LtxA, (ii) LtxA + 100% POPC liposomes, (iii) LtxA + 60% POPC/40% Chol liposomes, or (iv) LtxA + 60% POPC/40% Ergo liposomes. The mass of LtxA in each sample was 2 µg, and all liposome concentrations were 9.0 x 10^{-7} M. Controls included PBS, 100% POPC liposomes alone, 60%POPC/40%Chol liposomes alone, and 60%POPC/40%Ergo liposomes alone.

2.6.3 LtxA Cell Cytotoxicity with CRAC^{WT}

To measure the protective effect of the CRAC^{WT} peptide against LtxA, THP-1 cells were incubated with protein samples containing (i) LtxA, (ii) LtxA + CRAC^{WT}, or (iii) LtxA + CRAC^{SCR}. The mass of LtxA in each sample was 2 µg, and the molar LtxA:peptide ratio was 1:100. Controls included PBS, CRAC^{WT} alone, and CRAC^{SCR} alone.

2.6.4 SLO Cell Cytotoxicity with CRAC^{WT}

To measure the protective effect of the CRAC^{WT} peptide against SLO, THP-1 cells were incubated with protein samples containing (i) SLO, (ii) SLO + CRAC^{WT}, or (iii) SLO + CRAC^{SCR}. SLO-containing samples were incubated with cells for 24 hr. The mass of SLO in each sample was 40.5 μg.

2.6.5 PLO Cell Cytotoxicity with CRAC^{WT}

To measure the protective effect of the CRAC^{WT} peptide against PLO, THP-1 cells were incubated with protein samples containing (i) PLO, (ii) PLO + CRAC^{WT}, or (iii) PLO + CRAC^{SCR}. PLO-containing samples were incubated with cells for 2 hr. The mass of PLO in each sample was 1.6 μg.

2.7 Peptide Binding Centrifugation Assay

To measure the binding of the CRAC^{WT} and CRAC^{SCR} peptides to Chol, a centrifugation assay was performed [197]. The peptides (7.0×10^{-5} M) were incubated with 100% POPC or 60% POPC/40% Chol liposomes at a lipid-to-protein ratio of 100:1 for 30 min, then added to a centrifugal filter (Amicon® 30k MWCO, EMD Millipore, Billerica, MA) and centrifuged for 1 hr at 6,000 x g [198, 199]. The unbound peptide concentrations were determined by comparing the intrinsic fluorescence of the eluate at 305 nm to a set of standards of the same peptide with known concentrations. The fluorescence measurements were recorded on a Quantamaster® 400 spectrofluorometer (PTI Horiba, Edison, NJ) using an excitation wavelength of 281 nm. The bound peptide concentrations were then calculated from the total and free concentrations of peptide.

2.8 Peptide Design

Peptides used in this work were derived from the CRAC domain of LtxA including flanking residues (residues 328-346). $CRAC^{WT}$ is the CRAC domain and flanking residues with no alterations. Mutant peptides designed in this work are peptides that contain the same sequence of residues of $CRAC^{WT}$ but have had certain residues mutated (Table 3.2, Table 5.1, and Table 6.1).

2.9 Peptide Synthesis

The peptides used in this work (Table 3.2, Table 5.1, and Table 6.1) were prepared using Fmoc solid-phase synthesis. Briefly, the Fmoc group of H-Rink Amide ChemMatrix resin (0.47 mmol/g) was removed with a solution of 6% piperidine (wt%), 1% 1-hydroxybenzotriazole monohydrate (HOBt) (wt%) in dimethylformamide (DMF) for 30 min then washed with methanol (MeOH) and dichloromethane (DCM). Fmoc-amino acid (4.0 equiv.) was coupled with tetramethyl-O-(1H-benzotriazol-1-yl)uronium hexafluorophosphate (HBTU) (3.9 equiv.), and N,N-diisopropylethylamine (DIEA) (8.0 equiv.) in DMF (25 mL) for 90 min followed by washing with MeOH and DCM. Subsequent Fmoc groups were removed using the same deprotection and washing steps used for the resin, and the progress of the synthesis was periodically verified by matrix-assisted laser desorption/ionization time-of-flight mass spectrometry (MALDI-TOF MS) (Bruker Corporation, Billerica, MA). At the end of the solid phase synthesis, the N-terminal amino acid was capped using acetic anhydride with DIEA in DMF for 30 min. The peptide was then cleaved from the resin with a solution of 2.5% triisopropylsilane (vol%), 2.5% water (vol%), and 95% (vol%) trifluoroacetic acid (TFA) for 2 hr or a

solution of 2.5 thioanisole (vol%), 5% phenol (vol%), 5% water (vol%), 2.5% (vol%) 1,2-ethanedithiol, and 82.5% (vol%) TFA for 3 hr and precipitated with cold diethyl ether.

2.10 Peptide Purification

The peptide was purified by reversed-phase high-performance liquid chromatography (HPLC) on a Luna prep 10 μm, 250 mm × 21.2 mm C8 column (Phenomenex, Torrance, CA) (phase A: water, 0.1% TFA; phase B: acetonitrile, 0.1% TFA) using a gradient from 95/5 A/B to 0/100 A/B over 18 min. The identity of the peptide was confirmed with MALDI-TOF MS. The purified peptide was then lyophilized and stored at -80° C.

2.11 Isothermal Titration Calorimetry

To investigate the interaction of LtxA with Chol and the interaction of the $CRAC^{WT}$ peptide with Chol and three additional sterols, isothermal titration calorimetry (ITC) was performed. ITC measurements were performed at 30 °C in a Low Volume Nano ITC instrument (TA Instruments, New Castle, DE). For measurements of LtxA affinity, 50 μL of a liposome solution (10 mM) was injected into a cell containing 100 μM LtxA. The injected liposome solution was composed of either 100% POPC or 60% POPC and 40% Chol. For measurements of $CRAC^{WT}$ affinity, 50 μL of $CRAC^{WT}$ (7.65 mM) was injected into a cell containing a 2 mM liposome solution, composed of 100% POPC or 60% POPC and 40% sterol, where the sterol was Chol, Desmo, DHC, or CC. A control was also run by titrating $CRAC^{SCR}$ into liposome solutions of either 100% POPC or 60% POPC and 40% Chol. The thermodynamics of each reaction were determined by fitting curves of the raw heats to models within NanoAnalyze version 3.5.0. As shown in Figure 2.2, interactions between full-length LtxA or either peptide with 100% POPC membranes were

fit using the independent model, in which each protein/peptide can bind to n POPC molecules. Interactions between full-length LtxA or either peptide with membranes composed of POPC and sterol were fit using the multiple-sites model, with a ratio of sites of 1.5/1, corresponding to a lipid composition of 60% POPC and 40% sterol, where each protein/peptide can bind to n POPC molecules and m sterol molecules. The equations used for the fits performed by the independent model and the multiple-sites model utilize experimentally known quantities (total sample concentrations and individual heats measured) and have been detailed previously [200].

2.12 Peptide Structural Changes

To determine the structure of $CRAC^{WT}$ after binding to Chol and other sterols, CD spectra were collected using a Jasco J-815 CD spectrometer (Jasco Inc., Easton, MD). Spectral scans were performed from 240-190 nm, with a scanning speed of 20 nm/min, a bandwidth of 1.0 nm, and in 10 mM phosphate buffer using a peptide concentration of 0.25 mg/mL. A 0.01 cm path-length quartz cuvette was used for the measurements. To ensure that the spectra represent the structure of only bound peptide, unbound peptide was removed using centrifugal filters (Amicon® 30k MWCO, EMD Millipore, Billerica, MA) after 30 min [198, 199]. CD spectra were processed in ORIGIN® PRO 2016 (OriginLab, Northampton, MA). The secondary structure was determined with DICHROWEB using CONTIN/LL and either the SP175 references set (for solutions containing only peptide) or the SMP180 reference set (for solutions containing peptides and liposomes) [201-206].

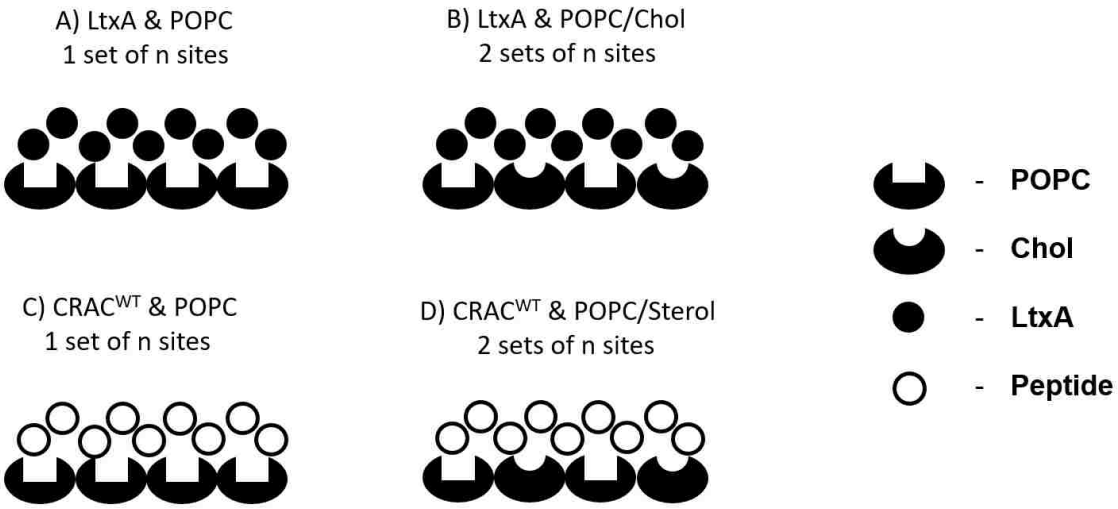

Figure 2.2 Isothermal Titration Calorimetry Experiments.
Types of ITC Experiments Performed. (A) 10 mM of 100% POPC liposomes were titrated into 100 μM of LtxA. LtxA interacts with one set of n sites (POPC lipid molecules). (B) 10 mM of 60% POPC/40% Chol liposomes were titrated into 100 μM of LtxA. LtxA interacts with two sets of n sites (POPC or Chol lipid molecules). (C) 7.65 mM of $CRAC^{WT}$ was titrated into 2 mM 100% POPC. $CRAC^{WT}$ interacts with one set of n sites (POPC lipid molecules). (D) 7.65 mM of $CRAC^{WT}$ was titrated into 2 mM 60% POPC/40% sterol liposomes. $CRAC^{WT}$ interacts with two sets of n sites (POPC or sterol lipid molecules).

2.13 Membrane Packing Assay

To investigate bilayer packing, a generalized polarization (GP) assay was performed. Laurdan was incorporated into liposomes containing 100% POPC, 80% POPC/20% sterol, or 60% DMPC/40% Chol. The liposomes were then incubated with either liposome buffer, $CRAC^{WT}$, or $CRAC^{SCR}$ at a lipid to peptide ratio of 50:1, at 23 °C for 15 min before the sample was excited at 340 nm using a Quantamaster® 400 spectrofluorometer (PTI Horiba, Edison, NJ). The GP was calculated using the following equation:

$$GP = \frac{I_{440} - I_{490}}{I_{440} + I_{490}}$$

where I_{440} and I_{490} are the fluorescence emission intensities at 440 nm and 490 nm, respectively.

2.14 Fluorescent LtxA Labeling

LtxA was labeled with Alexa Fluor® 555 NHS Ester (Molecular Probes, Eugene, OR) according to the manufacturer's instructions, with one modification. Specifically, after LtxA was labeled (AF555-LtxA), it was purified using a 40,000 MWCO Zeba™ Spin Desalting column (Pierce Biotechnology, Rockford, IL).

2.15 Confocal Microscopy

To stabilize THP-1 cells onto ibiTreat µ-Dishes (Ibidi, Martinsried, Germany), the cells were treated in one of two ways. 1) They were either differentiated into tissue-like macrophages using cell culture medium supplemented with PMA (100 ng/mL) over 72 hours and then the cells were incubated with 2 drops/mL NucBlue® Live ReadyProbes® reagent (Molecular Probes, Eugene, OR) for 20 min to label the cell nuclei, or 2) the cells were adhered onto ibiTreat µ-Dishes by treating the dishes with poly-L-lysine. Adherence of GUVs onto ibiTreat µ-Dishes was facilitated by treating the dishes with poly-L-lysine.

Each µ-Dish, containing either THP-1 cells or GUVs, was treated with a peptide or PBS for 30 min to allow binding of the peptide to occur before LtxA was added. Next, each µ-Dish was incubated with 30 ng of AF555-LtxA for 30 min. The molar peptide:toxin ratio in each dish was 100:1. Imaging was conducted using a Nikon C2si+ confocal microscope equipped with a LU-N4S laser unit and a 60x oil objective (NA = 1.4). The images were processed using Elements v4.3, Nikon's imaging software suite and Fiji [207].

2.16 CRAC^{WT} Long-Term Cell Cytotoxicity Assay

THP-1 cells obtained from ATCC were maintained at 37 °C under 5% CO_2 in RPMI 1640 medium containing 10% FBS, 0.05 mM 2-mercaptoethanol, and 40 μg/mL (15.9 μM) CRAC^{WT} peptide, alongside THP-1 cells grown in peptide-free media. Over a period of 65 days, cell viability was measured every two to three days using a Trypan blue assay.

2.17 Localized Surface Plasmon Resonance (LSPR)

To investigate the kinetics of binding of several peptides to Chol and/or other sterols, LSPR measurements were performed at 23 °C using an OpenSPR instrument (Nicoya Lifesciences, Kitchener, Canada). LSPR differs from SPR in that it produces a strong resonance absorbance peak that is very sensitive to the local refractive index that is surrounding the ligand and thus it measures changes to the peak's wavelength, whereas traditional SPR measures changes the angle of reflection [208]. For measurements of peptide affinity, a liposome solution, composed of 100% POPC or 60% POPC/40% Chol, was immobilized on a LIP-1 sensor chip (Nicoya Lifesciences). Next, 100 μL of peptide, at varying concentrations, was flowed over the immobilized liposomes. The kinetics of each reaction were determined by fitting the sensograms to models within TraceDrawer version 1.6.1. Reactions of peptide to 100% POPC were fit to a 1:1 binding model and reactions of peptide to 60%POPC/40%Chol were fit to 1:2 binding model.

2.18 Peptide Partitioning Measurements

Octanol-water partition coefficients were determined using the shake-flask method for each peptide. Vials containing varying volumes of 1-octanol and 18.2 MΩ/cm ultrapure water, from a Milli-Q Advantage A10 system, (always totaling 6 mL) were thoroughly shaken by hand for 1 min each, then left to stand over a period of 6 hours until both

substances had separated, and two distinct layers were observed. Each peptide was then added to the water phase at a final concentration of 40 mg/L and thoroughly shaken once more by hand for 1 min each, then left to stand for 6 hours until both substances had separated, and two distinct layers were observed. Serial dilutions of each peptide were created, and their fluorescence measured at 305nm using a Quantamaster™ 400 spectrofluorometer (PTI Horiba, Edison, NJ) to establish a concentration curve. The fluorescence of the water phase from the octanol-water samples was measured at 305 nm. Using the following equation, where the volume of water is (V_w), the final concentrations of peptide in water is (C_w^f), the volume of octanol is (V_o), the concentrations of peptide in octanol is (C_o), and the initial concentrations of peptide in water is (C_w^i):

$$V_w C_w^f + V_{oct} C_{oct} = V_w C_w^i$$

C_w^f and C_{oct} for the varying volumes were determined. The octanol-water partition coefficient for each volume set was determined by taking the log of K_{ow} from the following equation:

$$K_{ow} = \frac{C_{oct}}{C_w^f}$$

and averaged together [209, 210].

2.19 Zeta Potential Measurements

To measure the surface potential of liposomes containing 100%POPC and 60% POPC/40% Chol zeta potential measurements were conducted [211]. Measurements were performed on a Malvern Zetasizer Nano ZS (Malvern, Westborough MA). Liposomes

hydrated in liposome buffer were subjected to 10 runs each. The zeta potential was calculated as an average from those 10 runs.

2.20 Hemolysis Assay

Sheep erythrocytes were purchased from Colorado Serum Company (Denver, CO). Erythrocytes were washed and diluted with phosphate buffered saline (PBS) (pH 7.4) to a concentration of 2%. 200µL of 2% erythrocytes were pipetted into a 96 well plate. The positive control was treated with 20% Triton X-100, and a negative control was treated with PBS. Cells that were treated with $CRAC^{WT}$ were treated 30 min prior to the addition of the protein toxin. Once the protein toxin was added (1.6 µg), the 96 well plate was incubated at 37 °C and shaken minimally. The 96 well plate was centrifuged for 5 min at 500 x g. 100µL of the resulting supernatant of each sample was transferred to another 96 well plate and the absorbance was measured at 415 nm using an Infinite 200 Pro plate reader (Tecan Group Ltd., Männedorf, Switzerland). The background of each reading was subtracted using the negative control. All results were normalized to the positive control [212].

2.21 Statistical Analysis

Statistical analysis of the data was performed using ORIGIN® PRO 2016. In cases where $P > 0.05$, no statistically significant difference was reported between the two data sets in question.

Chapter 3

Inhibition of LtxA Toxicity by Using Cholesterol-Binding Peptides

3.1 Introduction

The pathogenicity of *A. actinomycetemcomitans* is regulated by several virulence factors, including LtxA that selectively kills human immune cells, allowing the organism to colonize the host [100, 213]. The mechanism by which LtxA kills cells is congruent with a wide variety of bacterial protein toxins, whereby target cell recognition initiates a multi-step process that culminates in cell death [214-218]. After binding to Chol within lipid raft enriched regions of the cell, LtxA triggers collapse of the microvilli on the outer surface of the cell and forms depressions on the cell surface followed by cavities in the membrane [89, 219-223].

In the current work, we have explored the possibility of inhibiting LtxA binding to Chol as a means of inhibiting activity. We found that the interaction between LtxA and Chol is highly specific, requiring both an intact CRAC sequence and a specific sterol structure, and disruption of this interaction in several different ways is sufficient to inhibit LtxA toxicity. We significantly reduced the ability of LtxA to kill THP-1 utilizing three different methods. First, we inhibited the association of LtxA with Chol in the target cell plasma membrane by removing Chol with methyl-β-cyclodextrin (MβCD), then we preincubated the toxin with Chol-containing liposomes which prevented the association of LtxA with membrane Chol, and lastly, we blocked the ability of LtxA to bind to membrane

Chol using a Chol-binding peptide that we designed. All three methods significantly reduced the ability of LtxA to kill THP-1 cells, demonstrating the potential therapeutic use of inhibiting the Chol-binding of LtxA to minimize cytotoxicity.

3.2 Results

3.2.1 LtxA toxicity is dependent on the presence of Chol

The association of LtxA with the membrane suggests that the toxin may interact with the cell plasma membrane lipids. Previously, it was found that LtxA must bind to Chol on the Jurkat (Jn.9) cell plasma membrane to kill the cells [102]. To investigate whether LtxA binding to the THP-1 membrane is likewise regulated by the presence of Chol, we extracted Chol from the THP-1 plasma membrane using MβCD and found that the toxicity of LtxA was significantly diminished in the absence of Chol (Figure 3.1). When the plasma membrane was replenished with Chol, using MβCD followed by MβCD-Chol, the cells again became susceptible to LtxA, indicating that the interaction of LtxA with Chol on the THP-1 plasma membrane is an essential element of the toxin's mechanism of action. One-way ANOVA followed by a Tukey test indicated that the Chol-dependence of LtxA activity is statistically significant (Table 3.1).

Neither treatment with MβCD nor treatment with MβCD followed by MβCD-Chol was toxic over the time course of the experiment (data not shown). The actual Chol concentrations in the cell membrane before and after MβCD treatment was determined using an Amplex® Red Cholesterol Assay. Untreated cells had a Chol concentration of 112.01 $\pm$ 1.87 µM, and after treatment with MβCD, the Chol concentration decreased 67.6% to 36.38 $\pm$ 1.34 µM. Replenishment of Chol with MβCD-Chol restored the Chol concentration to near original levels, 104.88 $\pm$ 1.34 µM.

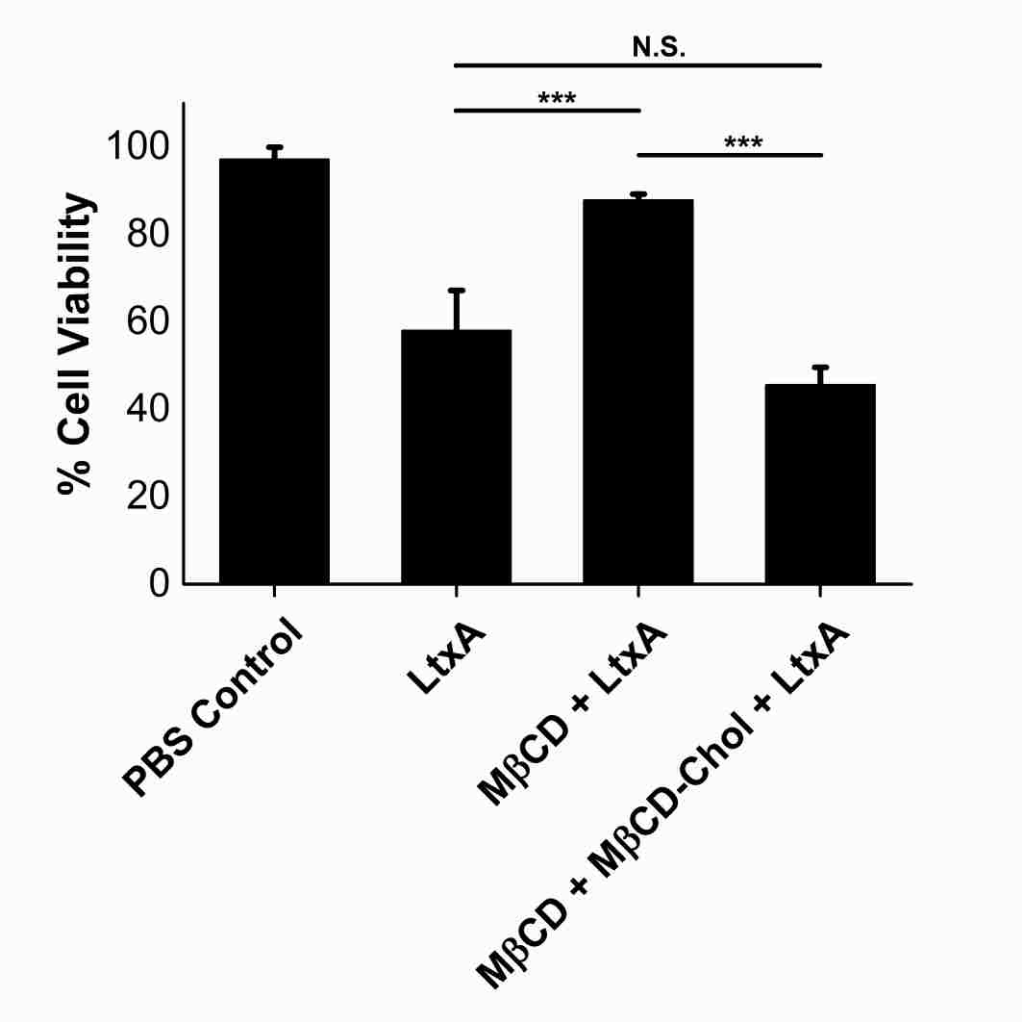

Figure 3.1 Cytotoxicity of LtxA after Chol extraction from THP-1 cells.
The toxicity of LtxA was measured in THP-1 cells as a function of Chol composition. THP-1 cells were either untreated, treated with methyl-b-cyclodextrin (MβCD) for 15 min to extract Chol, or treated with MβCD for 15 min followed by MβCD-Chol for 1 h to replenish Chol. Cells with reduced Chol compositions were significantly less susceptible to LtxA than were those with wild-type Chol levels. Replenishment of Chol restored susceptibility to LtxA. The data represents the average of three independent experiments, and the error bars represent the standard deviation. A one-way analysis of variance followed by a Tukey test was used to determine the level of significance between each experiment. ***P $\leq$ 0.001; N.S., not significant.

Table 3.1 Summary of statistical comparisons of data.
One-way ANOVA using the Tukey comparisons test within ORIGIN® PRO 2016. ***P ≤ 0.001; **P ≤ 0.01; N.S., not significant.

Comparison			P value	Significance
LtxA	vs.	MβCD + LtxA	0.00008	***
LtxA	vs.	MβCD + MβCD-Chol + LtxA	0.0724	N.S.
MβCD + LtxA	vs.	MβCD + MβCD-Chol + LtxA	0.00003	***
LtxA	vs.	LtxA + POPC	0.244	N.S.
LtxA	vs.	LtxA + POPC/Chol	0.000004	***
LtxA	vs.	LtxA + POPC/Ergo	0.464	N.S.
LtxA + POPC	vs.	LtxA + POPC/Chol	0.00225	**
LtxA + POPC	vs.	LtxA + POPC/Ergo	0.983	N.S.
LtxA + POPC/Chol	vs.	LtxA + POPC/Ergo	0.00103	**
$CRAC^{WT}$ + POPC	vs.	$CRAC^{WT}$ + POPC/Chol	0.00502	**
$CRAC^{WT}$ + POPC	vs.	$CRAC^{SCR}$ + POPC/Chol	0.00001	***
$CRAC^{WT}$ + POPC/Chol	vs.	$CRAC^{SCR}$ + POPC/Chol	0.00026	***
LtxA	vs.	LtxA + $CRAC^{WT}$	0.000003	***
LtxA	vs.	LtxA + $CRAC^{SCR}$	0.248	N.S.
LtxA + $CRAC^{WT}$	vs.	LtxA + $CRAC^{SCR}$	0.00001	***

3.2.2 Inhibition of binding to Chol inhibits LtxA toxicity

We investigated the possibility of blocking the binding of LtxA to Chol on the target cell plasma membrane as a means to inhibit the toxin's activity by preincubating the toxin with liposomes composed of 60% POPC and 40% Chol. First, we incubated LtxA with Chol-containing liposomes before incubating the mixture with THP-1 cells, with the idea that the LtxA would bind to Chol on the liposome and therefore be unable to bind to Chol on the cell membrane. Figure 3.3 demonstrates that this approach was successful. THP-1 cells were susceptible to free LtxA; however, when the LtxA was preincubated with 60% POPC/40% Chol liposomes, the cells remained viable throughout the experiment.

To determine the specificity of this inhibition, we repeated the experiment using two types of liposomes that did not contain Chol, 100% POPC liposomes and 60% POPC/40% Ergo liposomes. Ergo is a sterol found in yeast and other fungal membranes that differs in structure from Chol in both the ring and tail domains (Figure 3.2). As shown in Figure 3.3, neither type of liposome was able to inhibit LtxA toxicity. The additional double bonds in the body and tail of Ergo, plus the added methyl group to the tail of Ergo demonstrate that these structural changes create an unfavorable binding environment for LtxA and interfere with its ability to interact with the membrane. The decrease in affinity for Ergo-containing membranes could be a result of changes to membrane properties, (Ergo orders lipid chains more affectively and creates a more rigid bilayer than Chol), inability of the CRAC domain to favorably bind to Ergo based on structural differences, or both [19, 140, 224-227]. This indicates that the interaction between LtxA and Chol is unique and suggests that inhibiting the binding of LtxA to Chol could be an effective approach to

prevent LtxA toxicity. Furthermore, the specificity of this interaction was statistically significant as determined by a one-way ANOVA followed by a Tukey test (Table 3.1).

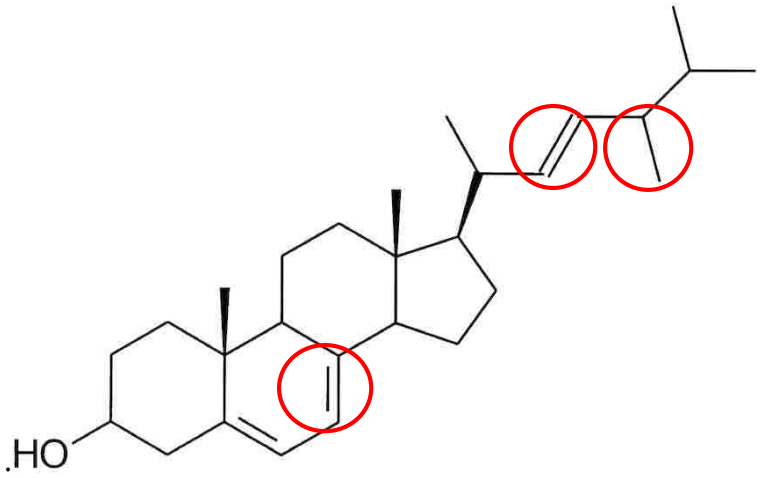

Figure 3.2 Structure of Ergosterol
Red circles indicate differences versus Chol.

3.2.3 Chol-binding peptides inhibit LtxA toxicity

We next investigated the possibility of inhibiting LtxA activity using a Chol-binding peptide derived from the $CRAC^{337}$ site of LtxA. A Chol-binding peptide ($CRAC^{WT}$), consisting of the $CRAC^{337}$ sequence of LtxA with six flanking residues on either side, and a scrambled control ($CRAC^{SCR}$), in which the CRAC motif was scrambled, were synthesized for this purpose. The sequences of the two peptides are shown in Table 3.2. An analytical centrifugation assay was used to demonstrate that the $CRAC^{WT}$ peptide binds more effectively to liposomes containing 40% Chol than it does to those without Chol (Figure 3.4), indicating that this peptide binds to Chol in the liposome. Additionally, the $CRAC^{WT}$ peptide bound to a greater extent to the 40% Chol liposomes than did the

$CRAC^{SCR}$ peptide, demonstrating that, as in the full-length toxin, the intact CRAC sequence is essential for this binding. The results of a statistical analysis of this data are included in Table 3.1.

Table 3.2 Sequences of Wild-Type and Scrambled Peptides
Residues underlined refer to the CRAC domain. Each peptide was acetylated at the N-terminus and amidated at the C-terminus.

Peptide	Sequence
$CRAC^{WT}$	FDRARM<u>LEEYSKR</u>FKKFGY
$CRAC^{SCR}$	FDRARM<u>YEKLERS</u>FKKFGY

This binding experiment was repeated with multiple liposome concentrations and the half maximal effective liposome concentration (EC_{50}) of $CRAC^{WT}$ binding to POPC/Chol liposomes was determined using a sigmoidal fit of the data (not shown). The results of this fit predict an EC_{50} of 3.2 μM, where EC_{50} represents the concentration of liposome solution that will generate a response halfway between the maximum response and baseline.

To inhibit LtxA binding to Chol and the resulting toxicity, we incubated THP-1 cells with LtxA alone or in combination with the $CRAC^{WT}$ peptide or the $CRAC^{SCR}$ peptide. As shown in Figure 3.5, the $CRAC^{WT}$ peptide, but not the $CRAC^{SCR}$ peptide, inhibited the activity of LtxA almost completely. A statistical analysis of these results is included in Table 3.1. Neither peptide was toxic to the cells at the concentrations used over the time course of the experiment.

To determine the half maximal peptide inhibitory concentration (IC_{50}) of the $CRAC^{WT}$ peptide, the experiment was repeated with several peptide concentrations, and

the data was fit to a sigmoidal curve (not shown). The results of this fit predict an IC_{50} of 6.1 µM for the $CRAC^{WT}$ peptide and demonstrates that an LtxA-derived Chol- binding peptide can be used to specifically alter the binding and subsequent toxicity of LtxA against several cell types, suggesting that the approach may have broad applicability in the treatment of *A. actinomycetemcomitans* infections. The IC_{50} represents the concentration of the peptide where the activity of LtxA is reduced by half.

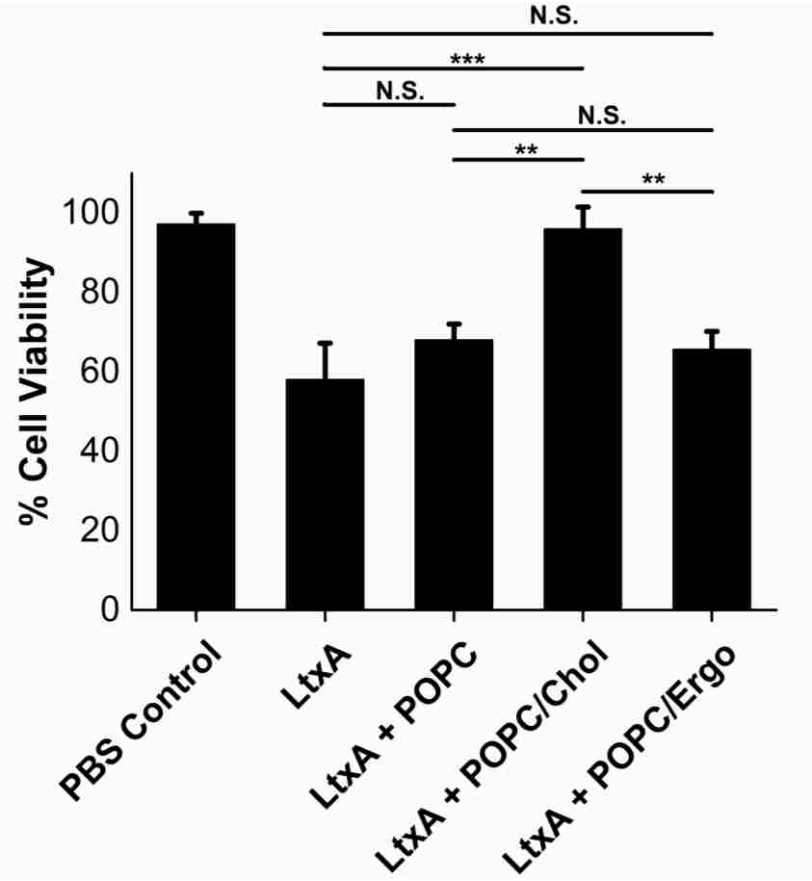

Figure 3.3 Pre-binding to Chol inhibits LtxA toxicity.
LtxA was preincubated with liposomes composed of 60% POPC and 40% Chol for 15 min before incubation with THP-1 cells for a period of 3 hrs. Preincubation of LtxA with these Chol-containing liposomes completely inhibited the toxicity of LtxA. Preincubation of LtxA with liposomes without Chol, composed of either 100% POPC or 60% POPC/40% Ergo, did not inhibit LtxA toxicity. A one-way analysis of variance followed by a Tukey test was used to determine the level of significance between each experiment. ***$P \leq 0.001$; **$P \leq 0.01$; N.S., not significant.

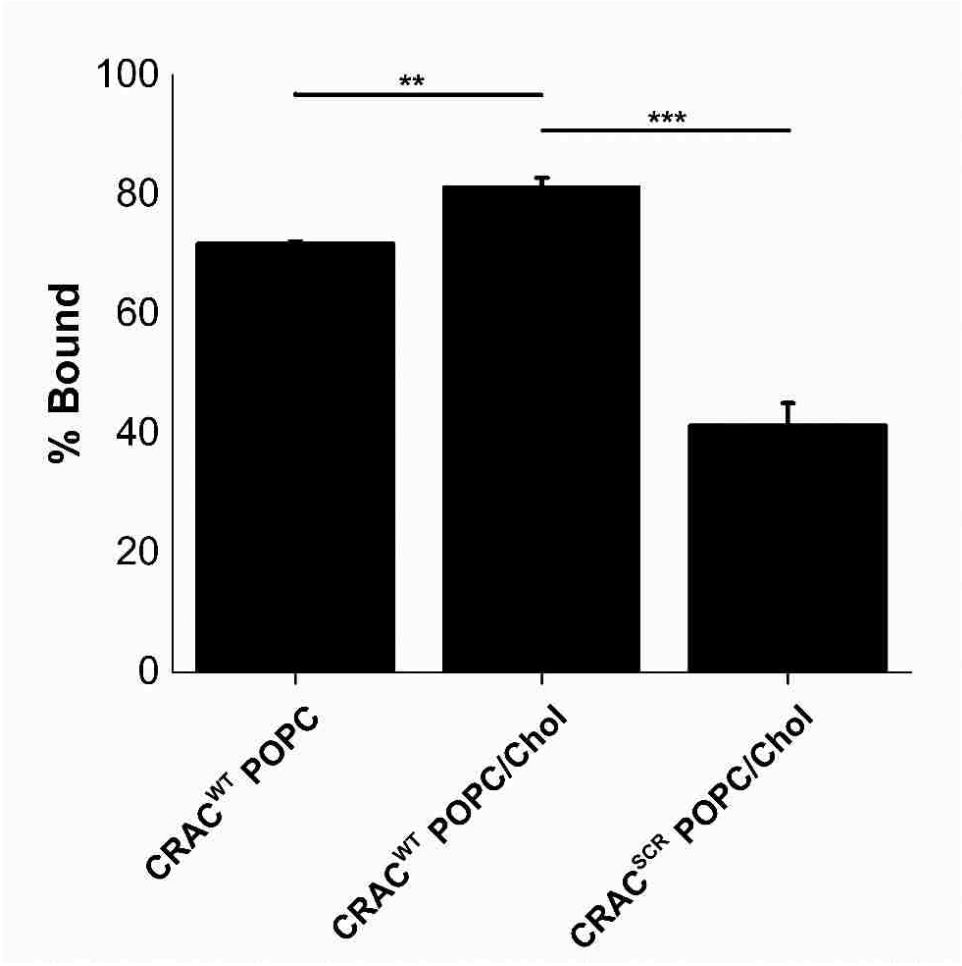

Figure 3.4 CRAC^{WT} peptide has an affinity for Chol.
A peptide corresponding to the Chol-binding motif in LtxA (CRAC^{WT}) was synthesized along with a control peptide in which the Chol-binding sequence was scrambled (CRAC^{SCR}). The peptides were incubated with liposomes composed of either 100% POPC or 60% POPC/40% Chol for 30 min. Unbound peptide was separated from the liposome–peptide complexes using a centrifugal filter, and the concentration of unbound peptide was determined by comparing the fluorescence intensity of the eluate to a set of standards. CRAC^{WT} bound significantly more to liposomes containing Chol than to those without Chol. CRAC^{SCR} bound with a lower affinity to the POPC/Chol liposomes than did CRAC^{WT}. A one-way analysis of variance followed by a Tukey test was used to determine the level of significance between each experiment. ***$P \leq 0.001$; **$P \leq 0.01$.

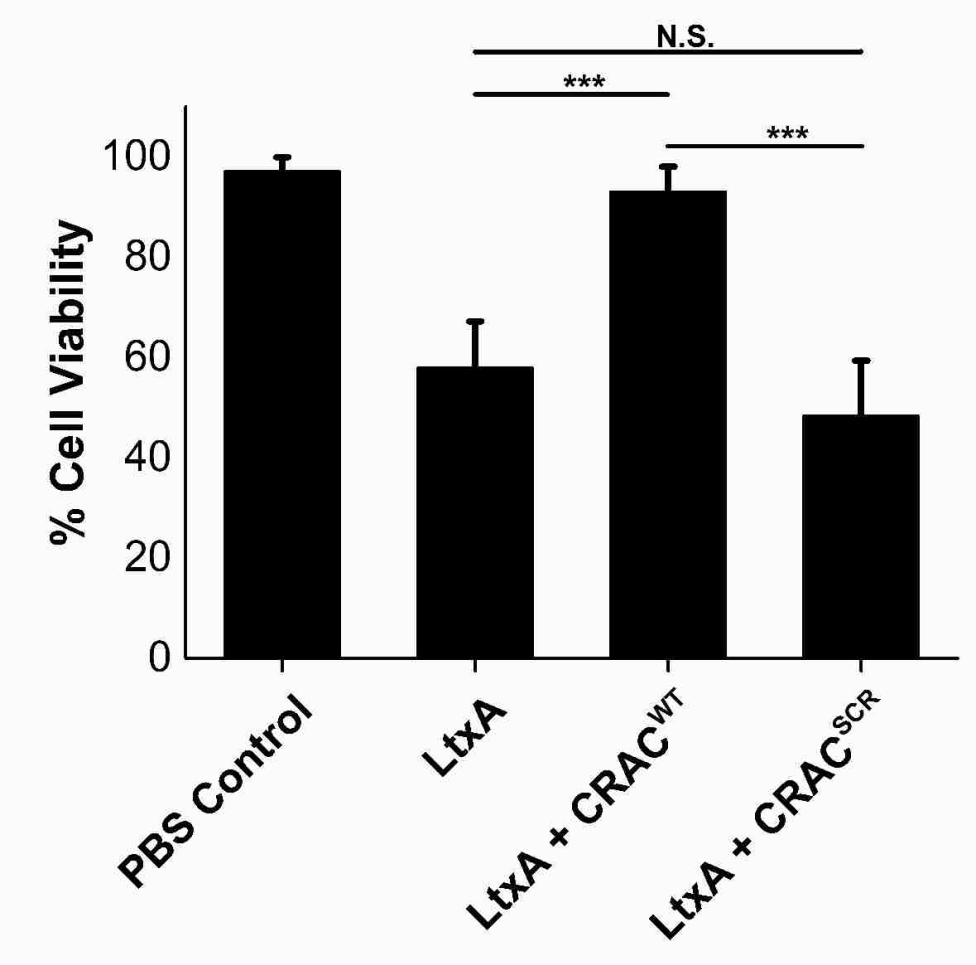

Figure 3.5 $CRAC^{WT}$ peptide inhibits LtxA toxicity.
LtxA and either $CRAC^{WT}$ or $CRAC^{SCR}$ were incubated with THP-1 cells for 3 h, and the viability of the cells was measured using a trypan blue assay. The $CRAC^{WT}$ peptide, which binds to Chol, inhibited the toxicity of LtxA, but the $CRAC^{SCR}$ peptide, which does not bind to Chol, did not inhibit LtxA toxicity. A one-way analysis of variance followed by a Tukey test was used to determine the level of significance between each experiment. ***P $\leq$ 0.001; N.S., not significant.

3.3 Discussion

Greater than 90% of cellular Chol resides at the plasma membrane and is essential for cell viability and proliferation [124, 228]. Chol is not uniformly dispersed throughout biological membranes; rather, it is sequestered in membrane microdomains known as lipid rafts, along with sphingolipids and specialized proteins, such as glycosylphosphatidylinositol (GPI)-anchored proteins, heterotrimeric G protein-coupled

receptors, and Src family kinases [229-233]. Many pathogens and their virulence factors have thus developed the ability to recognize and bind to lipid raft Chol on the surface of host cells. For example, Chol is required for the uptake of mycobacteria and *Leishmania* by host cells and allows these intracellular pathogens to avoid degradation by inhibiting lysosomal-phagosomal fusion [234-236]. In addition, the activity of several bacterial toxins depends on the presence of Chol in the target membrane [102, 135, 138, 221-223, 237-243]. Influenza, human immunodeficiency virus type 1, and the Ebola virus also require Chol in the host membrane for binding to and/or exit from the cell [244-246].

In the current study, we used THP-1, a human monocytic leukemia cell line, which expresses LFA-1, to investigate the role of Chol binding by LtxA on its toxicity [247]. While others have shown that LtxA cytotoxicity requires the expression of LFA-1 by the host cell, it has also been shown that LtxA is strongly membrane-active and has a particularly strong affinity (10^{-12} M) for membranes containing 40% Chol [89, 101, 248-250]. This membrane activity is correlated with subtle conformational changes in the entire protein structure, but a significant decrease in helicity within the Chol-binding domain upon association with Chol. These conformational changes are what allows the protein to move from a water-soluble to a membrane active state [182, 250, 251].

To determine the dependence of LtxA on Chol within the membrane, MβCD was utilized to remove and replenish Chol content and measure the effectiveness of LtxA in killing THP-1 cells in these two environments. This technique has been implemented previously in other studies to determine the effect of Chol in a specific interaction [119, 252, 253]. We found by removing Chol from the membrane, the cytotoxic ability of LtxA towards THP-1 cells was significantly inhibited (Figure 3.1). This was seen in other

pathogens with a dependence on membrane Chol as well, including poliovirus, PFO, and the CRAC domain containing cytolethal distending toxin (CDT) [138, 254, 255].

From our MβCD results, LtxA was observed to rely significantly on the presence of Chol. To determine if we could utilize LtxA's dependence on membrane Chol as an antivirulence approach to inhibit the toxin's activity toward THP-1 cells, we synthesized Chol-containing liposomes in which LtxA has previously shown to have an affinity for [102]. Using LtxA's strong affinity for Chol-containing liposomes, we introduced a novel approach at inhibiting LtxA cytotoxicity that deviates from the traditional role of liposomes serving as drug delivery vehicles [256-258]. Preincubating Chol-containing liposomes with LtxA prior to the introduction of THP-1 cells resulted in a significant decrease in cell cytotoxicity, as shown in Figure 3.3. LtxA's strong affinity for Chol within the liposome allowed it to bind to the liposomal membrane and stay bound throughout the incubation period, thus preventing LtxA from interacting with THP-1 cells. This type of approach, where a synthetic intermediate is used to compete against a host cell for toxin binding, has shown to be effective against several bacterial toxins *in vitro and in vivo* [75, 259]. In one case, synthetic liposomes were able to prevent fatalities from occurring in a murine model infected with septicemia from *S. aureus* and *Streptococcus pneumoniae* [259]. In a second case, a synthetic oligosaccharide scaffold was effective in binding to the bacterial toxin and preventing it from reaching the host cell, thus inhibiting toxin cytotoxicity *in vitro* and *in vivo* as well [75].

To build upon a previous study where CRAC peptides were used to inhibit LtxA from binding to Chol-containing liposomes, we investigated the ability of CRAC peptides to inhibit LtxA's ability to bind to THP-1 cells [102]. We found $CRAC^{WT}$ can also bind

to Chol within the THP-1 cell membrane, thus preventing the binding of LtxA and leading to a significant reduction of LtxA cytotoxicity (Figure 3.5). This study signifies the first-time a peptide, with an affinity for Chol, has been used to inhibit a pathogen that also has an affinity for Chol.

In conclusion, this work demonstrates the requirement of Chol binding by LtxA in cytotoxicity. Based on this and our previous results, we can conclude that LtxA requires Chol within the membrane to be available for binding in order for the toxin to kill the target cells.

Chapter 4

Use of a Cholesterol Recognition Amino Acid Consensus Peptide to Inhibit Binding of a Bacterial Toxin to Cholesterol

4.1 Introduction

Chol binding is usually the first step in the pathogenic mechanism of toxins or viruses as they move from the aqueous extracellular environment to hydrophobic membrane environment. Thus, disruption of this recognition process represents a possible method to inhibit bacterial and viral pathogenesis. Furthermore, we've previously demonstrated three alternative approaches to inhibit bacterial toxin activity. In the first we found that the removal of Chol from the cell's plasma membrane significantly reduced the toxic ability of the bacterial toxin LtxA by reducing the number of binding locations. In the second approach we demonstrated the use of synthetic vesicles that compete with the host cell to bind LtxA. Lastly in the third approach, we utilized a Chol-binding peptide containing a CRAC domain that can bind to Chol on the cell membrane thus preventing LtxA from binding and rendering the cell unsusceptible to the toxin's activity [17, 19].

Here, our goal was to investigate the interaction between $CRAC^{WT}$ and Chol and determine the effect this peptide's interaction has on LtxA's ability to bind to the membrane. Using several biophysical techniques, we found that $CRAC^{WT}$ has a strong

affinity for Chol. In addition, we determined that the hydroxyl group of Chol is key to the interaction between $CRAC^{WT}$ and Chol. Furthermore, using confocal microscopy we visualized the ability of $CRAC^{WT}$ to inhibit toxin binding to synthetic Chol-containing membranes. The ability of $CRAC^{WT}$ to prevent membrane binding led to its ability to prevent LtxA internalization and subsequent cytotoxicity to THP-1 cells as well. Through these studies, we found that the peptide interacts strongly near the surface of the membrane through the recognition of the hydroxyl group of Chol and as a result LtxA is unable to recognize and bind Chol, thus demonstrating an alternative approach to prevent the toxin from binding to the membrane and then killing the cells.

4.2 Results

4.2.1 LtxA and $CRAC^{WT}$ have a strong affinity for Chol

A total of six experiments were performed to investigate the thermodynamics of binding of LtxA to POPC and Chol, as well as binding of $CRAC^{WT}$ and $CRAC^{SCR}$ to POPC and Chol. These experiments were designed to be conducted at a lipid composition at which no phase separation is expected, so that the thermodynamic properties of binding to Chol could be extracted without the additional complications of phase separation [260-262].

To obtain the thermodynamic properties of binding of LtxA to membranes, liposomes composed of either 100% POPC or 60% POPC and 40% Chol were titrated into a solution of LtxA, and the data were fit using the independent model or the multiple-binding sites model, respectively (Figure 2.2). The heats of injection and the lines of best fit are shown in Figure 4.1, and the thermodynamic constants obtained are listed in Table 4.1. The equilibrium dissociation constant (K_D) of association of LtxA with POPC was

determined to be 8.75×10^{-4} M, and its negative entropic value suggests that desolvation effects from the hydrophobic interactions between LtxA and POPC dominate the reaction [263-265]. The K_D for the interaction between LtxA and Chol was determined to be 2.31×10^{-10} M, which was 6 orders of magnitude more favorable than the affinity of LtxA for POPC. As shown in Table 4.1, the Gibbs free energy (ΔG) of the interaction between LtxA and Chol is much more favorable than that between LtxA and POPC. The entropic (ΔS) contribution to ΔG is similar for both reactions, but the enthalpic (ΔH) contribution from the binding of LtxA to Chol is much more favorable than that for binding of LtxA to POPC, indicating that more and/or stronger noncovalent bonds are formed between LtxA and Chol relative to LtxA and POPC [264, 266, 267].

To determine the thermodynamic properties of binding of $CRAC^{WT}$ and $CRAC^{SCR}$ to Chol, each peptide was individually titrated into a solution of liposomes composed of either 100% POPC or 60% POPC and 40% Chol. The data were fit using the independent model or the multiple-binding sites model, respectively (Figure 2.2). The heats of injection and the lines of best fit are shown in Figure 4.2 and Figure 4.3, and the thermodynamic constants obtained are listed in Table 4.1. The results listed in Table 4.1 indicate that the $CRAC^{WT}$ peptide interacts weakly with membranes composed of 100% POPC, with a dissociation constant of 3.81×10^{-4} M. The affinity of this peptide for membranes containing 40% Chol was 5.05×10^{-8} M, four orders of magnitude stronger than the affinity of the peptide for POPC. ΔG is more favorable for binding of $CRAC^{WT}$ to Chol than to POPC, and like that for LtxA, this difference is due to differences in the enthalpic rather than entropic contributions to the free energy.

Because the $CRAC^{SCR}$ peptide lacks an intact CRAC sequence, we hypothesized that this peptide would have minimal affinity for Chol and could therefore be used in this work as a negative control. Using ITC, we found that the affinity of the $CRAC^{SCR}$ peptide for POPC membranes was reduced relative to that of $CRAC^{WT}$. In addition, the presence of Chol in the membrane did not enhance the affinity of $CRAC^{SCR}$ for the membrane (Table 4.1), demonstrating that this peptide has a significantly reduced affinity for Chol. Comparison of the free energy values and affinity constants of LtxA and $CRAC^{WT}$ for membranes (Table 4.1) indicates that both LtxA and $CRAC^{WT}$ have a significantly greater affinity for Chol than for POPC. Furthermore, the similarity between the thermodynamics of the interaction of $CRAC^{WT}$ and LtxA with Chol suggests that the affinity of LtxA for Chol is driven primarily by the toxin's CRAC motif.

4.2.2 $CRAC^{WT}$ secondary structure is altered upon binding to Chol

The favorable enthalpy change observed in the ITC experiment upon $CRAC^{WT}$ binding to Chol indicates that this reaction results in more and/or stronger noncovalent bonds between the peptide and Chol than between the peptide and POPC. To investigate whether conformational changes are involved in this difference in binding, we conducted a CD experiment.

The mean residue ellipticity (MRE), which measures the molar CD of each residue within the peptide, was calculated for each CD spectrum (Figure 4.4). The MRE was measured for $CRAC^{WT}$ in solution and after $CRAC^{WT}$ interacted with membranes composed of 100% POPC or 60% POPC/40% Chol (Figure 4.5). Initially, $CRAC^{WT}$ in solution is roughly composed of 25% α-helices and 25% β-sheets with the remaining structure containing random coils and being unordered. Similarly, other CRAC peptides

of similar length including molecular dynamics simulations of $CRAC^{WT}$ have produced comparable solution structures to $CRAC^{WT}$ [182, 268].

As the peptide moved from solution to a POPC membrane, the helicity decreased slightly, and the fraction of β-sheet structure increases slightly. The structural changes as the peptide moved from solution to a Chol-containing membrane were much more pronounced, with a large decrease in helicity and a large increase in β-sheet structure, indicating that at least some of the differences in the enthalpic contributions to free energy observed by ITC are due to conformational changes in the peptide upon binding to Chol.

4.2.3 $CRAC^{WT}$ membrane affinity depends on sterol structure

To characterize recognition by $CRAC^{WT}$ of Chol in the membrane, we performed ITC experiments using liposomes composed of POPC and one of four sterols. As shown in Figure 4.7, each sterol varied only slightly in structure from that of Chol, allowing us to determine if $CRAC^{WT}$ recognition of the sterol occurs at the head, body, or tail of the molecule. Relative to Chol, Desmo, has an altered tail, DHC has an altered A ring, and CC has an altered headgroup. The results, shown in Figure 4.6 and Table 4.2, indicate that $CRAC^{WT}$ has the lowest affinity (6.86×10^{-2} M) for liposomes containing CC, which has a modified headgroup, followed by liposomes containing Desmo (2.39×10^{-4} M), which has a modified tail relative to that of Chol. Slightly reduced affinity, relative to Chol, was measured for liposomes containing DHC (2.53×10^{-7} M), which has a modified ring structure relative to that of Chol. These results suggest that the recognition of Chol by $CRAC^{WT}$ occurs primarily at the hydroxyl group and hydrocarbon groups of Chol.

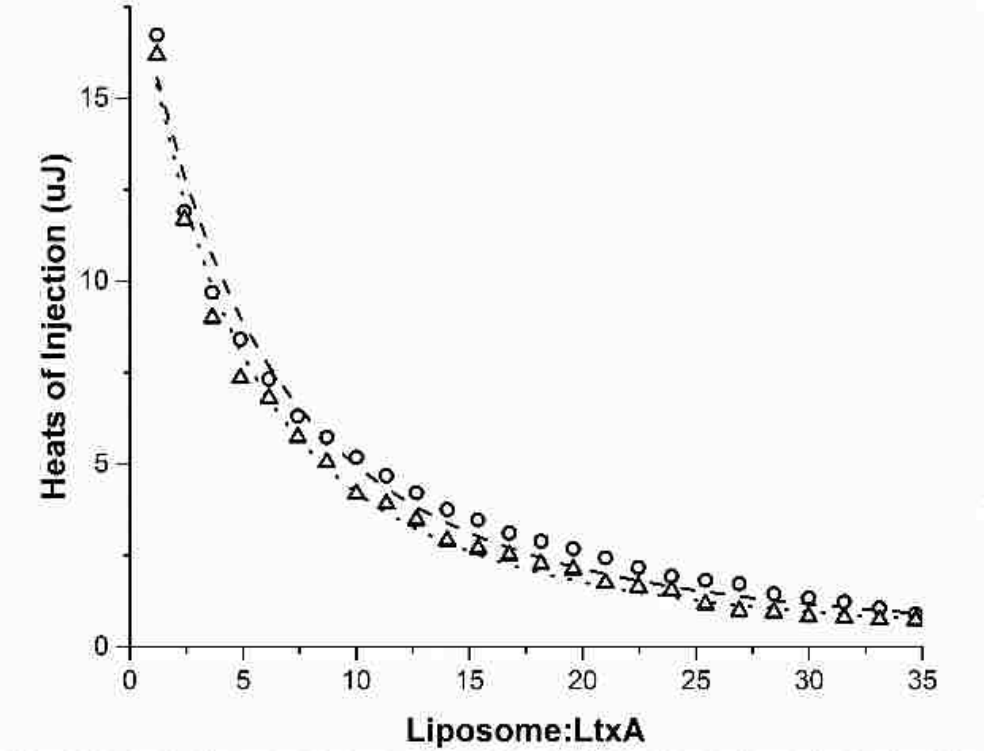

Figure 4.1 Raw ITC Heats of Injection for LtxA and POPC, POPC/Chol.
ITC measurements were performed at 30 °C in a Low Volume Nano ITC. 50 μL of a liposome solution (10 mM) was injected into a cell containing 100 μM LtxA. Triangles depict each 1 μL injection of 100% POPC titrated into LtxA. Circles depict each 1 μL injection of 60% POPC/40% Chol titrated into LtxA. Lines of best fit are shown, with long dashes depicting POPC/Chol and short dashes depicting POPC.

Table 4.1 Thermodynamics of the Interactions of LtxA and $CRAC^{WT}$ with Chol.
Liposomes composed of 100% POPC or 60% POPC/40% Chol were titrated into a solution containing either LtxA or $CRAC^{WT}$. The affinity and thermodynamic properties were obtained using one of two models, as described in the Methods section.

	K_D (M)	**ΔH (kJ/mol)**	**-TΔS (kJ/mol)**	**ΔG (kJ/mol)**
LtxA + POPC	$8.75 \times 10^{-4} \pm 2.40 \times 10^{-5}$	15.24	-32.99	-17.8
LtxA + Chol	$2.31 \times 10^{-10} \pm 9.80 \times 10^{-11}$	-29.76	-26.15	-55.9
$CRAC^{WT}$ + POPC	$3.81 \times 10^{-3} \pm 2.13 \times 10^{-3}$	32.58	-46.8	-14.2
$CRAC^{WT}$ + Chol	$5.05 \times 10^{-8} \pm 3.47 \times 10^{-3}$	2.81	-46.2	-43.4
$CRAC^{SCR}$ + POPC	$5.36 \times 10^{-5} \pm 2.25 \times 10^{-5}$	−7.65	−17.27	−24.9
$CRAC^{SCR}$ + Chol	$4.07 \times 10^{-4} \pm 4.13 \times 10^{-5}$	−5.45	−14.24	−19.7

To verify that the observed inhibition of $CRAC^{WT}$ binding in the presence of Desmo, CC, and DHC, relative to that with Chol, is due specifically to changes in sterol structure and not a decrease in membrane fluidity that could prevent peptide association, a GP experiment was performed. Using POPC liposomes containing Laurdan, a fluorescent molecule that is sensitive to the presence of water within the membrane, we measured the GP of membranes composed entirely of POPC or of POPC and one of the four sterols [269]. As shown in Figure 4.7B, Chol significantly decreased fluidity in the membrane relative to that of 100% POPC, measured by an increase in GP, as expected. Both DHC and Desmo decreased the fluidity similar to Chol. CC decreased the fluidity of the POPC membrane slightly, but much less so than Chol, DHC, or Desmo. This result indicates that the reduction in the level of binding observed in the ITC experiments is due to sterol structure and not overly tight packing of the membrane.

4.2.4 $CRAC^{WT}$ does not disrupt membrane packing

To determine if $CRAC^{WT}$ perturbs bilayer packing in its interaction with the membrane, another Laurdan fluorescence experiment was performed. Using Laurdan-labeled liposomes of varying compositions, we calculated the GP before and after peptide addition, to measure water penetration into the membrane core, as a measure of bilayer disruption by the peptide. Figure 4.7B shows the GP of the membrane in the presence of $CRAC^{WT}$ or $CRAC^{SCR}$ normalized by the membrane's GP value in the absence of peptide. No statistical difference between the GP profiles of any of the membranes in the presence or absence of either $CRAC^{WT}$ or $CRAC^{SCR}$ was found. This result indicates that neither peptide induces water penetration into the hydrophobic core of the membrane, suggesting that the peptides do not penetrate deeply into the membrane.

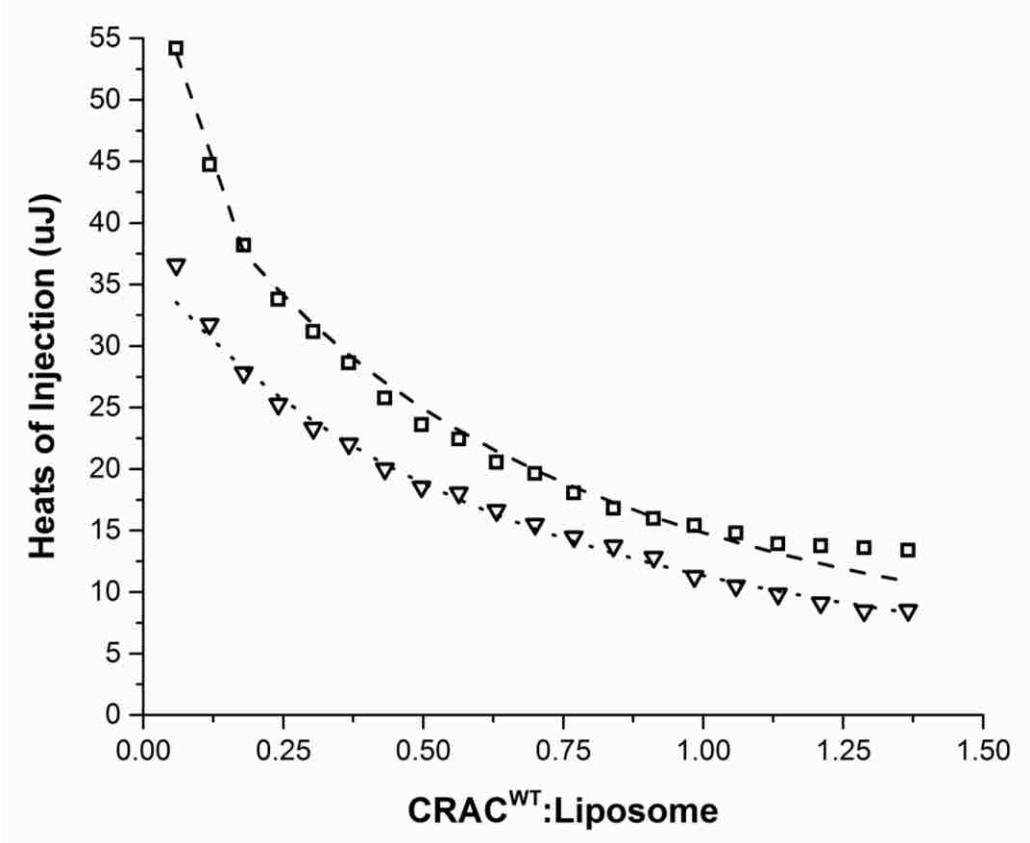

Figure 4.2 Raw ITC Heats of Injection for $CRAC^{WT}$ and POPC, POPC/Chol. ITC measurements were performed at 30 °C in a Low Volume Nano ITC. 50 µL of $CRAC^{WT}$ (7.65 mM) was injected into a cell containing 2 mM liposome solution. Inverted triangles depict each 2.5 µL injection of $CRAC^{WT}$ titrated into 100% POPC. Squares depict each 2.5 µL injection of $CRAC^{WT}$ titrated into 60% POPC/40% Chol. Lines of best fit are shown, with long dashes depicting POPC/Chol and short dashes depicting POPC.

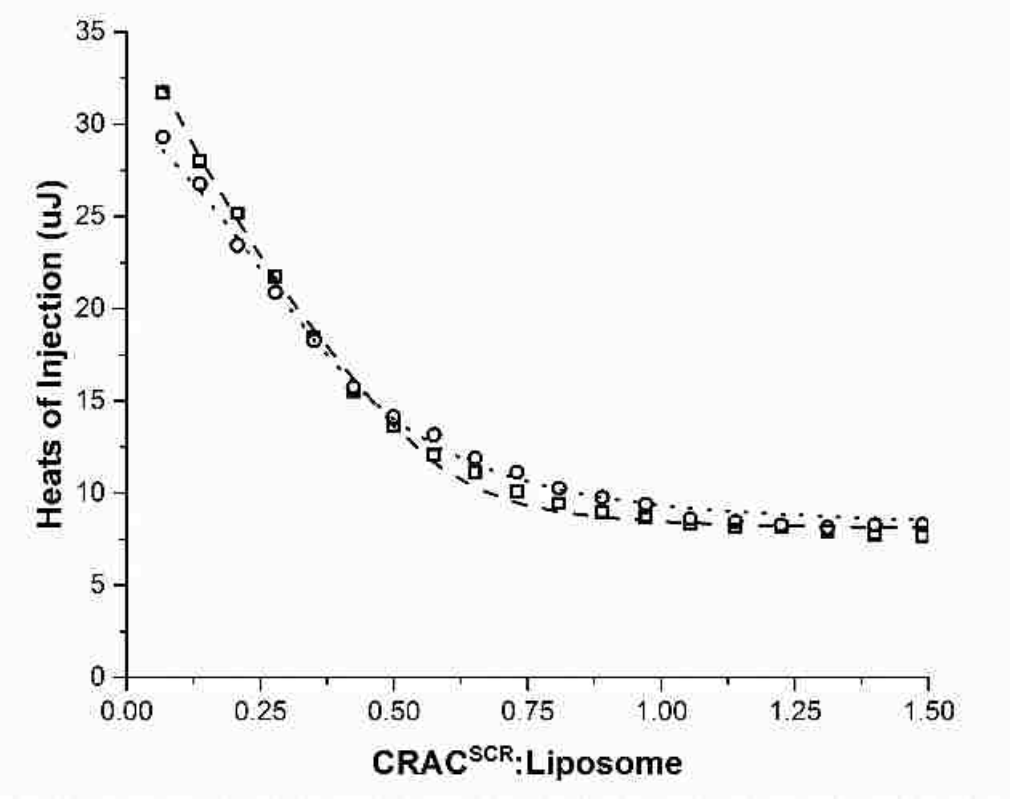

Figure 4.3 Raw ITC Heats of Injection for $CRAC^{SCR}$ and POPC, POPC/Chol. ITC measurements were performed at 30 °C in a Low Volume Nano ITC. 50 µL of $CRAC^{SCR}$ (7.65 mM) was injected into a cell containing 2 mM liposome solution. Squares depict each 2.5 µL injection of $CRAC^{SCR}$ titrated into 100% POPC. Circles depict each 2.5 µL injection of $CRAC^{SCR}$ titrated into 60% POPC/40% Chol. Lines of best fit are shown, with short dashes depicting POPC/Chol and long dashes depicting POPC.

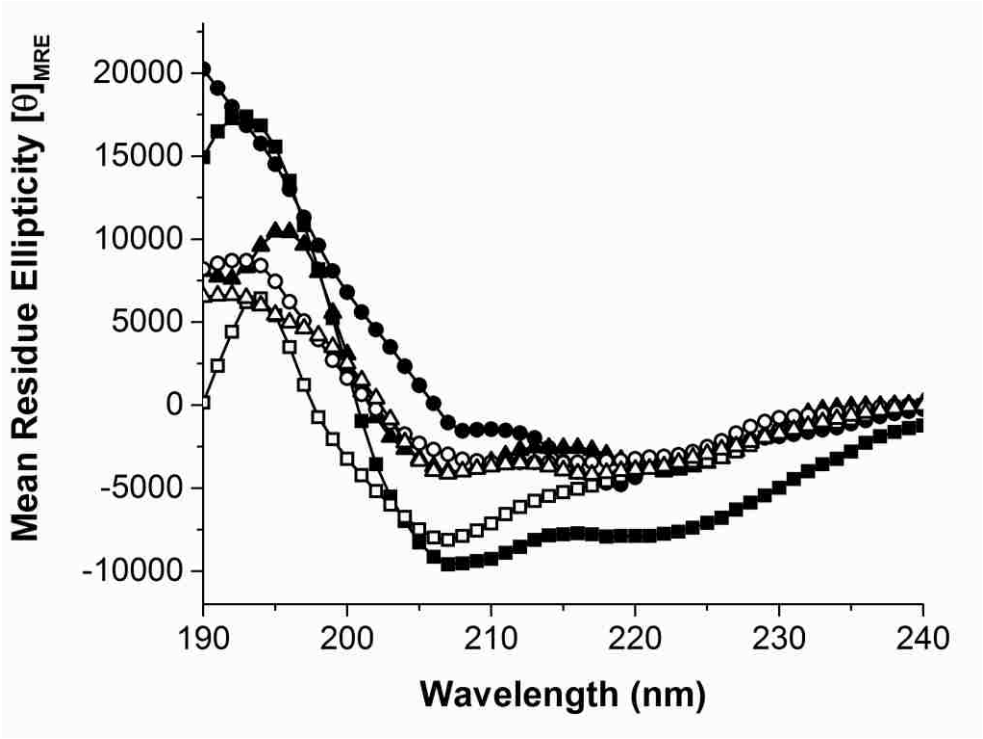

Figure 4.4 MRE CD Spectroscopy Data of $CRAC^{WT}$.
Spectral scans were performed in 10 mM phosphate buffer, using a peptide concentration of 0.25 mg/mL. To ensure that the spectra represent the structure of only bound peptide, unbound peptide was removed using centrifugal filters. MRE was calculated for each spectrum. Filled in squares depict spectrum of $CRAC^{WT}$ in solution. Filled in triangles depict spectrum of $CRAC^{WT}$ in 100% POPC. Filled in circles depict spectrum of $CRAC^{WT}$ in 60% POPC/40% Chol. Empty squares depict spectrum of $CRAC^{WT}$ in 60% POPC/40% Desmo. Empty circles depict spectrum of $CRAC^{WT}$ in 60% POPC/40% DHC. Empty triangles depict spectrum of $CRAC^{WT}$ in 60% POPC/40% CC.

4.2.5 CRAC^{WT} peptides inhibit LtxA internalization

Previously, we showed that CRAC^{WT} is able to inhibit LtxA activity in target cells, and here, we have demonstrated that the peptide has a strong affinity for Chol [17]. We therefore investigated the hypothesis that the peptide inhibits LtxA activity by preventing the toxin from binding to Chol and being subsequently internalized by the cell. To visually confirm the affinity of LtxA for Chol we performed a confocal imaging experiment using GUVs composed of DOPC/DPPC/Chol (1:1:1). The GUVs were labeled with the fluorescent probe NBD-PE. As shown in Figure 4.8A, AF555-LtxA was able to bind to the GUVs. When the GUVs were preincubated with CRAC^{WT} (Figure 4.8B), LtxA was unable to bind to the membranes, indicating that the peptide does block the ability of LtxA to bind Chol. The scrambled peptide, CRAC^{SCR}, had no effect on LtxA binding to the membranes (Figure 4.8C). Quantification of the total LtxA intensity is shown in Figure 4.8D.

In addition to Chol binding, LtxA must also recognize and bind a cell surface receptor, LFA-1 [247, 249, 270]. We therefore investigated whether CRAC^{WT} mediated inhibition of LtxA binding to Chol is sufficient to inhibit LtxA internalization into target cells. When AF555-LtxA was incubated for 30 min with THP-1 cells in the absence of CRAC peptide, internalization of the toxin into THP-1 cells was observed, as shown in Figure 4.9A. In contrast, significantly less AF555-LtxA was detected inside the cells when the same amount of the AF555-LtxA was incubated with THP-1 cells pretreated with CRAC^{WT}, as shown in Figure 4.9A, demonstrating that CRAC^{WT} mediated inhibition of AF555-LtxA binding to Chol prevents the toxin from being internalized. THP-1 cells pretreated with CRAC^{SCR}, the control peptide, did not inhibit AF555-LtxA activity, as

shown in Figure 4.9A. Quantification of the total AF555-LtxA intensity is shown in Figure 4.9B.

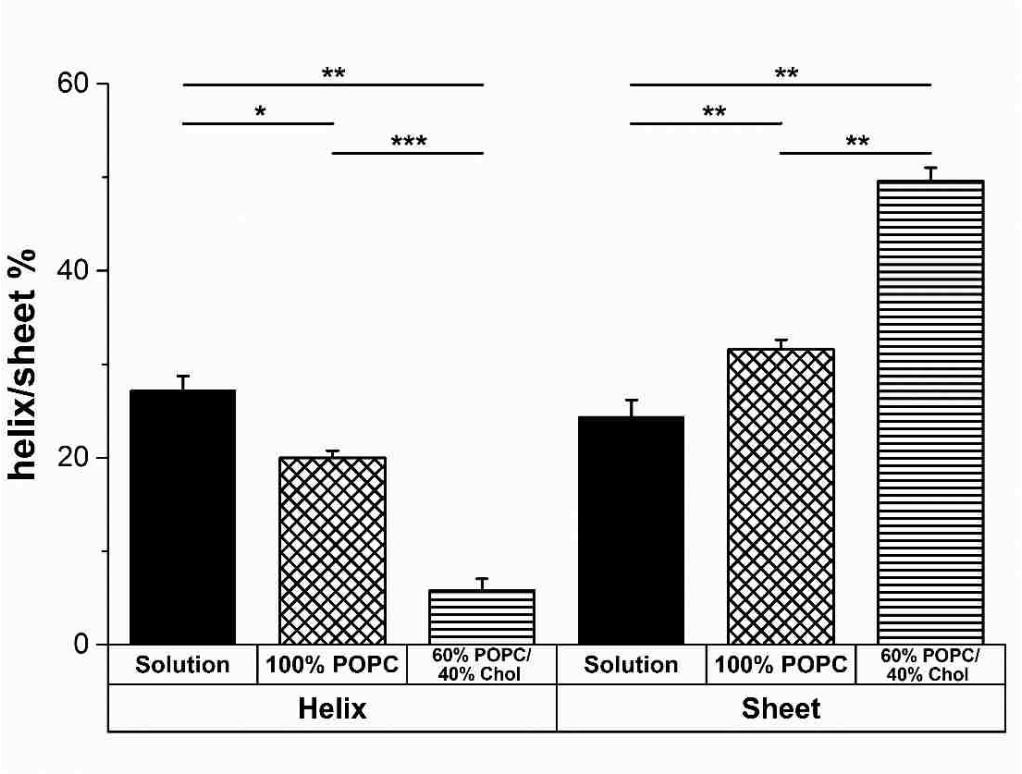

Figure 4.5 Predicted secondary structure of $CRAC^{WT}$ in solution or in membranes composed of 100% POPC or 60% POPC/40% Chol.

As the $CRAC^{WT}$ peptide transitions from a membrane free environment, to a Chol-free membrane environment, and lastly to an environment with Chol-containing membranes, the helical structure of $CRAC^{WT}$ decreases and the sheet structure of $CRAC^{WT}$ increases. Results were obtained with DICHROWEB using CONTIN/LL and either the SP175 or the SMP180 reference set. The bar graph is split into an α-helical structure section (left) and a β-sheet structure section (right). Each bar graph represents data averaged over three independent experiments. The level of significance was determined using an unpaired two-sample t-test. ***$P \leq 0.001$; **$P \leq 0.01$; *$P \leq 0.05$; N.S. $P > 0.05$.

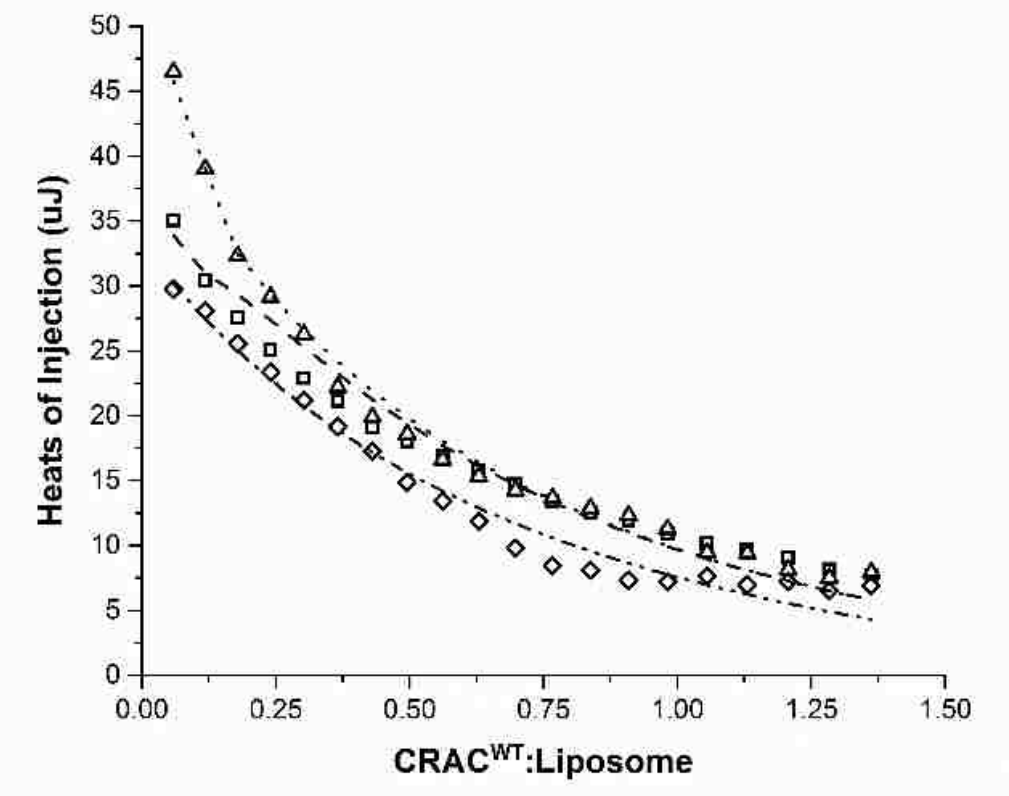

Figure 4.6 Raw ITC Heats of Injection for $CRAC^{WT}$ and POPC/DHC, POPC/Desmo, and POPC/CC.

ITC measurements were performed at 30 °C in a Low Volume Nano ITC. 50 µL of $CRAC^{WT}$ (7.65 mM) was injected into a cell containing 2 mM liposome solution. Triangles depict each 2.5 µL injection of $CRAC^{WT}$ titrated into 60% POPC/40% DHC. Squares depict each 2.5 µL injection of $CRAC^{WT}$ titrated into 60% POPC/40% Desmo. Diamonds depict each 2.5 µL injection of $CRAC^{WT}$ titrated into 60% POPC/40% Desmo. Lines of best fit are shown, with short dashes depicting POPC/DHC, long dashes depicting POPC/Desmo, and combined long and short dashes depicting POPC/CC.

4.2.6 $CRAC^{WT}$ does not exhibit long-term toxicity to cells

To determine if the $CRAC^{WT}$ peptide is toxic to cells over a period of time, which would prevent its future therapeutic use, we conducted a long-term viability study. THP-1 cells were cultured in media containing 40 µg/mL (15.9 µM) peptide of $CRAC^{WT}$ alongside THP-1 cells grown in peptide-free media. Over a period of 65 days, no peptide-mediated toxicity was observed in the cells, as shown in Figure 4.10, suggesting that this

peptide may represent a non-toxic method for blocking bacterial toxin and pathogen binding to Chol in host cells. Furthermore, the concentration used in the long term toxicity assay is five times greater than the half maximal effective concentration (EC_{50}) found previously for $CRAC^{WT}$ and liposomes composed of 60% POPC/40% Chol [17].

Table 4.2 Thermodynamic Parameters of the $CRAC^{WT}$ Interactions with sterols and $CRAC^{SCR}$ Interaction with Chol

Liposomes composed of 100% POPC or 60% POPC/40% sterol were titrated into a solution containing either $CRAC^{WT}$ or $CRAC^{SCR}$. The affinity and thermodynamic properties were obtained using one of two models, as described in the Methods section.

	K_D (M)	**ΔH (kJ/mol)**	**-TΔS (kJ/mol)**	**ΔG (kJ/mol)**
$CRAC^{WT}$ + POPC	$3.81 \times 10^{-3} \pm 2.13 \times 10^{-3}$	32.58	-46.8	-14.2
$CRAC^{WT}$ + Chol	$5.05 \times 10^{-8} \pm 3.47 \times 10^{-3}$	2.81	-46.2	-43.4
$CRAC^{WT}$ + Desmo	$2.39 \times 10^{-4} \pm 8.21 \times 10^{-5}$	1.508	-22.42	-20.9
$CRAC^{WT}$ + DHC	$2.53 \times 10^{-7} \pm 4.24 \times 10^{-8}$	2.66	-40.91	-38.3
$CRAC^{WT}$ + CC	$6.86 \times 10^{-2} \pm 1.01 \times 10^{-2}$	-0.80	-5.76	-4.96
$CRAC^{SCR}$ + POPC	$5.36 \times 10^{-5} \pm 2.25 \times 10^{-5}$	-7.65	-17.27	-24.9
$CRAC^{SCR}$ + Chol	$4.07 \times 10^{-4} \pm 4.13 \times 10^{-5}$	-5.45	-14.24	-19.7

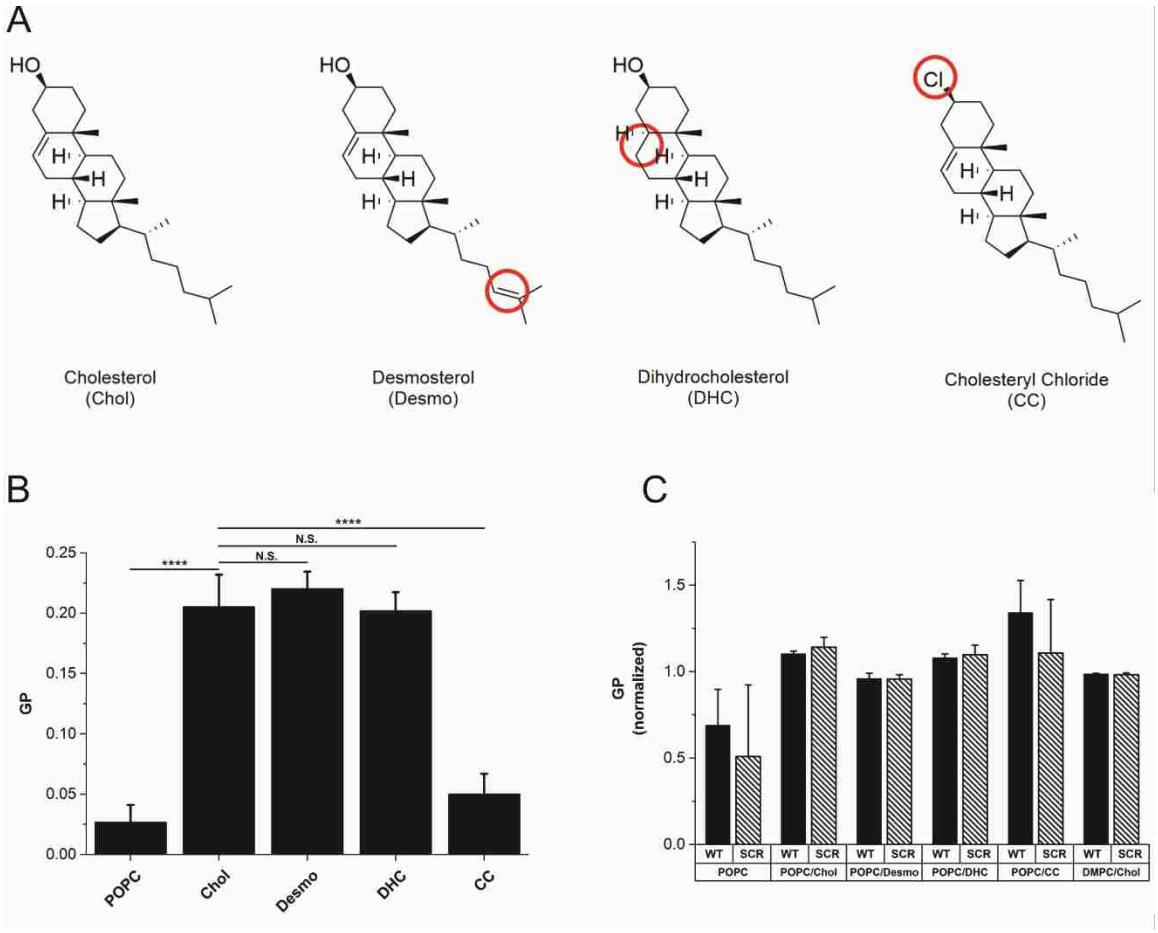

Figure 4.7 Structures of the sterols, Chol, DHC, Desmo, and CC, used in this work and the quantification of membrane packing effect from the GP values of Laurdan.
(A) The structural differences in each sterol relative to Chol are circled. (B) Laurdan was incorporated into liposomes containing 100% POPC, or 80% POPC/20% sterol at 23 °C. The fluidity of each membrane was quantified by the GP value of Laurdan, with a lower GP indicating a more fluid membrane. This graph represents data averaged over six independent experiments. (C) Laurdan was incorporated into liposomes containing 100% POPC, 80% POPC/20% sterol, or 60% DMPC/40% Chol at 23 °C. Disruption of bilayer packing after peptide incorporation was quantified by the GP value of Laurdan, with a lower GP value indicating the presence of water in the membrane core. Each GP value was normalized with respect to the GP value of the specified membrane in the absence of peptide. This graph represents data averaged over three independent experiments. The level of significance for both figures was determined using an unpaired two-sample t-test. ****$P \leq 0.0001$; ***$P \leq 0.001$; **$P \leq 0.01$; N.S. $P > 0.05$.

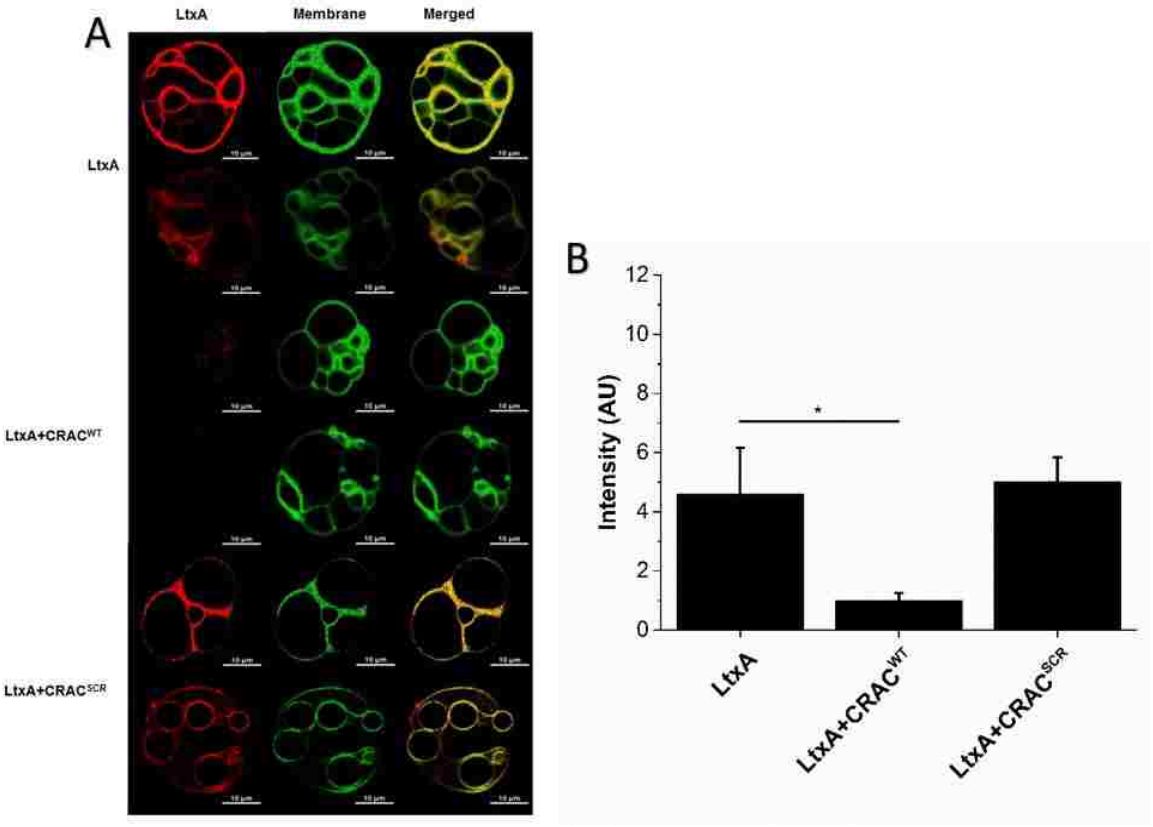

Figure 4.8 Peptide-mediated inhibition of LtxA binding to Chol in GUVs. GUVs were composed of DOPC/DPPC/Chol (1:1:1), labeled with NBD-PE (green). (A) In the absence of peptide, AF555-LtxA (red) binds to the membrane. In the presence of $CRAC^{WT}$ at a peptide:toxin ratio of 100:1, LtxA was inhibited from binding to the membrane. In the presence of $CRAC^{SCR}$ at a peptide:toxin ratio of 100:1, LtxA was able to bind to the GUV membrane. The scale bar in the bottom right corner of each micrograph represents 10 μm. (B) Region of interest (ROI) analysis was performed to measure the fluorescence intensity of LtxA in the confocal images. The bar graph represents data averaged over 5 independent GUV image captures for each of the three conditions. The level of significance was determined using an unpaired two-sample t-test. $*P \leq 0.05$.

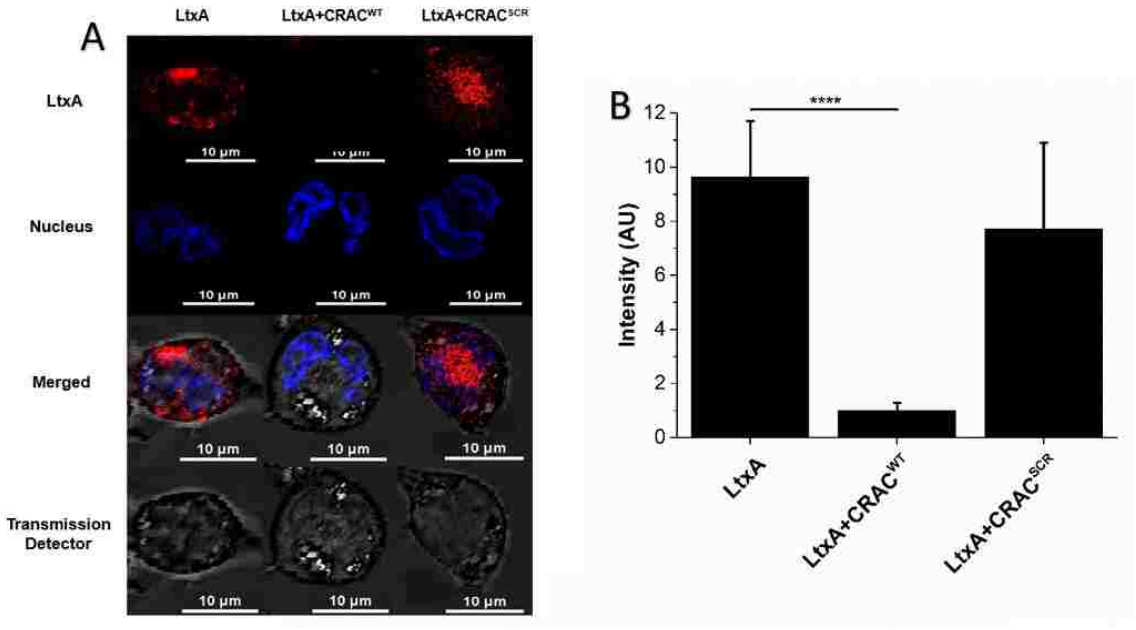

Figure 4.9 Peptide-mediated inhibition of LtxA internalization in THP-1 cells. THP-1 cells were differentiated into tissue-like macrophages, and the nuclei were labeled with NucBlue® Live ReadyProbes® reagent (Thermo Fisher Scientific, blue). (A) In the absence of peptide, AF555-LtxA (red) is located within THP-1 cells. When the cells were preincubated with $CRAC^{WT}$ for 30 min at a peptide:toxin ratio of 100:1, AF555-LtxA was unable to be internalized by the cells. Preincubation of the cells with $CRAC^{SCR}$ for 30 min at a peptide:toxin ratio of 100:1 did not inhibit AF555-LtxA internalization. The scale bar in the bottom right corner of each micrograph represents 10 µm. (B) Region of interest (ROI) analysis was performed to measure the fluorescence intensity of LtxA. The bar graph represents data averaged over every cell for each image captured, for each of the three conditions (images were enlarged for clarity and not every cell measured is shown). ****$P \leq 0.0001$.

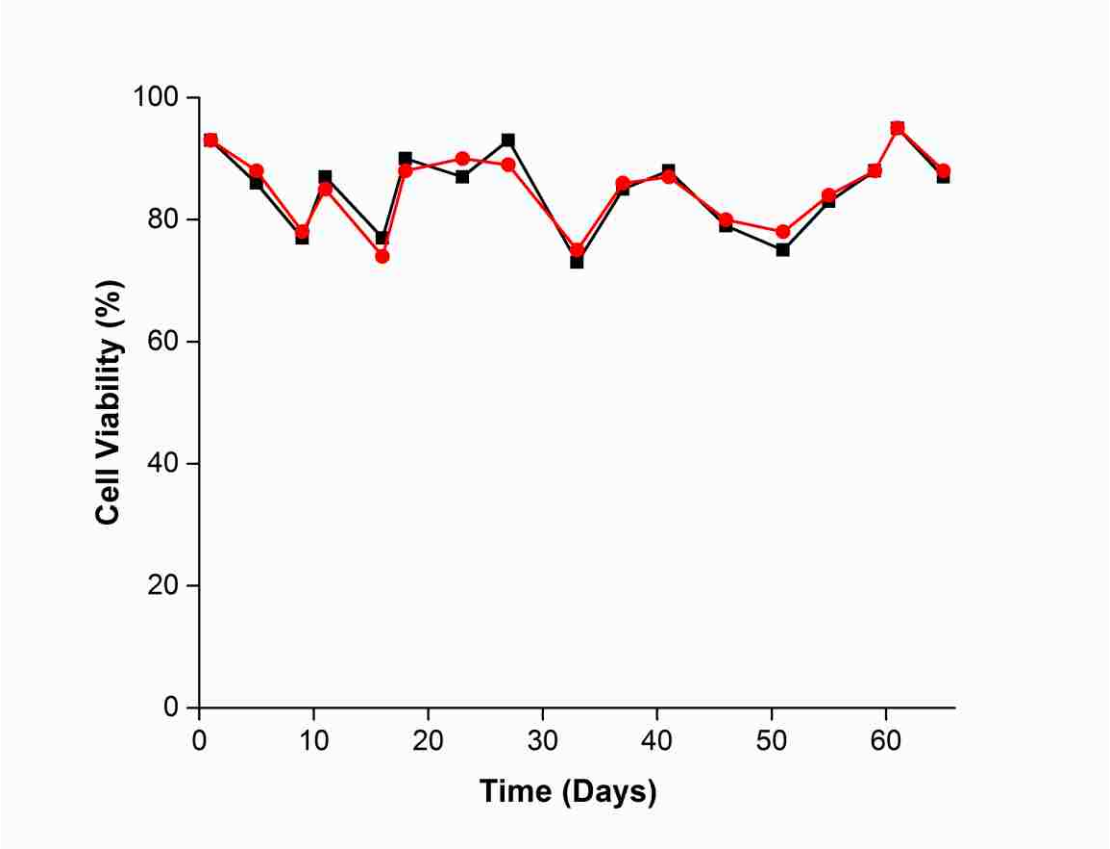

Figure 4.10 Long-term Effect of $CRAC^{WT}$ on THP-1 Cell Viability
THP-1 cells (5 x 10^5 cell/mL) were grown in medium supplemented with 40 µg/mL $CRAC^{WT}$ or in the absence of peptide. Cell viability was measured using a Trypan blue assay.

4.3 Discussion

Treatment of bacterial illnesses has become increasingly difficult as the number of antibiotic-resistant organisms increases, and the development of new antibiotics slows to record low numbers. In the last two years, both the CDC and World Health Organization (WHO) have issued recommendations for battling the issue of antibiotic resistance, which include preventing infections from occurring, improved tracking of resistant organisms, more conscientious use of current antibiotics, and the development of new antibiotic strategies [3, 5].

In this work, we have demonstrated the effective use of a Chol-binding peptide to inhibit the activity of a bacterial toxin, LtxA, a strategy that represents a novel antivirulence approach that has broad potential for the treatment of bacterial illnesses. We demonstrated that the $CRAC^{WT}$ peptide has a strong affinity for Chol and resides near the membrane surface, where it blocks toxin recognition of Chol to inhibit membrane binding and subsequent internalization and activity of the toxin. Importantly, the peptide exhibits no long-term toxicity to the cells.

In considering the use of this peptide to inhibit toxin activity, we considered two essential components: (1) localization at the membrane interface to reduce negative interactions with essential membrane components, which may lead to cytotoxicity and (2) strong binding energetics to outcompete binding by a toxin with a reported strong interaction with Chol [102]. A previous molecular dynamics study suggested that the $CRAC^{WT}$ peptide interacts with the membrane interface but not the core, and investigation of the amino acid sequence suggested that the peptide would reside in a location where it could interact with both aqueous solution and the membrane environment [182]. A snapshot from this molecular dynamics study displays the trajectories of $CRAC^{WT}$ interacting with PC/Chol membranes (Figure 4.11). In this figure the central tyrosine, shown in green, is seen to be interacting with Chol (magenta) within the membrane.

Previously, we have demonstrated that a peptide corresponding to the CRAC motif in LtxA is able to outcompete the binding of the toxin for Chol and inhibit activity, suggesting that the peptide itself has a strong affinity for Chol [17]. We therefore undertook this work to demonstrate that our hypotheses were correct and to establish the potential use of this peptide in the inhibition of Chol-binding by a range of pathogens.

To determine the membrane location of the $CRAC^{WT}$ peptide, we used Laurdan fluorescence to demonstrate that the peptide does not disrupt membrane packing, suggesting that the peptide sits near the interface of the membrane rather than deep in the hydrophobic core. In addition, we found that replacement of the hydroxyl group of Chol significantly decreases binding of the peptide, while substitutions to the B ring or hydrocarbon chains have smaller effects on binding, indicating that recognition of Chol by the peptide occurs near the membrane surface. These findings are consistent with previous findings regarding the CRAC motif found in the fusion protein, gp41, of HIV-1, LWYIK. A nearest neighbor recognition (NNR) study demonstrated that the peptide is sensitive to the packing of the bilayer, suggesting that the peptide must at least partially penetrate into the membrane [271]. However, a molecular simulation experiment of the same peptide, along with some derivatives, demonstrated that the peptides prefer the membrane interface over the membrane core and interact with the hydroxyl group of Chol electrostatically [172]. Magic-angle spinning nuclear magnetic resonance (MAS-NMR) demonstrated, in Chol-containing membranes, that the peptide interacts with the A ring of Chol, near the membrane interface as well [272].

Recognition of the hydroxyl group of Chol may be conserved among pathogens, as it would be the first structural element of Chol they encounter upon interaction with a host cell membrane. For example, although they do not use a CRAC motif to recognize Chol, the CDCs produced by Gram positive bacteria likewise require the presence of a sterol with an intact hydroxyl group; variation in this region completely inhibits activity of the toxins, while changes in the ring structure of the sterol reduce activity slightly, and changes to the hydrocarbon tail have no effect on toxin activity [150]. In the case of $CRAC^{WT}$ (Table

4.2), similar requirements can be found when compared to CDCs. $CRAC^{WT}$ also requires the presence of a hydroxyl group for binding. Changes to the ring structure result in slight reduction in affinity as well, but the key difference lie in the intact hydrocarbon tail and hydroxyl group of Chol. For $CRAC^{WT}$, changes to the hydrocarbon tail of Chol result in a reduced affinity for the sterol, which is not the case for CDCs as no effect is seen with that change.

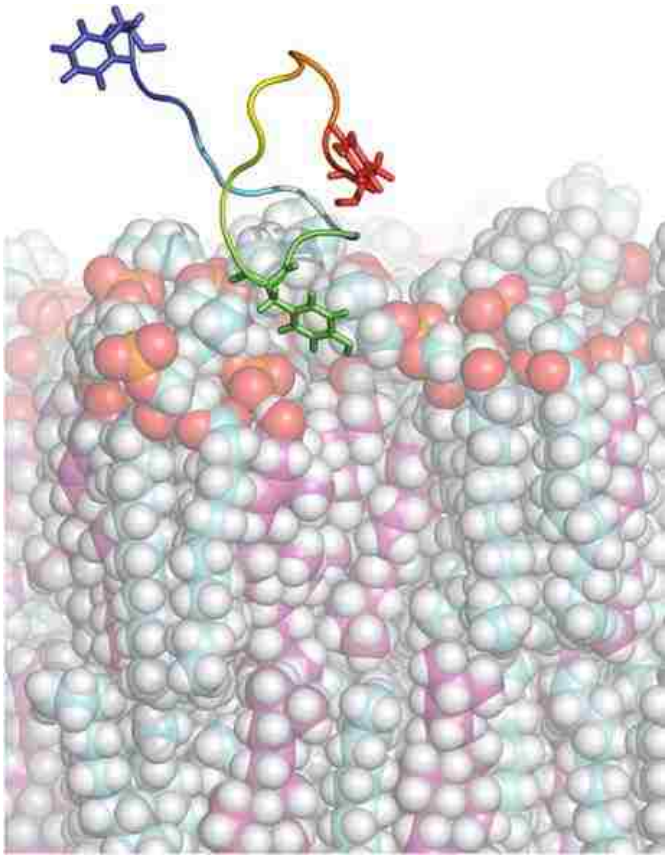

Figure 4.11 A Molecular Dynamics Snapshot of $CRAC^{WT}$ Interacting with a PC/Chol Membrane.
An interaction can be visualized between Tyr337 residue (green) and the membrane that is composed of PC carbons (cyan) and Chol (magenta) [182]. The Phenylalanine residue is show in blue and the terminal Tyr is shown in red.

In addition to localization at the membrane interface, we hypothesized that strong affinity for Chol would be required for the peptide to efficiently outcompete binding to Chol by pathogens with reported affinity for Chol. For this reason, we investigated the $CRAC^{WT}$ peptide of LtxA. Previously, it was shown that LtxA has a very strong affinity, on the order of 10^{-12} M, for liposomes containing 40% Chol [102]. Here, we have shown that much of the affinity of LtxA for Chol is driven by the CRAC motif, as the peptide alone has a comparable affinity for Chol as the full-length protein. The affinity of the $CRAC^{WT}$ peptide is several orders of magnitude stronger than reported affinities of PLO (4×10^{-7} M), Cdt produced by *A. actinomycetemcomitans* (2×10^{-6}) , α-hemolysin (HlyA) produced by *Escherichia coli* (1.6×10^{-5}) , and the invasion plasmid antigen B (ipaB) produced by *Shigella flexneri* (1.8×10^{-5}), suggesting that the peptide may be able to outcompete binding of these and other pathogenic proteins [273-276].

Because many pathogens recognize Chol in their activity against host cells, we investigated the ability of a peptide to inhibit protein toxicity by binding to Chol at the membrane surface. We predicted that a CRAC peptide that binds Chol at the membrane surface would be able to block the pathogen's recognition of Chol. Our results here represent proof-of-concept of this idea and we expect that this peptide will have broad applications for the treatment of viral and bacterial diseases, as there are currently no viable approaches to inhibit this interaction. Previously proposed strategies include cyclodextrins, which have a strong affinity for Chol and are able to extract the sterol from the membrane [277]. This molecule has been shown to extract Chol from HIV-1 and SIV-1 virions, resulting in decreased infectivity and was therefore proposed as a possible topical microbicide [278]. In addition, β-cyclodextrins have been proposed for the treatment of

intracellular Leishmania infections; however, due to cyclodextrins' alteration of cell processes and viability, this therapeutic use is limited [235]. Here, we have demonstrated that the $CRAC^{WT}$ peptide, perhaps because its interaction with Chol occurs only near the membrane interface, does not induce cytotoxicity in host cells (Figure 4.10). The ability of the $CRAC^{WT}$ peptide to inhibit toxin activity by blocking its interaction with Chol in the host cell plasma membrane is a novel concept that has wide-ranging applications in bacterial and viral pathogenesis.

Chapter 5

Role of Peptide Net Charge on the Affinity of a Cholesterol Recognition Amino Acid Consensus Peptide for Membrane Cholesterol

5.1 Introduction

A major problem that we face in creating a potential therapeutic utilizing a CRAC domain is that the CRAC definition is not well defined. It over predicts Chol binding, making this domain difficult to study [102, 148, 151]. In the present work, we look to improve the binding of $CRAC^{WT}$ to the membrane and refine the current CRAC definition. We hypothesize that by decreasing the net charge of the $CRAC^{WT}$ peptide we would increase peptide partitioning into the hydrophobic membrane thus increasing affinity, while increasing the net charge would lead to an opposite effect.

To investigate the effect of net charge on a CRAC peptide's affinity for membrane Chol, we engineered four peptides, derived from our wild-type $CRAC^{WT}$ peptide, with a varying degree of net charge. Net charges were altered by substituting Lys and/or Arg for a glutamate (Glu), or a Glu for a Lys (Table 5.1). To determine the effect of these substitutions we measured the peptide's affinities for Chol as well as their ability inhibit our model protein toxin's (LtxA) cytotoxicity to leukocytes utilizing LSPR and cell-based

assays respectively. We found that changes to the net charge of $CRAC^{WT}$ led to a decrease in the peptide's affinity for Chol and its ability to inhibit LtxA activity.

5.2 Results

5.2.1 Peptide Design

Peptides used in this study were derived from the CRAC domain of LtxA, including residues that surround the domain. As shown in Table 5.1, $CRAC^{WT}$, is the CRAC domain including surrounding residues and is composed of LtxA residues 328-346 (Figure 1.3). $CRAC^{-1D}$, $CRAC^{-1F}$, $CRAC^{-7}$, and $CRAC^{+7}$ are peptides that contained the same residues as $CRAC^{WT}$ but have had certain residues substituted. The residues that have been substituted are depicted in red as shown in Table 5.1. The superscript of these four peptides denotes their overall net charge.

Two classes of peptides were synthesized for this study, polyelectrolytes and polyampholytes as shown in Figure 5.1. Polyelectrolytes which are classified as peptides composed by mostly positive or negatively charged residues, indicated by the orange or blue regions respectively (Figure 5.1), include peptides $CRAC^{+7}$ and $CRAC^{-7}$. Polyampholytes contain both positively and negatively charged residues, as indicated by the green region in Figure 5.1. This group of peptides include $CRAC^{-1F}$, $CRAC^{-1D}$, and $CRAC^{WT}$.

5.2.2 Highly charged peptides favor a hydrophilic environment

To determine the tendency of each peptide to partition into a hydrophobic environment versus a hydrophilic environment we performed an octanol-water experiment to measure each peptide's octanol-water coefficient (log K_{ow}). $CRAC^{-7}$ and $CRAC^{+7}$, classified as polyelectrolytes, have the highest overall net charge (Figure 5.1), and

displayed the greatest partitioning into the hydrophilic environment, as indicated by the lowest log K_{ow} coefficient (Figure 5.3). $CRAC^{-1D}$ and $CRAC^{-1F}$, which are classified as polyampholytes, and have the lowest overall net charge (Figure 5.1), displayed the greatest partitioning into the hydrophobic environment, as indicated by the highest log K_{ow} coefficients (Figure 5.3). $CRAC^{WT}$, also a polyelectrolyte, displayed a log K_{ow} between $CRAC^{-7}$/$CRAC^{+7}$ and $CRAC^{-1D}$/$CRAC^{-1F}$ which correlates with it having a net charge between the two groups of peptides mentioned.

Table 5.1 Peptide Sequences of Peptide mutants
Residues underlined refer to the CRAC domain. Residues highlighted in red and bolded are the residues we mutated from $CRAC^{WT}$ peptide. Each peptide was acetylated at the N-terminus and amidated at the C-terminus.

Peptide	**Sequence**
$CRAC^{WT}$	FDRARML<u>LEEYSKRFKK</u>FGY
$CRAC^{-1D}$	FDRARML<u>LEEYS</u>**E**<u>RF</u>**E**<u>K</u>FGY
$CRAC^{-1F}$	FD**E**A**E**M<u>LEEYSKRFKK</u>FGY
$CRAC^{-7}$	FD**E**A**E**M<u>LEEYS</u>**EE**<u>F</u>**E**<u>K</u>FGY
$CRAC^{+7}$	FDRARML<u>**KK**YSKRFKK</u>FGY

5.2.3 Highly charged peptides have a reduced affinity for the membrane

To determine the affinity of each peptide for membranes composed of 100% POPC and membranes composed of 60% POPC/40% Chol we performed an LSPR experiment, as shown in Table 5.2 and Table 5.3 respectively. $CRAC^{-1D}$ and $CRAC^{-1F}$, which are classified as polyampholytes along with $CRAC^{WT}$ (Figure 5.1) have affinities (K_D (M)) for Chol-containing membranes that were measured to be 6.84 x 10^{-7} M and 3.37 x 10^{-7} M

respectively (Table 5.3), which are comparable to $CRAC^{WT}$. $CRAC^{-7}$ and $CRAC^{+7}$, which are polyelectrolytes (Figure 5.1), with K_D values of 1.21 x 10^{-4} M and 1.47 x 10^{-6} M, respectively, have a weaker affinity for Chol compared to $CRAC^{WT}$, $CRAC^{-1D}$ and $CRAC^{-1F}$ (Table 5.3), but this difference is not statistically significant. $CRAC^{+7}$ though having a weaker affinity for Chol compared to $CRAC^{WT}$, $CRAC^{-1D}$ and $CRAC^{-1F}$, has an affinity for Chol that is one hundred times stronger than that of $CRAC^{-7}$. Zeta potential measurements performed on 100% POPC and 60% POPC/40% Chol liposomes, suggest that the increased affinity of $CRAC^{+7}$ to Chol containing membranes arises from electrostatic interactions. Introducing Chol into liposomes decreases the liposomes' zeta potential, shifting it from an overall positive charge to an overall negative charge (Figure 5.2), thus leading to a more favorable interaction between the negatively charged liposome surface and the positively charged peptide. We hypothesize that this peptide may associate with the surface of the liposome through this electrostatic interaction without necessarily interacting with membrane cholesterol.

5.2.4 Structural changes do not correlate with increased membrane affinity

CD spectroscopy measurements for the peptides were performed in solution, with liposomes composed of 100% POPC, and with liposomes composed of 60% POPC/40% Chol and are shown in Figure 5.4, Figure 5.5, and Figure 5.6. Furthermore, CD spectra of each peptide in each environment were consolidated and are shown in Figure 5.7.

$CRAC^{WT}$ exhibits typical α-helical characteristics in solution and in 100% POPC membranes, with a maximum at 195 nm and a double minima at 208 nm and 222 nm [279]. In 60% POPC/40% Chol membranes the minima and maximum of $CRAC^{WT}$ increase, suggesting a decrease of α-helical structure that we have shown previously [19]. Changes

to the spectrum of CRAC^{-1F} suggests it transitions from an unordered state in solution to a state with increased α-helical structure, containing a double minima at 208 nm and 222 nm.

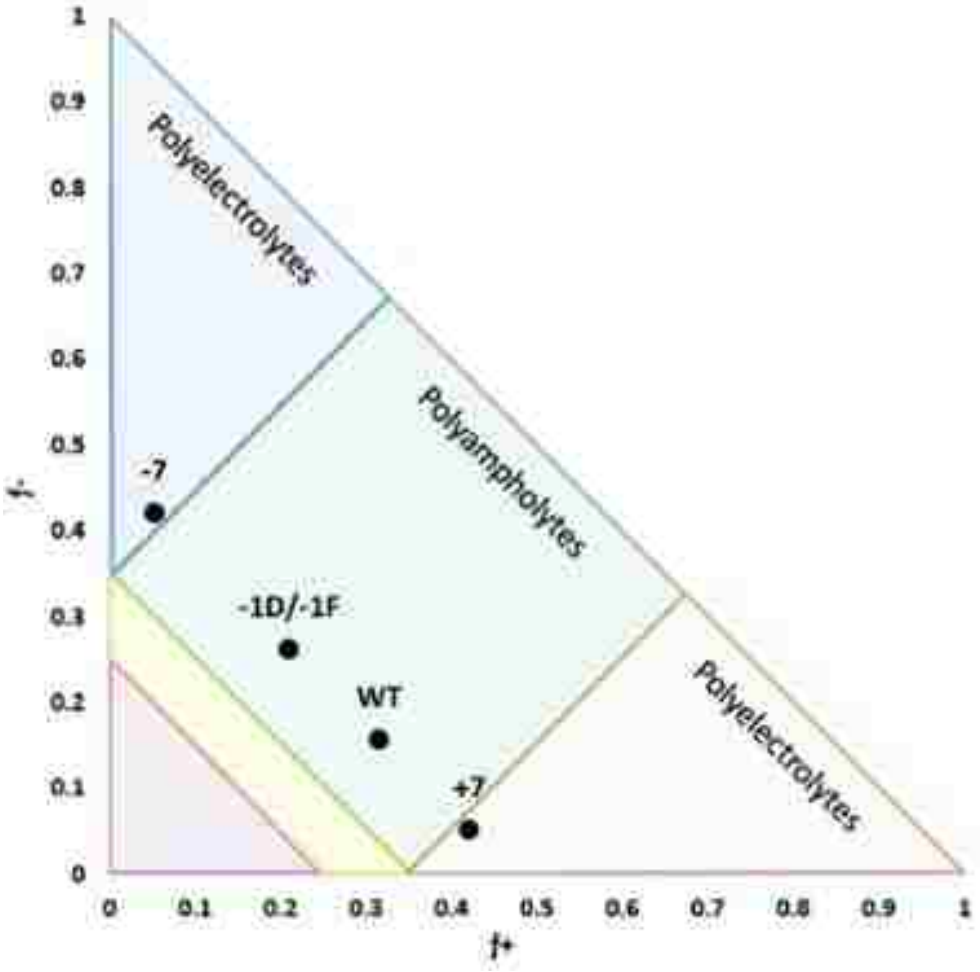

Figure 5.1 Peptide Charge Distribution.
Polyelectrolytes are classified as peptides that are composed by mostly positive or negatively charged residues, indicated by the orange or blue regions respectively. These groups include CRAC^{+7} and CRAC^{-7}. Polyampholytes contain both positively and negatively charged residues, indicated by the green region. This group includes CRAC^{-1F}, CRAC^{-1D}, and CRAC^{WT} [280].

In the case of $CRAC^{WT}$ and $CRAC^{-1F}$ conformational changes are correlated with an increase in affinity for Chol-containing membranes as seen in Table 5.3. On the other hand, $CRAC^{-1D}$ undergoes minimal conformational changes while transitioning from an environment of 100% POPC liposomes to an environment containing 60% POPC/40% Chol liposomes (Figure 5.7) but exhibits a stronger affinity for 60% POPC/40% Chol liposomes versus 100% POPC liposomes (Table 5.3 and Table 5.2 respectively). This suggests that affinity for Chol is not necessarily correlated with conformational changes with the peptide.

For the peptides $CRAC^{-7}$ and $CRAC^{+7}$, the MRE data (Figure 5.4, Figure 5.5, Figure 5.6, and Figure 5.7) suggests that they occupy a random coil structure in each condition with the most noticeable differences occurring when each peptide is interacting with 60% POPC/40% Chol membranes. The maximum at 195 nm for $CRAC^{+7}$ is more positive than $CRAC^{-7}$, suggesting a more pronounced α-helical structure for $CRAC^{+7}$.

5.2.5 CRAC mutants display decreased ability to inhibit LtxA internalization and cytotoxicity

To measure the ability of each CRAC mutant to inhibit LtxA binding to Chol-containing GUV membranes, we used confocal microscopy to visualize the differences in the association of AF555-LtxA to NBD-labeled GUVs. We found that $CRAC^{-1D}$ and $CRAC^{-1F}$, which have reduced affinities to Chol as $CRAC^{WT}$, were the only peptides that could prevent a majority of LtxA from binding to GUVs, as indicated by the reduced red intensity associated with the GUVs compared to the control (Figure 5.9). The moderate amount of binding affinity displayed by $CRAC^{+7}$ for Chol, which Figure 5.2 suggests to be a result of electrostatic interactions, had no significant effect on inhibiting LtxA binding

and internalization as indicated by the colocalized toxin (red) and membrane (green) in Figure 5.9. This finding is consistent with our hypothesis that this peptide associates with the membrane through electrostatic interactions but does not fully interact with cholesterol. Furthermore, $CRAC^{-7}$ displayed the weakest affinity for Chol and was unable to prevent LtxA binding and internalization.

To determine if inhibition of LtxA binding to Chol by the peptides could prevent toxin internalization in cells, we performed a confocal experiment, in which THP-1 cells were pretreated with each peptide for 30 min before the mixture was incubated with AF555-LtxA, as shown in Figure 5.9. $CRAC^{-1D}$ and $CRAC^{-1F}$ were able to inhibit LtxA internalization, as indicated by the very low number of red pixels inside of the cells. Peptides $CRAC^{-7}$ and $CRAC^{+7}$ failed to prevent LtxA internalization, as indicated by the large number of red pixels present within the THP-1 cells that they were incubated with (Figure 5.9). The ability of these peptides to inhibit LtxA binding to Chol in GUVs correlates with their ability to inhibit LtxA activity in THP-1 cells.

Table 5.2 Affinity of Peptides for 100% POPC Liposomes Measured by LSPR

Reaction	**K_D (M)**
$CRAC^{WT}$ binding to POPC	$2.38 \times 10^{-5} \pm 2.04 \times 10^{-6}$
$CRAC^{-1D}$ binding to POPC	$3.17 \times 10^{-5} \pm 5.36 \times 10^{-6}$
$CRAC^{-1F}$ binding to POPC	$1.05 \times 10^{-5} \pm 2.46 \times 10^{-6}$
$CRAC^{-7}$ binding to POPC	$1.66 \times 10^{-5} \pm 2.54 \times 10^{-5}$
$CRAC^{+7}$ binding to POPC	$5.32 \times 10^{-5} \pm 5.41 \times 10^{-6}$

Table 5.3 Affinity of Peptides for 60% POPC and 40% Chol Liposomes Measured by LSPR

Reaction	**K_D (M)**
$CRAC^{WT}$ binding to Chol	$9.12 \times 10^{-8} \pm 4.87 \times 10^{-10}$
$CRAC^{-1D}$ binding to Chol	$6.84 \times 10^{-7} \pm 7.30 \times 10^{-9}$
$CRAC^{-1F}$ binding to Chol	$3.37 \times 10^{-7} \pm 9.73 \times 10^{-8}$
$CRAC^{-7}$ binding to Chol	$1.21 \times 10^{-4} \pm 5.43 \times 10^{-4}$
$CRAC^{+7}$ binding to Chol	$1.47 \times 10^{-6} \pm 1.48 \times 10^{-5}$

5.2.6 *Efficacy of peptide mutants to inhibit LtxA cytotoxicity correlates with their affinity for membrane Chol*

To determine if peptide-mediated inhibition of LtxA internalization by $CRAC^{-1D}$ and $CRAC^{-1F}$ resulted in reduced LtxA cytotoxicity, we performed a cell cytotoxicity assay that measured cell viability in each of these cases. As shown in Figure 5.10, our results indicate that $CRAC^{-1D}$ and $CRAC^{-1F}$ inhibit LtxA cytotoxicity, but $CRAC^{-7}$ and $CRAC^{+7}$ do not. Inhibition of LtxA toxicity by $CRAC^{-1D}$ and $CRAC^{-1F}$ are slightly less effective than inhibition by $CRAC^{WT}$, although this is not a statistically significant difference (data not shown). Cell viability measurements correlate with the ability of these peptides to inhibit LtxA binding and internalization as shown in Figure 5.8 and Figure 5.9.

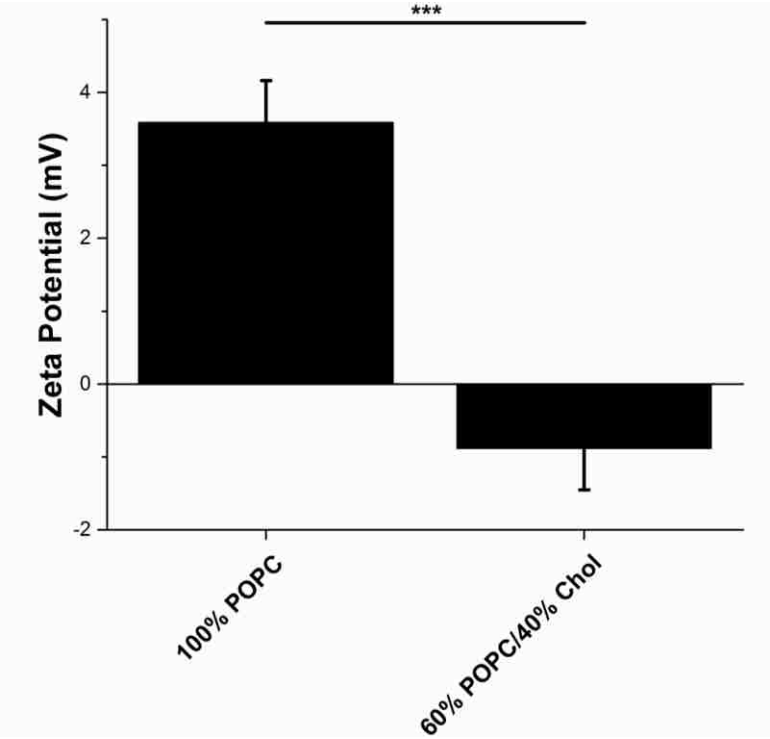

Figure 5.2 Zeta Potential Measurements of Lipid Bilayers with and without Chol. Zeta potential was measured for liposomes composed of 100% POPC or 60% POPC/40% Chol. As liposome Chol content increases, the zeta potential decreases suggesting the ions bound to the membrane also decrease. A two-sample t-test was used to determine the level of significance between each experiment. ***$P \leq 0.001$.

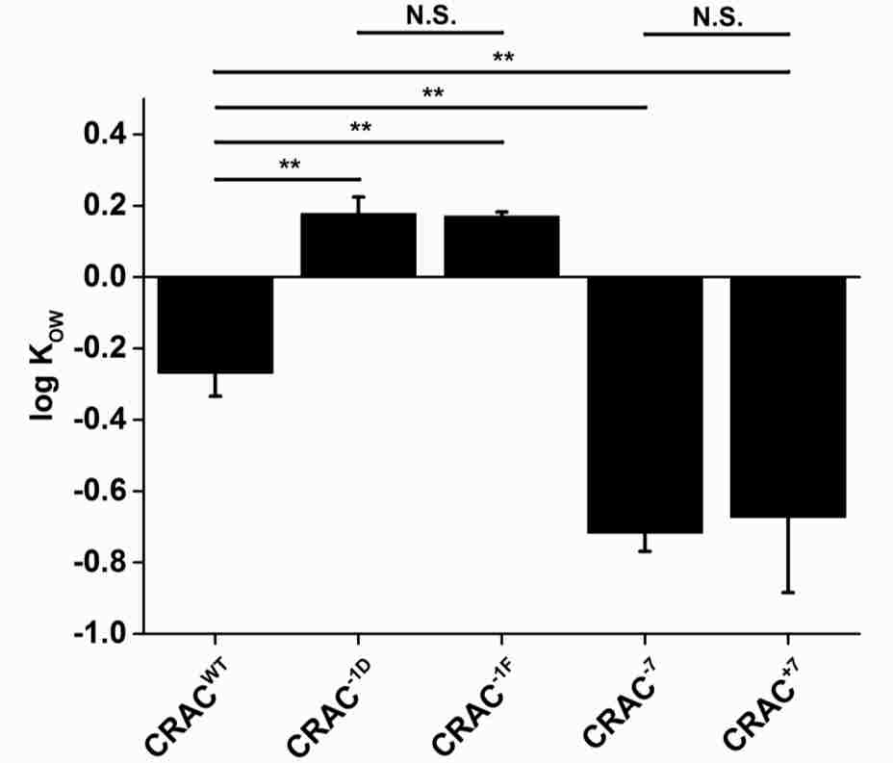

Figure 5.3 Octanol-Water Coefficients (log K_{ow}) of the peptides.
Octanol-water partition coefficients for each peptide were determined using the shake-flask method. $CRAC^{-7}$ and $CRAC^{+7}$ have the highest overall net charge and greatest partitioning into the hydrophilic environment, as indicated by the lowest log K_{ow} coefficient. $CRAC^{-1D}$ and $CRAC^{-1F}$ have the lowest overall net charge and displayed the greatest partitioning into the hydrophobic environment, as indicated by the highest log K_{ow} coefficients. $CRAC^{WT}$ displayed a log K_{ow} between $CRAC^{-7}$/$CRAC^{+7}$ and $CRAC^{-1D}$/$CRAC^{-1F}$. A one-way analysis of variance followed by a Tukey test was used to determine the level of significance between each experiment. **$P \leq 0.01$; N.S., not significant.

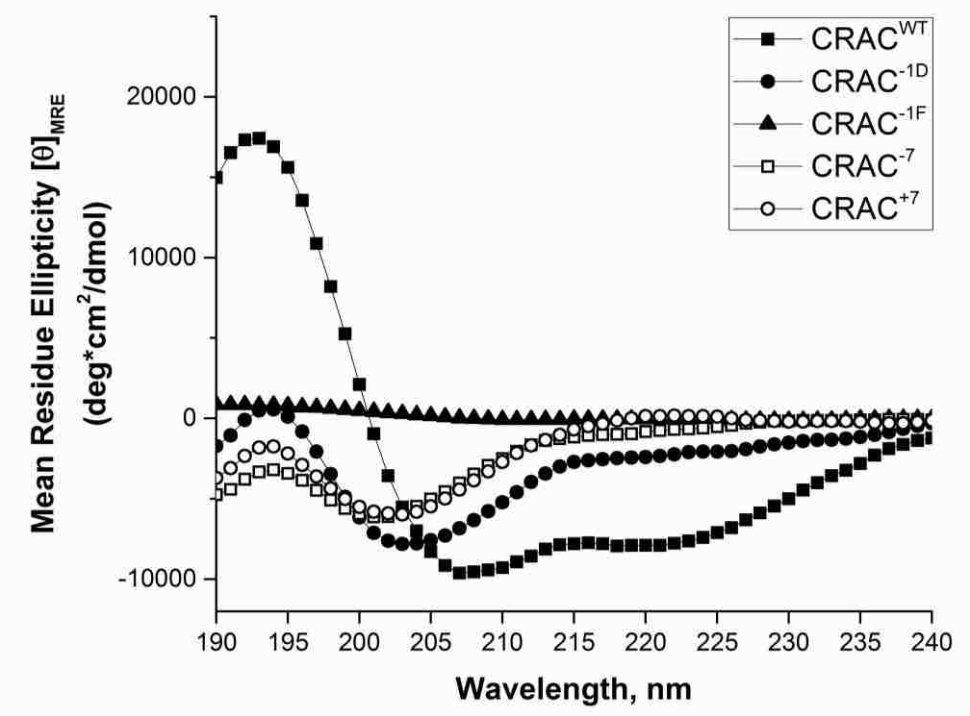

Figure 5.4 MRE CD Spectroscopy Data of Peptide Mutants in Solution.
Spectral scans were performed in 10 mM phosphate buffer, using a peptide concentration of 0.25 mg/mL. To ensure that the spectra represent the structure of only bound peptide, unbound peptide was removed using centrifugal filters. MRE was calculated for each spectrum. Filled in squares depict spectrum of $CRAC^{WT}$ in solution. Filled in circles depict spectrum of $CRAC^{-1D}$ in solution. Filled in triangles depict spectrum of $CRAC^{-1F}$ in solution. Open squares depict spectrum of $CRAC^{-7}$ in solution. Open circles depict spectrum of $CRAC^{+7}$ in solution.

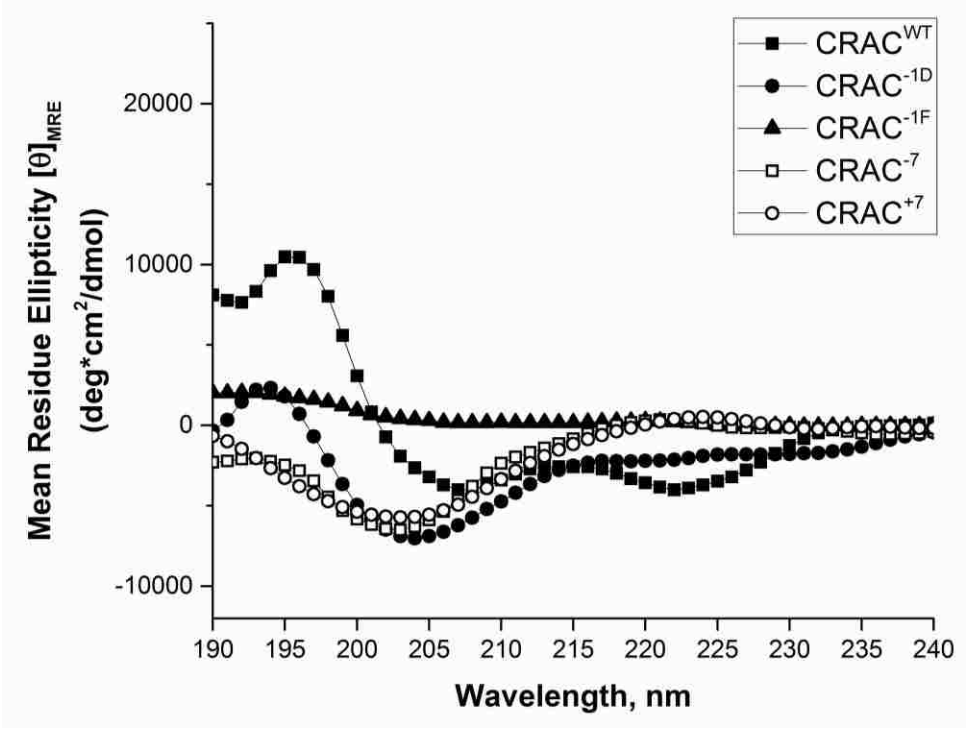

Figure 5.5 MRE CD Spectroscopy Data for Peptides Binding to 100% POPC Liposomes. Spectral scans were performed in 10 mM phosphate buffer, using a peptide concentration of 0.25 mg/mL. To ensure that the spectra represent the structure of only bound peptide, unbound peptide was removed using centrifugal filters. MRE was calculated for each spectrum. Filled in squares depict spectrum of $CRAC^{WT}$ in 100% POPC. Filled in circles depict spectrum of $CRAC^{-1D}$ in 100% POPC. Filled in triangles depict spectrum of $CRAC^{-1F}$ in 100% POPC. Open squares depict spectrum of $CRAC^{-7}$ in 100% POPC. Open circles depict spectrum of $CRAC^{+7}$ in 100% POPC.

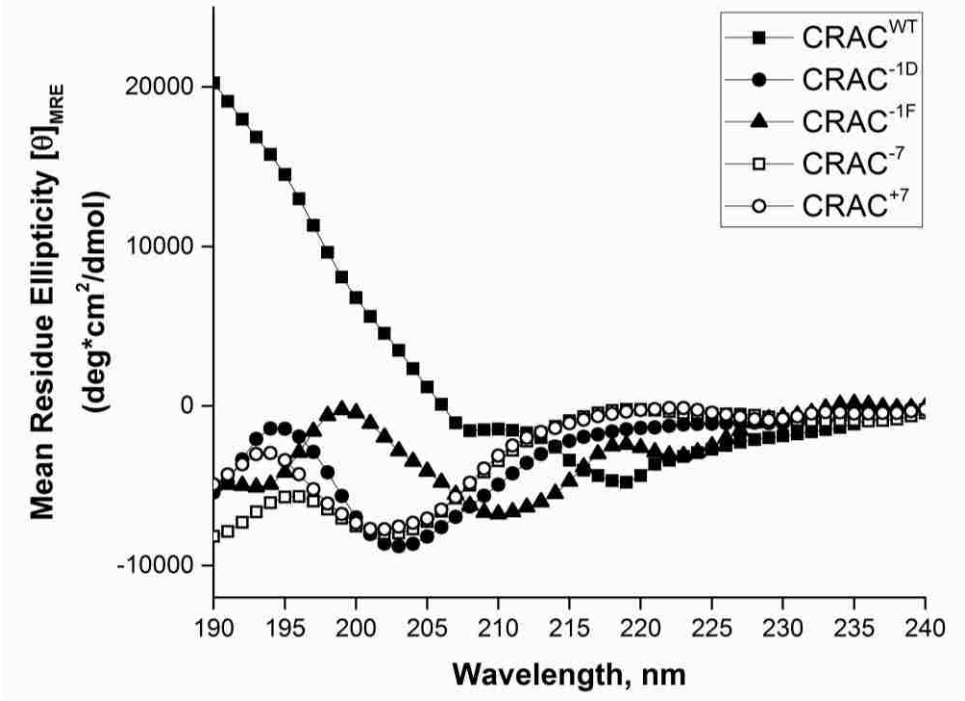

Figure 5.6 MRE CD Spectroscopy Data for Peptides Binding to 60% POPC/40% Chol Liposomes.

Spectral scans were performed in 10 mM phosphate buffer, using a peptide concentration of 0.25 mg/mL. To ensure that the spectra represent the structure of only bound peptide, unbound peptide was removed using centrifugal filters. MRE was calculated for each spectrum. Filled in squares depict spectrum of $CRAC^{WT}$ in 60% POPC/40% Chol. Filled in circles depict spectrum of $CRAC^{-1D}$ in 100% POPC. Filled in triangles depict spectrum of $CRAC^{-1F}$ in 60% POPC/40% Chol. Open squares depict spectrum of $CRAC^{-7}$ in 60% POPC/40% Chol. Open circles depict spectrum of $CRAC^{+7}$ in 60% POPC/40% Chol.

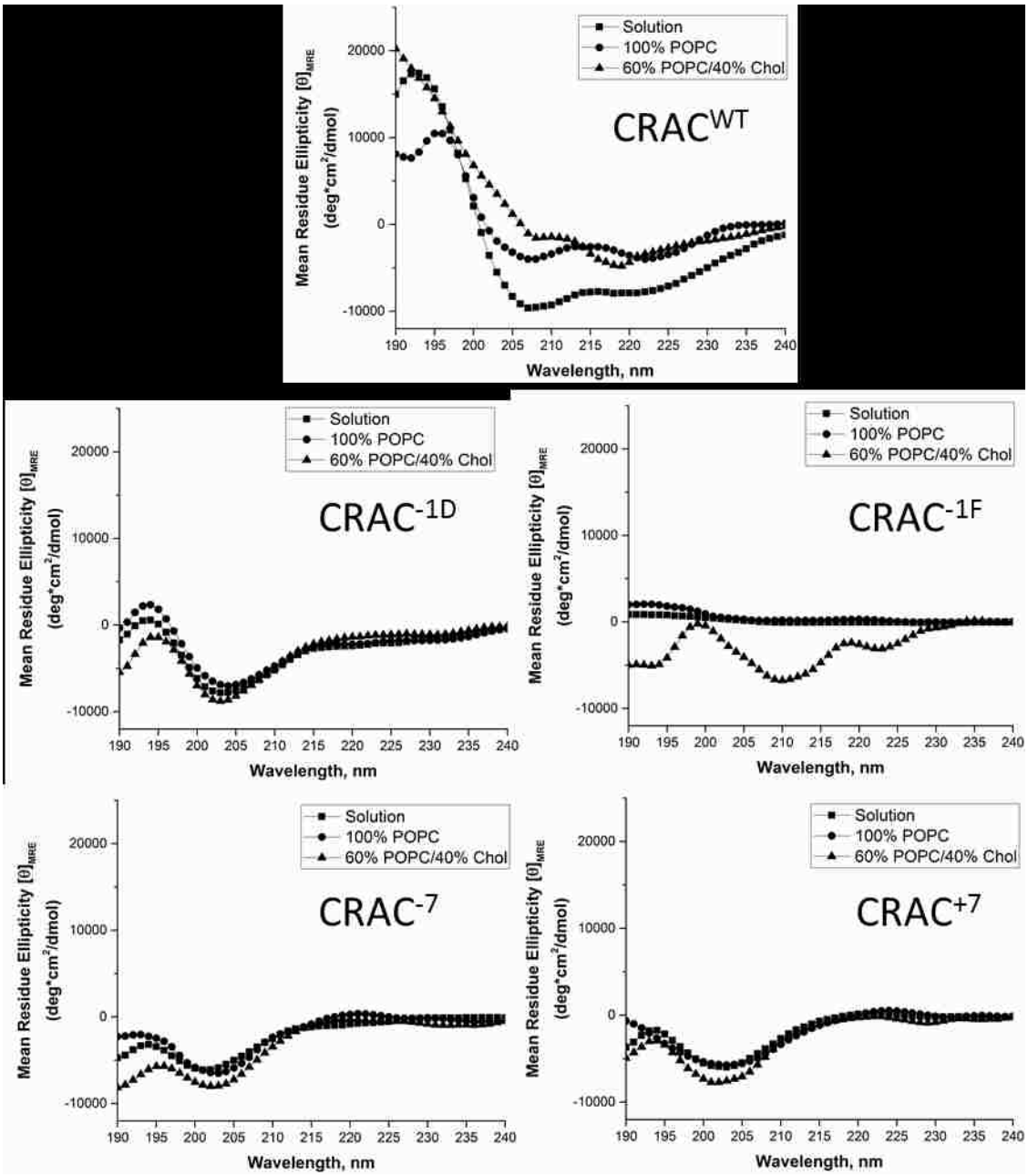

Figure 5.7 MRE CD Spectroscopy Data for Each Peptide in Each Environment. Spectral scans were performed in 10 mM phosphate buffer, using a peptide concentration of 0.25 mg/mL. To ensure that the spectra represent the structure of only bound peptide, unbound peptide was removed using centrifugal filters. MRE was calculated for each spectrum. Filled in squares depict spectrum of each peptide in solution. Filled in circles depict spectrum of each peptide in solution in 100% POPC. Filled in triangles depict spectrum of each peptide in 60% POPC/40% Chol.

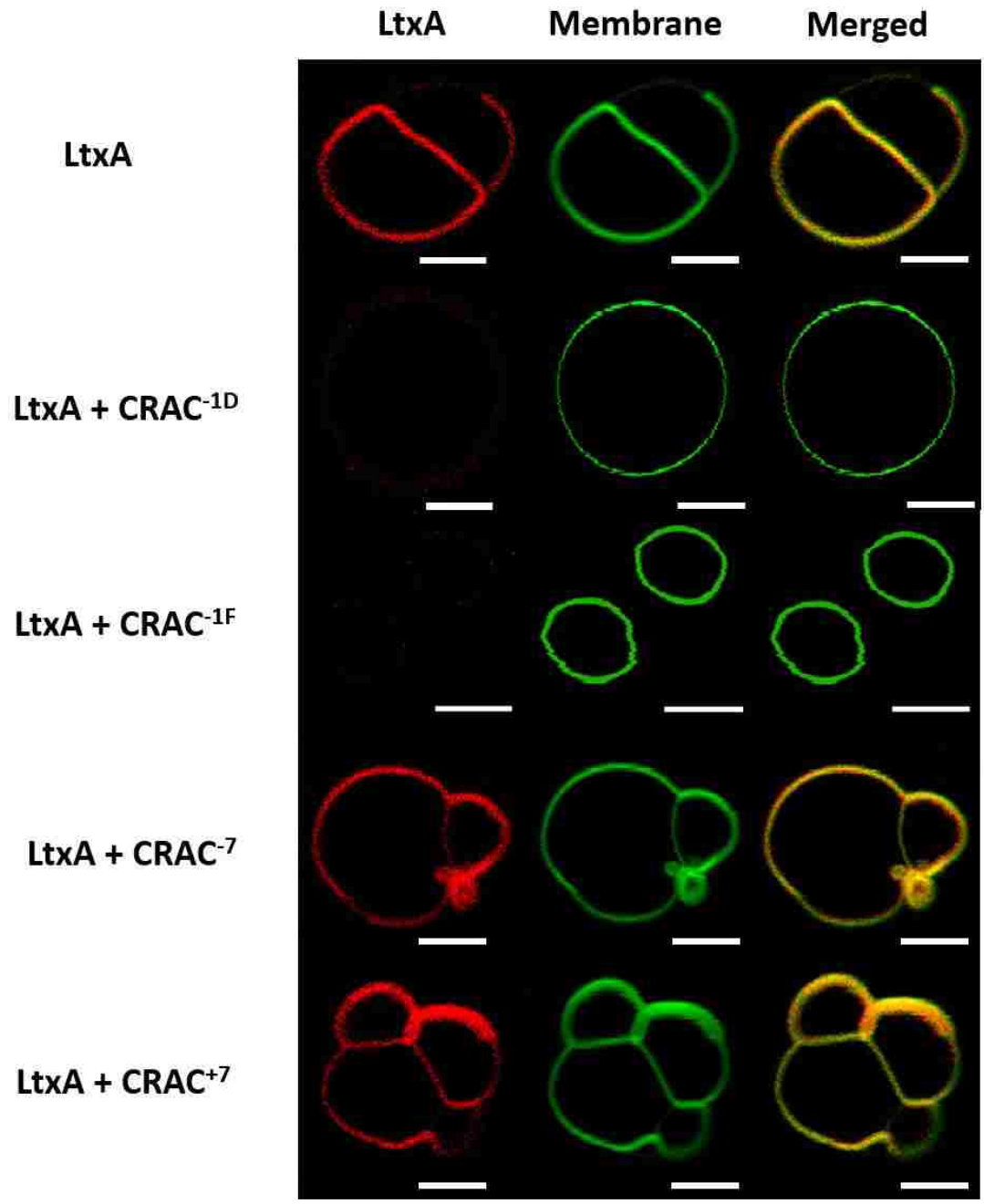

Figure 5.8 Peptide-mediated inhibition of LtxA binding to Chol in GUVs.
GUVs were composed of 66% POPC/33% Chol/1% NBD-PE (green). In the absence of peptide, AF555-LtxA (red) bound to the membranes. In the presence of $CRAC^{-1D}$ and $CRAC^{-1F}$, at a peptide:toxin ratio of 100:1, LtxA was inhibited from binding to the membrane. In the presence of $CRAC^{-7}$ and $CRAC^{+7}$, at a peptide:toxin ratio of 100:1, LtxA was able to bind to the GUV membrane. The scale bar in the bottom right corner of each micrograph represents 10 µm.

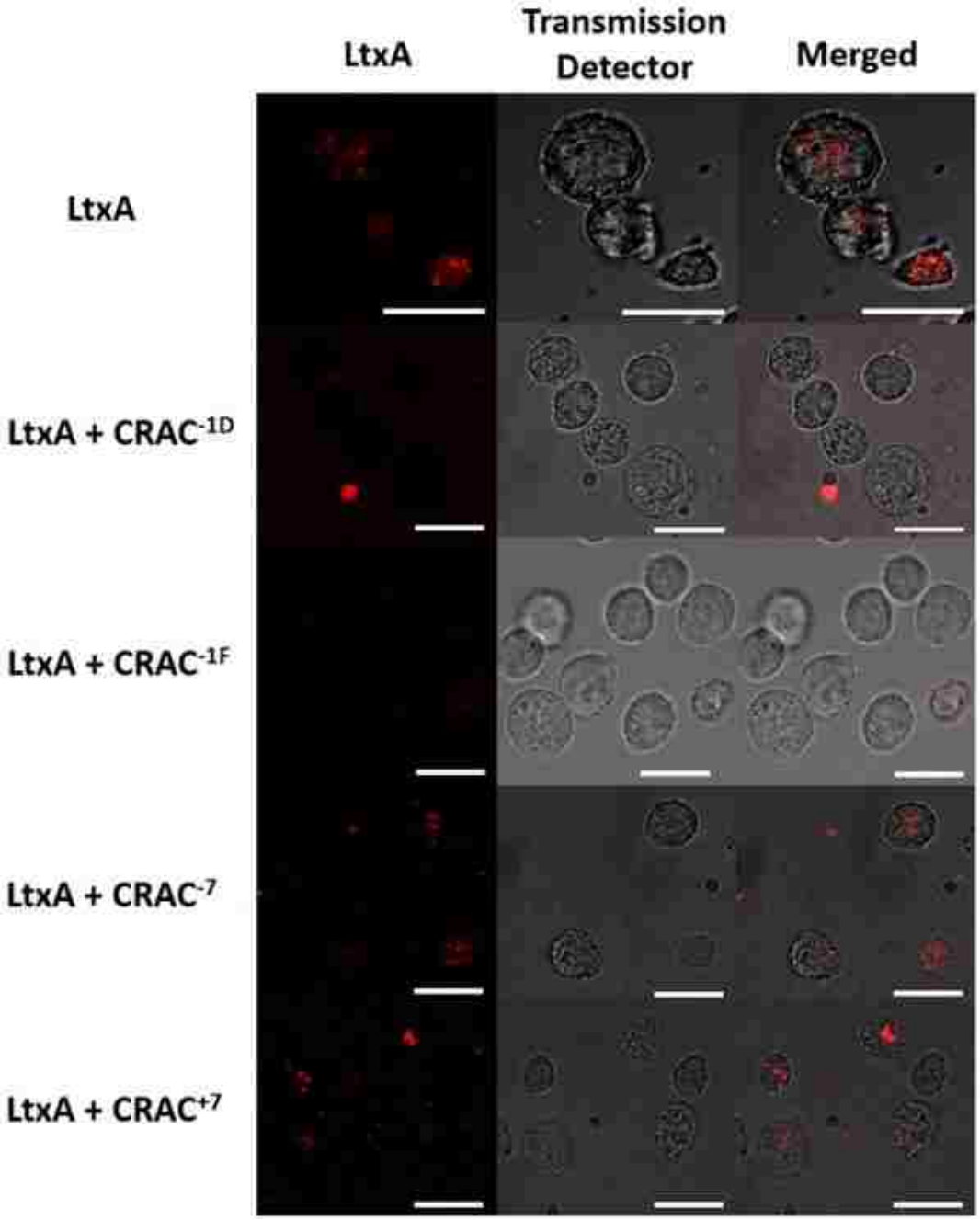

Figure 5.9 Peptide-mediated inhibition of LtxA internalization in THP-1 cells. In the absence of peptide, AF555-LtxA (red) is located within THP-1 cells. When the cells were preincubated with $CRAC^{-1D}$ and $CRAC^{-1F}$ for 30 min at a peptide:toxin ratio of 100:1, AF555-LtxA was unable to be internalized by the cells. Preincubation of the cells with $CRAC^{-7}$ and $CRAC^{+7}$ for 30 min at a peptide:toxin ratio of 100:1 did not inhibit AF555-LtxA internalization. The scale bar in the bottom right corner of each micrograph represents 10 μm.

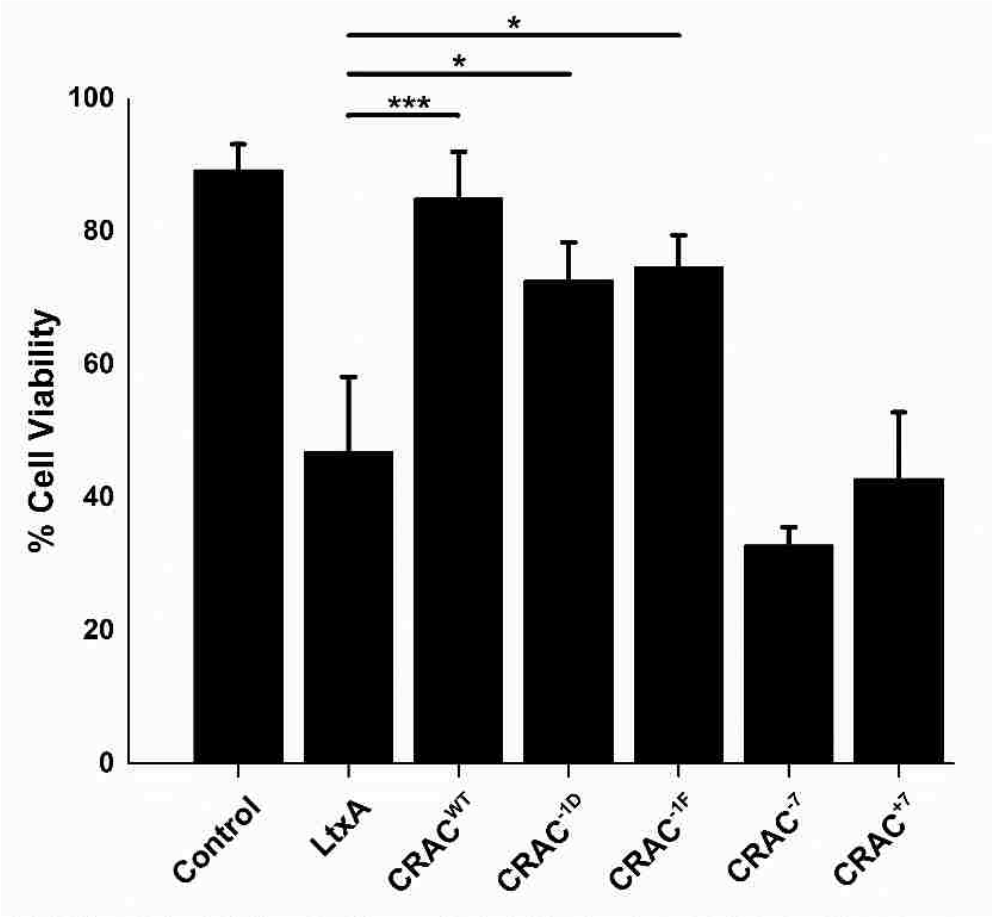

Figure 5.10 Effect of Mutant Peptides Inhibiting LtxA Cytotoxicity.
LtxA and either $CRAC^{WT}$, $CRAC^{-1D}$, $CRAC^{-1F}$, $CRAC^{-7}$, or $CRAC^{+7}$were incubated with THP-1 cells for 3 hr, and the viability of the cells was measured using a trypan blue assay. The $CRAC^{WT}$, $CRAC^{-1D}$, and $CRAC^{-1F}$ peptide, which bind to Chol, significantly inhibited the toxicity of LtxA. The $CRAC^{-7}$and $CRAC^{+7}$ peptide, which do not bind to Chol, did not inhibit LtxA toxicity. A one-way analysis of variance followed by a Tukey test was used to determine the level of significance between each experiment. ***$P \leq 0.001$; *$P \leq 0.05$; N.S., not significant.

5.3 Discussion

A key issue with designing peptides that include CRAC domains is that the CRAC domain over predicts Chol binding, and a peptide which is designed to contain it may not display an affinity for Chol [102, 148, 151]. We undertook this work to improve upon the binding of $CRAC^{WT}$ to the membrane and refine the current CRAC definition.

The interaction of peptides with lipid bilayers involves both electrostatic and hydrophobic forces [281]. We hypothesized that by decreasing the net charge of $CRAC^{WT}$ we would increase peptide partitioning by increasing its propensity to bury into the hydrophobic membrane. To accomplish this, we engineered four peptides, derived from our $CRAC^{WT}$ peptide, with a varying degree of net charge.

The four engineered variants of the $CRAC^{WT}$ peptide were $CRAC^{-1D}$, $CRAC^{-1F}$, $CRAC^{-7}$, and $CRAC^{+7}$. The net charges were altered by substituting Lys and/or Arg for a Glu, or a Glu for a Lys as shown in Table 5.1. To determine the effect of these substitutions, we measured their affinities for Chol as well as their ability inhibit LtxA-mediated cytotoxicity in leukocytes. We found that changes to the net charge of $CRAC^{WT}$ affected the peptide's affinity for Chol and its ability to inhibit LtxA activity.

To understand how each mutant's lipophilicity compared to that of our wild-type peptide, we performed a series of octanol-water partition measurements [282, 283]. The octanol-water coefficient (log K_{ow}) measurements for $CRAC^{-1D}$ and $CRAC^{-1F}$, both with values greater than $CRAC^{WT}$, suggested they would have an increased partitioning into the hydrophobic membrane over the wild-type peptide thus leading to a greater affinity for Chol-containing model membranes. Affinity measurements though, contradict this hypothesis, as the affinities of $CRAC^{-1D}$ and $CRAC^{-1F}$ for Chol were both one order of magnitude weaker than that of $CRAC^{WT}$. It has been found that amphiphilic peptides with reduced helical structures in solution have a lower propensity to bind to minimally charged zwitterionic membranes such as the ones used in this study [281]. This finding is supported by our CD spectroscopy and LSPR results. Peptides $CRAC^{-1D}$, $CRAC^{-1F}$, $CRAC^{-7}$, and $CRAC^{+7}$ have reduced secondary structures in solution compared to $CRAC^{WT}$ in solution

and additionally these peptides have reduced affinities (Table 5.3) for the minimally charged 60% POPC/40% Chol liposomes (Figure 5.2).

On the other end of the spectrum, $CRAC^{-7}$ and $CRAC^{+7}$ displayed a lower octanol-water coefficient than $CRAC^{WT}$, which would suggest that they prefer to be in the hydrophilic environment more so than the wild-type peptide. Our affinity measurements (Table 5.3) show this is the case for $CRAC^{-7}$, but $CRAC^{+7}$ displayed an affinity two orders of magnitude greater than $CRAC^{-7}$. A follow up zeta-potential measurement demonstrates that Chol decreases the surface charge of the membrane, leading to a more favorable binding environment for the positively charged $CRAC^{+7}$. Although there is an increase in binding, $CRAC^{+7}$ fails to inhibit LtxA cytotoxicity, suggesting that when $CRAC^{+7}$ interacts with the membrane, it does not specifically interact with Chol over POPC molecules.

The low correlation between log K_{ow} values and affinity suggest that the amino acid residues have a larger impact on the ability of the peptide to bind to Chol-containing membranes than we previously thought. Studies have found the arrangement of amino acids and certain substitutions can lead to significant effects on the biological properties of peptides; our findings suggest that this could be the reason an increase in membrane affinity was absent in the mutant peptides with a reduced net charge [172, 284].

Our findings also suggest that substitutions to the (X_{1-5}) residues within the CRAC domain and residues that flank the CRAC domain (demonstrated with $CRAC^{-1D}$ and $CRAC^{-1F}$) influence the peptide's ability to bind to Chol-containing membranes. The influence of these substitutions is unsurprising as Lys, Arg, and Glu can facilitate significant interactions with membrane lipids. Studies have shown that Arg and Lys can form hydrogen bonds to the carbonyl and phosphate groups of lipids because of their

positive charge [184, 186]. Furthermore, a distinctive trait of charged amino acids is that they can snorkel (become incorporated within a lipid membrane and have their charged side chains remain at the water-membrane interface) and use their hydrogen bonding groups to attract water molecules and/or lipid headgroups [185, 285]. Arg has been shown to snorkel less efficiently than Lys due to its extra NH_3 group, allowing it to attract more water into the membrane, increasing its ability to bind interfacially and perturb the membrane [184, 286]. On the opposite end of the spectrum, the acidic residues Glu and aspartate (Asp) require hydrogen bond donors, leading to more favorable interactions with the choline groups of phospholipids and water molecules at the water-membrane interface [184, 186]. These findings correlate with the snapshot obtained of $CRAC^{WT}$ interacting with a PC/Chol membrane *in silico* (Figure 5.11). The CRAC domain residues Glu, Lys, and Arg that surround the central Tyr are observed to reside at the membrane-water interface or just below the interface within the bilayer membrane.

Accounting for the behavior of Arg and Lys, a substitution to one of these residues could disrupt a reaction that facilitates Chol binding. For an Arg to Glu substitution as seen in $CRAC^{-1F}$ and a Lys to Glu substitution as seen in $CRAC^{-1D}$, these changes could disrupt crucial hydrogen bonds between Arg and Lys and the carbonyl and phosphate groups of membrane lipids, thus decreasing the affinity of our peptides for the membrane and Chol [184, 186]. It is worth noting that these changes only highlight interactions with PC lipids and such changes do not induce differences in theses peptides' affinity for 100% POPC liposomes. With that in mind, the changes in affinities of these mutants for Chol-containing membranes cannot be compared to the lack of change observed with these same mutants and 100% POPC. The introduction of Chol within 60% POPC/40% Chol

liposomes alters the physical and chemical properties of the membrane which could allow such changes to have an effect on the peptide's ability to bind to the membrane and its affinity for Chol-containing membranes [211, 287, 288].

The hydroxyl group of Chol is another key component in the interaction of a CRAC domain with the membrane [19, 140]. In the case of both $CRAC^{-1D}$ and $CRAC^{-1F}$ the basic Lys or Arg residues were substituted with acidic Glu residues. The ability of the CRAC mutants, $CRAC^{-1D}$ and $CRAC^{-1F}$, to form hydrogen bonds with lipid phosphate groups that reside near the hydroxyl groups of Chol diminished by 33% when compared to $CRAC^{WT}$ [289]. Furthermore, the introduction of Glu residues, which hydrogen bond with choline and water, near the surface of the membrane, make it energetically less favorable for these polar residues to adopt a position near the Chol headgroups that are positioned further into the bilayer [184, 186, 290] further supporting the decreased affinity that was observed for $CRAC^{-1D}$ and $CRAC^{-1F}$.

In summary, our studies show that factors other than overall net charge of the peptide are important for the binding of $CRAC^{WT}$ to Chol. For the first time, these studies differentiate the possible role that the charged acidic and basic residues can have in altering the biological activity of our wild-type peptide, demonstrating that the interaction of $CRAC^{WT}$ with Chol depends not only on the key Leu/Val, Tyr, and Lys/Arg residues but potentially on the residues surrounding these amino acids.

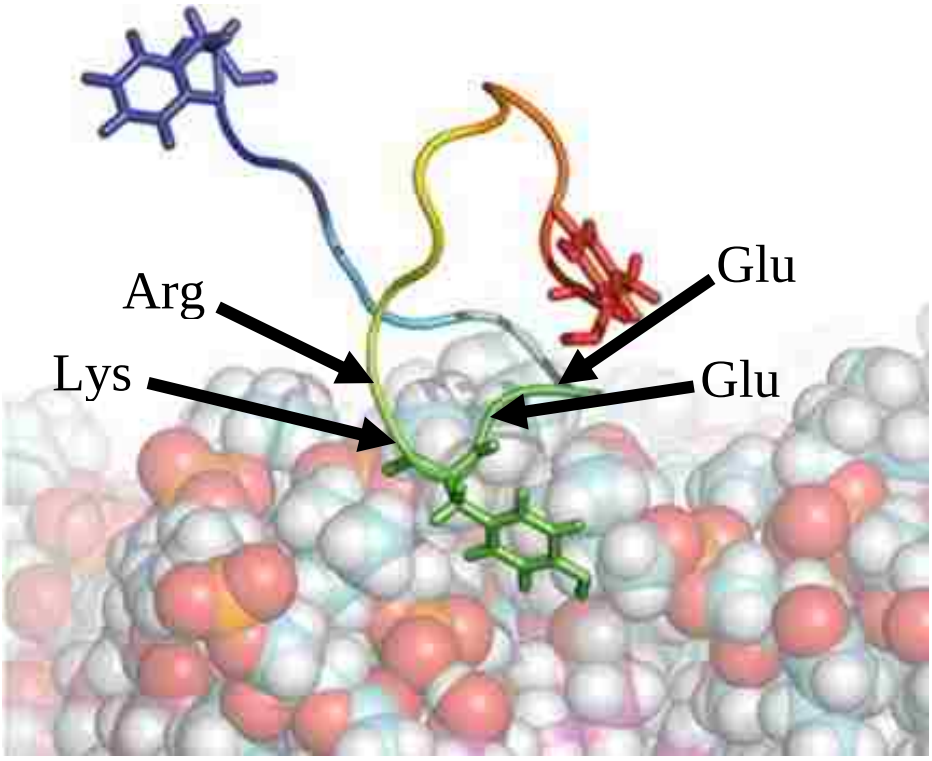

Figure 5.11 Zoomed in snapshot of $CRAC^{WT}$ near a PC/Chol membrane. The Glu, Lys, and Arg residues can be seen at the water-membrane interface where they could potentially be interacting with PC lipid headgroups and/or Chol molecules. The membrane is composed of PC carbons (cyan) and Chol molecules (magenta) [182]. The Phenylalanine residue is show in blue and the central and terminal Tyr residues are shown in green and red respectively.

Chapter 6

Implementing Alanine Substitutions to Examine Key Residues in the Binding of a CRAC Domain to Cholesterol

6.1 Introduction

The biggest issue pertaining to the CRAC domain is still unaddressed, which is that the algorithm is not well defined and is very inaccurate. This leads to the algorithm overpredicting Chol-binding domains and many of these domains found that contain a CRAC motif end up not having an affinity for Chol [102, 148, 150, 151].

Previously, other groups have tried to investigate certain characteristics that regulate the CRAC domain's affinity for Chol. Studies were performed in which multiple mutations were investigated, including Tyr substitution with another aromatic amino acid (phenylalanine or tryptophan), alterations to the Leu/Val residue, which is thought to bury itself into the membrane and play a role in the CRAC domain's ability to conform to the structure of Chol, and lastly alterations to the Lys/Arg residue, which is believed to allow the peptide to gravitate toward the water-membrane interface by way of their polar side chain [140, 143, 180, 181]. These studies did not reveal anything that is not already known and concluded that Tyr is necessary for Chol binding and that substitutions to either the first or last residue in the CRAC motif results in a decrease in affinity for Chol.

Literature has also suggested that the residues labeled as X must be nonpolar because those amino acids are assumed to span the nonpolar region of the membrane [140]. $CRAC^{WT}$, which we have previously shown to have a strong affinity for Chol, contains two polar Glu residues in the X_1 and X_2 position. In conjunction with studies that indicate Glu forms favorable interactions with the choline groups of PC lipids that facilitate binding to the membrane, this contradicts the notion that the X residues should be nonpolar [186].

The goal of this project was to demonstrate the role of each residue in the affinity for Chol, beyond the established requirements of Leu/Val, Tyr, and Arg/Lys and to gain a better understanding of the requirements needed for a CRAC domain to bind to Chol. To accomplish this, a panel of ten peptides was synthesized based on the $CRAC^{WT}$ peptide, where each peptide had one residue within the CRAC domain substituted with an alanine (Ala) residue, as listed in Table 6.1 [291, 292]. We hypothesized that this study would confirm Leu or Val, Tyr, and either the Arg or Lys as the key residues in the interaction with Chol. Furthermore, measuring the affinity of each peptide for Chol will give us insight on each residue's significance in the CRAC domain's affinity for Chol and assist us and others in the future design of Chol-binding peptides.

6.2 Results

6.2.1 Mutations to the polar residues and to the central Tyr of $CRAC^{WT}$ significantly increases log K_{ow}

To determine the tendency of each peptide to partition in a hydrophobic environment versus a hydrophilic environment we performed an octanol-water experiment to measure each peptide's octanol-water coefficient (log K_{ow}). In this experiment, 1-octanol serves as our model hydrophobic membrane and water serves as our model aqueous

environment. Mutations to either Lys or Arg residues within $CRAC^{WT}$ had the most pronounced effect on the log K_{ow} as shown in Figure 6.1. Each of these changes reduced the net charge of the peptide from +3 to +2 and increased the peptides hydrophobicity, resulting in an increased log K_{ow}. In addition, mutation of the central Tyr (Y10A) also increased log $K_{ow,}$ as Ala is more hydrophobic than Tyr, and led the peptide to favor a more hydrophobic environment as seen from the 10-fold increase in log K_{ow} (Figure 6.1) [293, 294].

Table 6.1 Peptide Sequences of Alanine mutants

Residues underlined refer to the CRAC domain. Residues highlighted in red and bolded are the residues we mutated from $CRAC^{WT}$ peptide. Each peptide was acetylated at the N-terminus and amidated at the C-terminus.

Peptide	**Sequence**
$CRAC^{WT}$	FDRARMLEEYSKRFKKFGY
$CRAC^{L7A}$	FDRARMAEEYSKRFKKFGY
$CRAC^{E8A}$	FDRARMLAEYSKRFKKFGY
$CRAC^{E9A}$	FDRARMLEAYSKRFKKFGY
$CRAC^{Y10A}$	FDRARMLEEASKRFKKFGY
$CRAC^{S11A}$	FDRARMLEEYAKRFKKFGY
$CRAC^{K12A}$	FDRARMLEEYSARFKKFGY
$CRAC^{R13A}$	FDRARMLEEYSKAFKKFGY
$CRAC^{F14A}$	FDRARMLEEYSKRAKKFGY
$CRAC^{K15A}$	FDRARMLEEYSKRFAKFGY
$CRAC^{K16A}$	FDRARMLEEYSKRFKAFGY

6.2.2 Amino acid mutations L7A, Y10A, and R13A of CRAC^{WT} have the largest effect on its affinity for Chol-containing membranes

The three key residues in a CRAC definition are the initial Leu/Val, the central Tyr, and the final Lys/Arg. To determine the effect of the initial, central, and final residues on the peptide's affinity for Chol, we synthesized mutants with a substituted Ala at each of these positions and measured each mutant peptide's affinity for Chol using LSPR measurements. Affinity results for Chol-containing liposomes shown in Table 6.2 corroborate with the CRAC definition that Leu, Tyr, and Arg are the key residues that facilitate the binding to Chol. The affinities of these mutants for Chol were, on average, four orders of magnitude weaker than that of the wild-type peptide.

6.2.3 Flanking residues facilitate binding to Chol

Initially we did not know where the CRAC domain ended in CRAC^{WT}, as the CRAC definition proposed four possibilities: K12, R13, K15, and K16. Utilizing LSPR we measured the change in affinity for Chol of four peptides, in which each peptide had a single mutation to either K12, R13, K15, or K16 and compared them to CRAC^{WT}. We determined that R13 is the final residue of the CRAC domain as seen by the largest decrease in affinity between the four mutants and the third largest decrease overall (5.10×10^{-9} M to 2.07×10^{-5} M), as seen in Table 6.2. Furthermore, we found through changes to our wild-type peptide that residues flanking the CRAC domain influence our wild-type peptide's affinity for Chol. These mutations (F14A, K15A, and K16A) decreased binding to Chol, on average, by two orders of magnitude. The reduction in their affinity for Chol, as shown in Table 5.3, is much smaller than what we observed for the key CRAC residues (L7A, Y10A, and R13A). These results suggest that residues between the key amino acids and

the residues flanking key amino acids could play a facilitative role in the binding of $CRAC^{WT}$ to Chol-containing membranes.

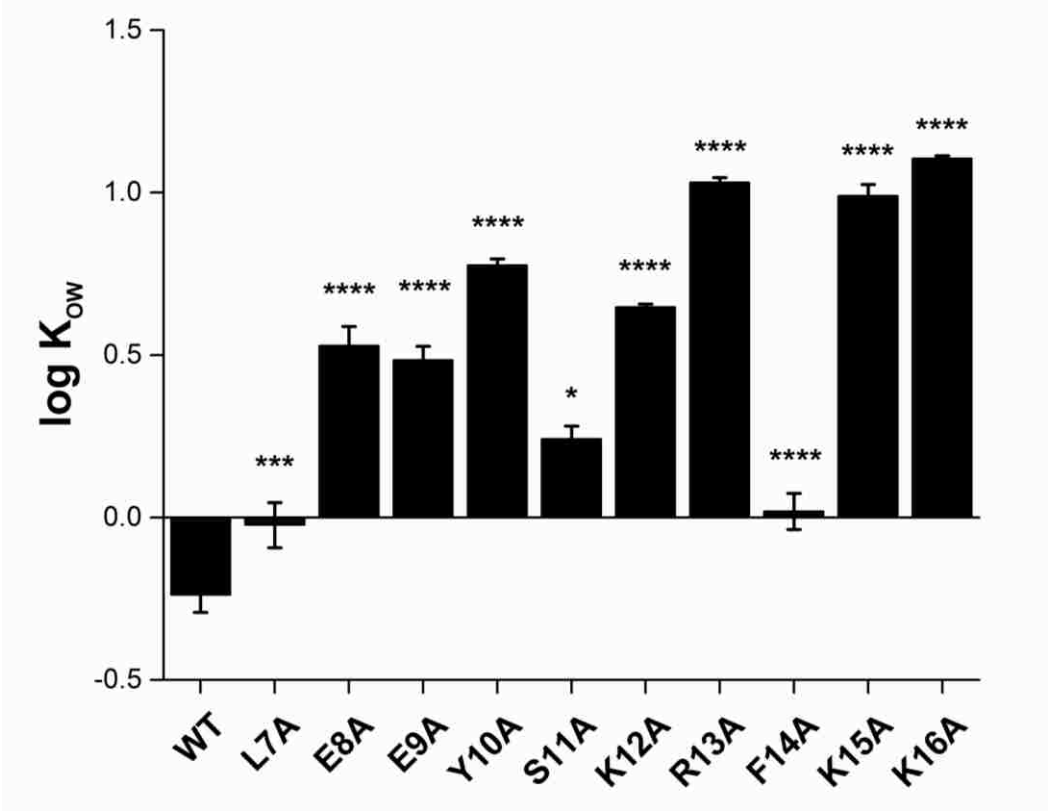

Figure 6.1 Octanol-Water Coefficients (log K_{ow}) of Alanine Scanning Mutants. Octanol-water partition coefficients for each peptide were determined using the shake-flask method. Mutations to Y10, R13, K15, and K16 produced the largest log K_{ow} coefficients suggesting that these residues play a significant role in the wild-type peptide's tendency to partition in a hydrophilic environment. A one-way analysis of variance followed by a Tukey test was used to determine the level of significance between each mutant and $CRAC^{WT}$. **** ($P \leq 0.0001$). *$P \leq 0.05$; N.S., not significant.

Table 6.2 Affinity Values of Mutant Peptides Binding to 60% POPC/40% Chol Liposomes by LSPR

Reaction	$K_{D\ SPR}$ (M)
$CRAC^{WT}$ binding to Chol	$5.10 \times 10^{-9} \pm 4.37 \times 10^{-9}$
$CRAC^{L7A}$ binding to Chol	$4.27 \times 10^{-5} \pm 2.02 \times 10^{-5}$
$CRAC^{E8A}$ binding to Chol	$1.96 \times 10^{-8} \pm 1.37 \times 10^{-9}$
$CRAC^{E9A}$ binding to Chol	$2.76 \times 10^{-8} \pm 2.70 \times 10^{-9}$
$CRAC^{Y10A}$ binding to Chol	$3.64 \times 10^{-5} \pm 2.68 \times 10^{-5}$
$CRAC^{S11A}$ binding to Chol	$1.64 \times 10^{-8} \pm 5.59 \times 10^{-9}$
$CRAC^{K12A}$ binding to Chol	$1.53 \times 10^{-7} \pm 1.51 \times 10^{-8}$
$CRAC^{R13A}$ binding to Chol	$2.07 \times 10^{-5} \pm 4.21 \times 10^{-6}$
$CRAC^{F14A}$binding to Chol	$3.48 \times 10^{-7} \pm 6.42 \times 10^{-8}$
$CRAC^{K15A}$ binding to Chol	$2.77 \times 10^{-7} \pm 1.20 \times 10^{-7}$
$CRAC^{K16A}$ binding to Chol	$3.19 \times 10^{-6} \pm 3.63 \times 10^{-7}$

6.3 Discussion

The largest issue surrounding the CRAC domain is that it over predicts Chol binding, thus requiring experiments to determine if a motif has an affinity for Chol [102, 148, 151]. We undertook this work to investigate the key residues that drive our wild-type peptide's affinity for Chol with a secondary aim of trying to refine the CRAC motif's definition to assist us and other groups in the future design of Chol-binding peptides.

To accomplish our goal, we performed an alanine scanning procedure where each residue within the CRAC domain of our wild-type peptide was substituted with an alanine residue. This method is widely employed to determine key residues involved in specific

interactions [292, 295-297]. Replacing a residue with alanine removes the side chain atoms after the β-carbon, which includes the functional group of the amino acid. This allows us to study the effects that a specific residue has on our interaction of interest.

Among the mutants studied, we found that L7A, Y10A, and R13A had the largest effect on the wild-type peptide's affinity for Chol. Our results (Table 6.2) indicate that these residues are the three key amino acids defined in the CRAC definition, (L/V)-(X_{1-5})-Y-(X_{1-5})-(K/R), and confirm our initial hypothesis while supporting the long standing CRAC motif definition [131]. Other groups have also demonstrated similar results; studies into single point mutations on CRAC segments found that mutations on either of the key residues resulted in a decreased or abolished ability to interact with Chol [142, 143, 145].

The initial Leu or Val uses its branched side chains to associate with the β face of Chol through van der Waals interactions [140, 180]. The final Lys or Arg can bury itself into the membrane bilayer and have its charged group sitting at the membrane surface, allowing it to attract and hydrogen bond water molecules and/or lipid headgroups [140, 183-186]. Finally, the central Tyr is the most critical amino acid between the binding of the CRAC domain to Chol. Tyr uses its hydroxyl group to electrostatically interacts with the sterol's hydroxyl group while facilitating a CH-π stacking interaction with the B ring of Chol as well [140, 142, 182].

Sites on a target protein that have a high tendency to bind to proteins, membranes, or other biomolecules, are referred to as "hot spots" [17, 19, 102, 298]. Systematic analyses of hot spots have found that these regions overlap with structurally conserved residues, as shown in the $CRAC^{337}$ motif of LtxA [102, 298-302]. Furthermore, two of the most conserved residues found in "hot spots" are Arg, and Tyr which are also key residues within

the CRAC definition [131, 302, 303]. Although there have been no reports of protein hot spots containing CRAC domains or that a CRAC domain could be classified as one, the two share many similarities. Taking this into account hot spot analyses could shed further light into why Tyr and Arg as well as the other key amino acids are significant in the CRAC motif's interactions with Chol.

Studies pertaining to CRAC domains have shown Tyr hydrogen bonds using its hydroxyl group, but hot spot analyses have shown that the hydrophobic surface, aromatic π interactions, and minimal rotatable bonds of Tyr are what allow it to contribute to the binding energy of its interaction without taking a large entropic penalty [304, 305]. Furthermore, hot spot analyses suggests Arg can form up to five hydrogen bonds and due to the guanidinium π-system it can give the residue quasi-aromatic characteristics facilitating a stacking interaction with the membrane [304, 306-308].

In summary, our studies show that the key residues of the CRAC definition, Leu/Val, Tyr, and Lys/Arg, are important for the binding of the wild-type peptide to Chol. Furthermore, our results suggest that residues between key amino acids are not as critical in the binding of our CRAC wild-type peptide to Chol-containing membranes, but they could play a supporting role. The results of this study have given us a clearer picture on the amino acid requirements for the CRAC domain as well as the significance of each residue within our wild-type peptide $CRAC^{WT}$ which will allow us to improve our wild-type peptide's affinity for Chol. Lastly, with recent advances in peptide synthesis and screening, peptides are in a favorable spot to become successful drug discovery candidates and our findings could facilitate the development of a Chol-binding therapeutic peptide [309].

Chapter 7

Inhibiting the Bacterial Toxins Streptolysin O and Pneumolysin O Utilizing Cholesterol Binding Peptides

7.1 Introduction

Many pathogens including bacterial toxins, recognize Chol as an initial step in their activity against cells [237, 310-312]. One class of toxins, the Chol-dependent cytolysins, depend on the presence of Chol for toxicity [310]. Previously, we described the potential of a peptide engineered to contain a CRAC motif ($CRAC^{WT}$) as a therapeutic agent against a toxin that targets Chol [19]. We demonstrated that $CRAC^{WT}$ has a strong affinity for Chol and can inhibit a Chol-binding bacterial protein toxin. Demonstrating the effectiveness of this Chol-binding peptide to inhibit the interaction between a virulence factor and Chol introduced a novel strategy that may have potential applications against other pathogens that bind to Chol. This enables us to attack any Chol-dependent illnesses, as there are currently no viable approaches to inhibit this interaction. More importantly, $CRAC^{WT}$ exhibits no long-term toxicity to white blood cells, further bolstering its potential as an alternative therapeutic (Figure 4.10) [19]. This strategy has enormous potential for the treatment of bacterial infections, including ones that pose an antibiotic-resistant threat. Furthermore, the use of these types of peptides has the potential to replace or supplement

the use of antibiotics, which could lead to a decrease in the increasingly rising number of antibiotic resistant bacteria.

In this work we focused on investigating the potential use of our antivirulence strategy in inhibiting other Chol-binding bacterial toxins. Our model toxins include SLO and PLO. SLO and PLO are secreted by bacteria that fall under the CDC's list of emerging bacterial threats and both toxins utilize Chol in their method of action [3, 310]. Both toxins are structurally homologous and are secreted by most bacterial strains in the genus *Streptococcus* [310, 313, 314]. They are toxic to leukocytes and erythrocytes, and SLO and PLO require Chol for binding and cytotoxicity [273, 315, 316].

To measure the efficacy of $CRAC^{WT}$ in inhibiting these toxins, white blood cell cytotoxicity and red blood cell hemolytic assays were performed using THP-1 cells and sheep erythrocytes. The affinity of the $CRAC^{WT}$ peptide for Chol is several orders of magnitude stronger than reported affinity of PLO for Chol (4×10^{-7} M) suggesting that the peptide may inhibit binding of PLO to Chol-containing membranes [19, 273]. The affinity of SLO for Chol has yet to be determined but due to the mechanistic similarities of both toxins we hypothesize that $CRAC^{WT}$ will inhibit SLO as well [4, 310, 314]. From our study we found that $CRAC^{WT}$ is an effective agent in inhibiting the toxicity of SLO and PLO toward THP-1 cells, and the toxicity of PLO towards sheep erythrocytes, thus demonstrating the peptide's potential as a novel alternative therapy for bacterial toxin-mediated infections.

7.2 Results

7.2.1 CRAC^{WT} inhibits SLO cytotoxicity in THP-1 cells

To investigate the possibility of inhibiting SLO cytotoxicity using the Chol-binding peptide CRAC^{WT} we employed a cell cytotoxicity experiment with THP-1 cells. We incubated THP-1 cells with SLO alone or in combination with the CRAC^{WT} peptide for 24 hr. As shown in Figure 7.2, CRAC^{WT} inhibited the activity of SLO almost completely at a peptide to toxin ratio of 40:1. To determine the half maximal peptide inhibitory concentration (IC_{50}) of the CRAC^{WT} peptide, the data were fitted to a sigmoidal curve in ORIGIN® PRO 2016. The results of this fit predict an IC_{50} of 7.4 μM for CRAC^{WT} peptide against SLO in THP-1 cells, that is, a peptide to toxin molar ratio of 1.3.

7.2.2 CRAC^{WT} inhibits PLO cytotoxicity

We next investigated the possibility of inhibiting PLO activity using the Chol-binding peptide CRAC^{WT}. To determine if CRAC^{WT} can inhibit PLO binding to Chol and subsequent toxicity, we incubated THP-1 cells with PLO alone or in combination with the CRAC^{WT} peptide for 2 hr. As shown in Figure 7.4, CRAC^{WT} inhibited the activity of PLO almost completely at a peptide to toxin ratio of 1000:1. The results of this fit predict an IC_{50} of 8.5 μM for CRAC^{WT} peptide, that is, a peptide to toxin molar ratio of 36.5.

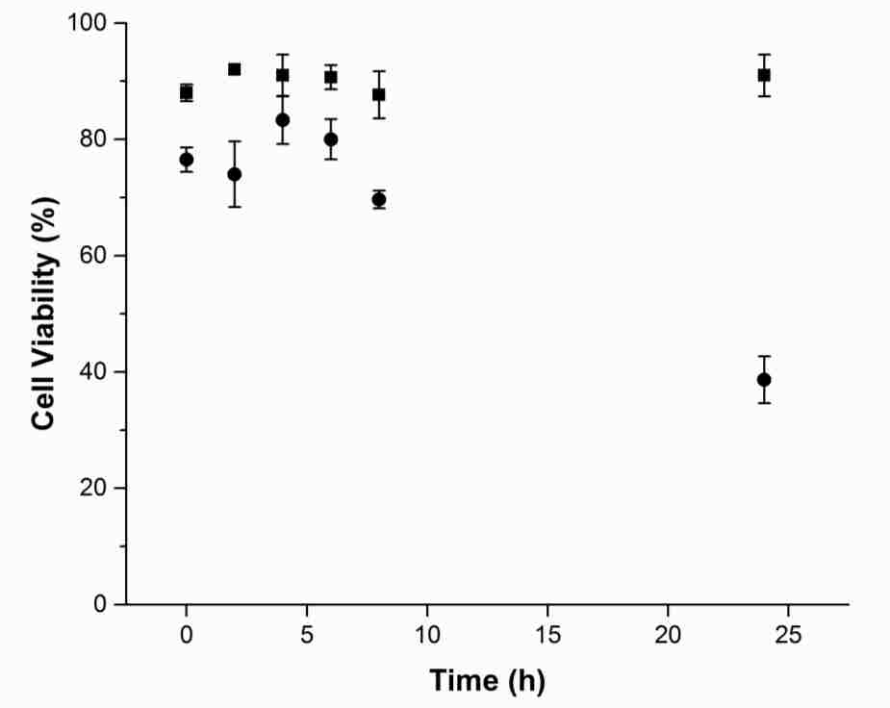

Figure 7.1 SLO is toxic to THP-1 Cells over time.
THP-1 cells were treated with 40.5 µg of SLO for 24 hr, and the viability of the cells was measured using a trypan blue assay. Squares represent the control group without SLO, circles represent cells incubated with SLO.

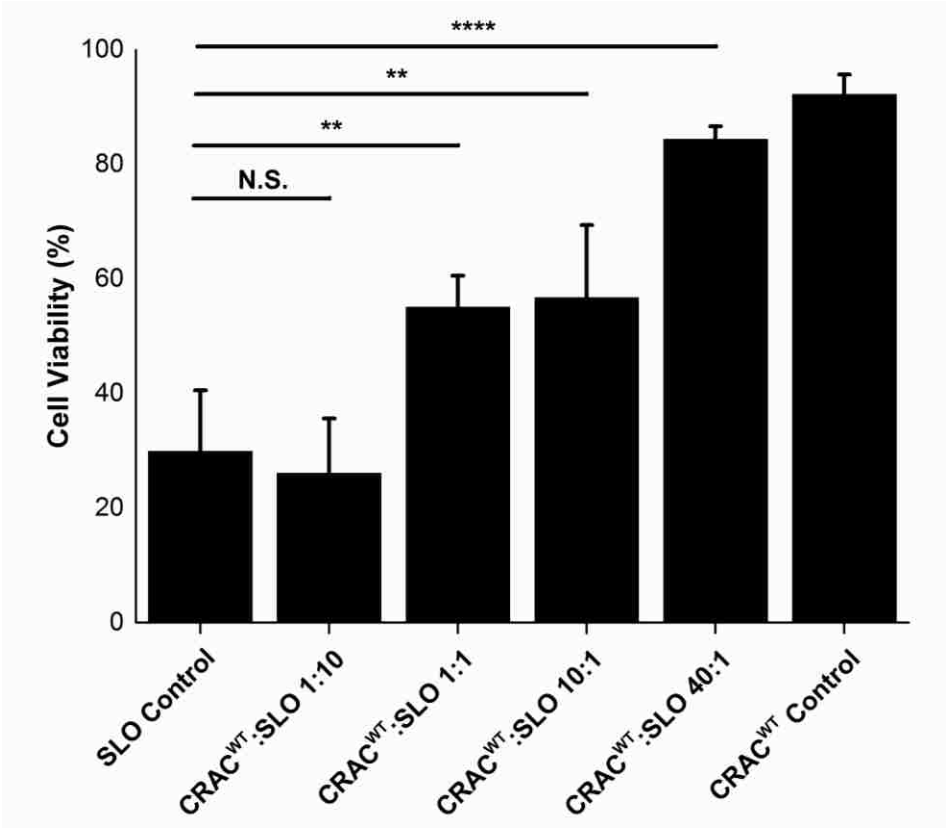

Figure 7.2 $CRAC^{WT}$ peptide inhibits SLO-mediated toxicity.
SLO and $CRAC^{WT}$ were incubated with THP-1 cells for 24 h, and the viability of the cells was measured using a trypan blue assay. The $CRAC^{WT}$ peptide, which binds to Chol, inhibited the toxicity of SLO. A one-way analysis of variance followed by a Tukey test was used to determine the level of significance between each experiment. $^{**}P \leq 0.01$; $^{*}P \leq 0.05$; N.S., not significant.

7.2.3 CRAC^{WT} inhibits PLO hemolysis

Lastly, we investigated the possibility of inhibiting PLO hemolysis of sheep erythrocytes using the Chol-binding peptide CRAC^{WT}. To determine if CRAC^{WT} could prevent the hemolytic activity of PLO, we incubated sheep erythrocytes with PLO alone or in combination with the CRAC^{WT} peptide. As shown in Figure 7.5, CRAC^{WT} inhibited the activity of PLO almost completely at a peptide to toxin ratio of 1:1. The results of this fit predict an IC_{50} of 40.6 nM for CRAC^{WT} peptide, that is, a peptide to toxin molar ratio of 0.4.

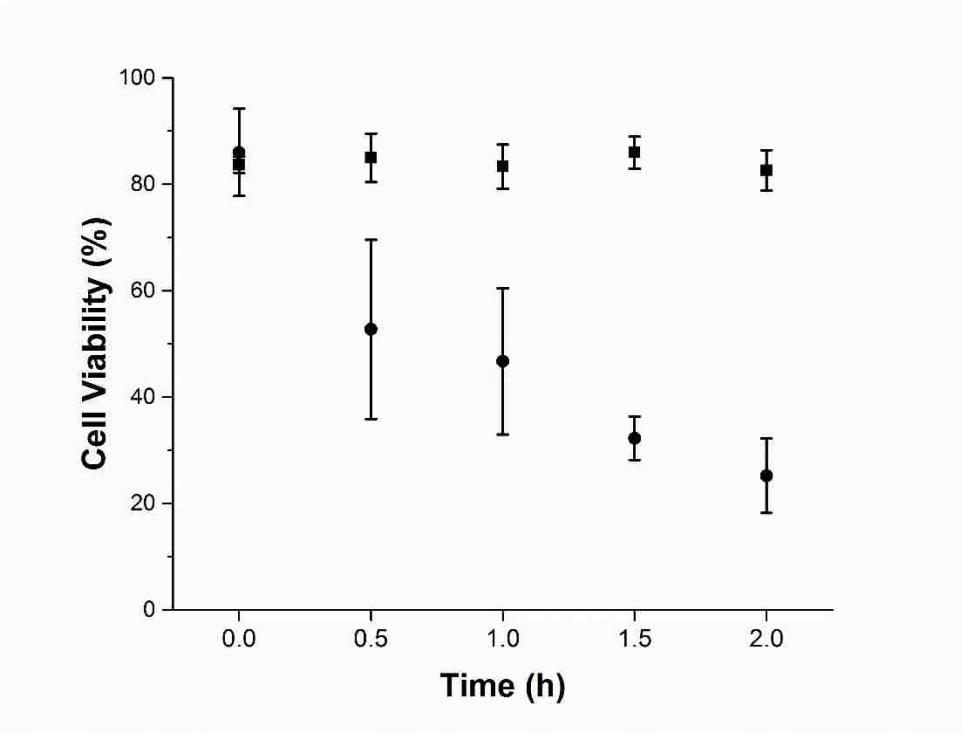

Figure 7.3 PLO is toxic to THP-1 Cells over time.
PLO was incubated with THP-1 cells for 2 h, and the viability of the cells was measured using a trypan blue assay. Squares represent the control group without PLO, circles represent cells incubated with 4 μg of PLO.

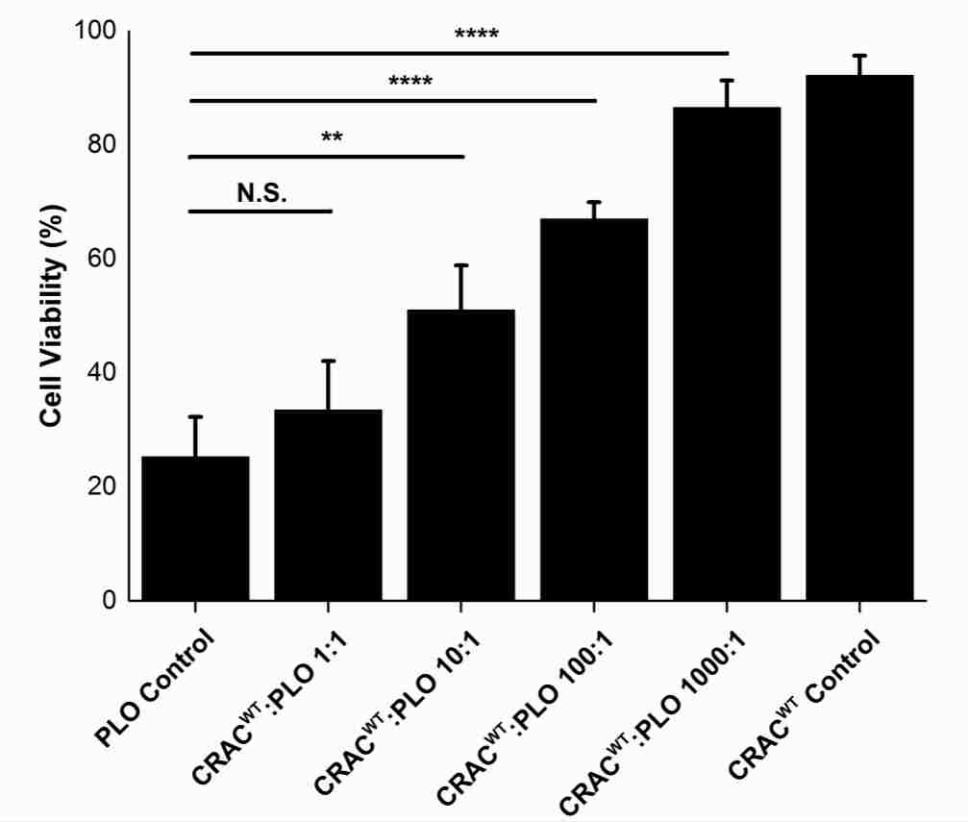

Figure 7.4 $CRAC^{WT}$ peptide inhibits PLO toxicity.
PLO and $CRAC^{WT}$ were incubated with THP-1 cells for 2 h, and the viability of the cells was measured using a trypan blue assay. The $CRAC^{WT}$ peptide, which binds to Chol, inhibited the toxicity of PLO. A one-way analysis of variance followed by a Tukey test was used to determine the level of significance between each experiment. **$P \leq 0.01$; *$P \leq 0.05$; N.S., not significant.

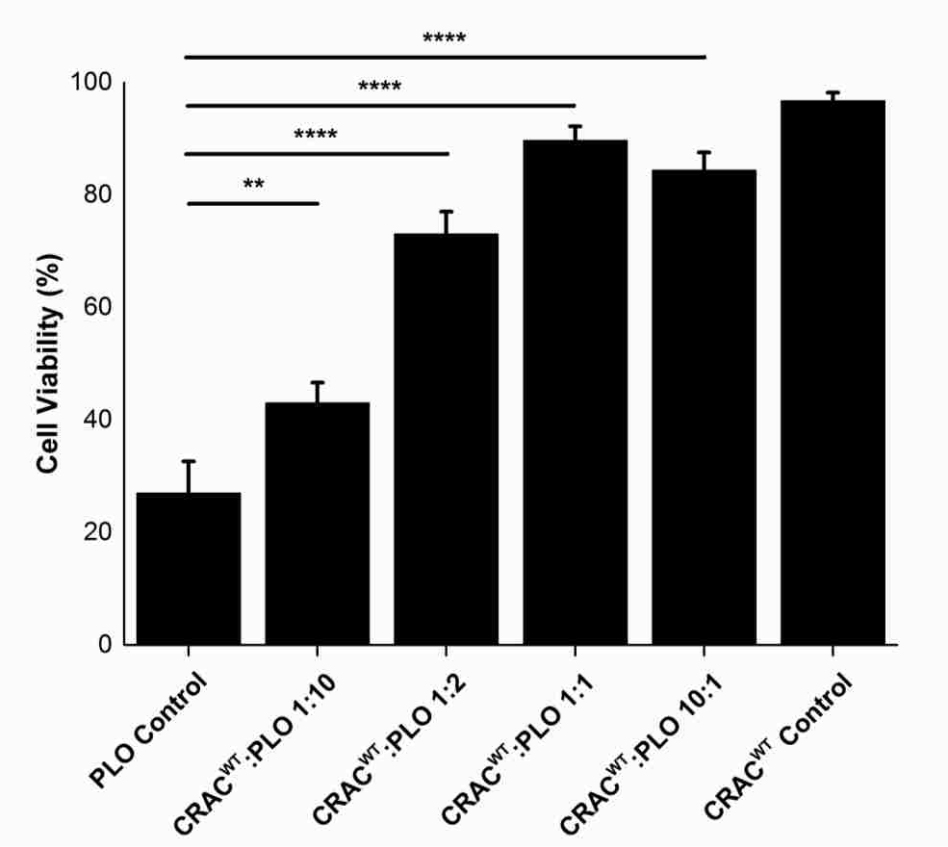

Figure 7.5 $CRAC^{WT}$ peptide inhibits PLO hemolysis.
PLO and $CRAC^{WT}$ were incubated with sheep erythrocytes for 1 h, and the viability of the cells was determined by measuring the absorbance of the supernatant. The $CRAC^{WT}$ peptide, which binds to Chol, inhibited the toxicity of PLO. A one-way analysis of variance followed by a Tukey test was used to determine the level of significance between each experiment. ***$P \leq 0.001$; **$P \leq 0.01$; *$P \leq 0.05$; N.S., not significant.

7.3 Discussion

Traditional antibiotics are the usual route of treatment with patients presenting with *Streptococcus* infections [317]. In conjunction with the increasing number of other bacterial infections, the number of antibiotics prescribed annually has reached 250 million [318]. Due to the overuse of antibiotics to treat bacterial infections, there are greater opportunities for infectious bacteria to evolve and develop antibiotic resistance [3, 319]. Furthermore, it is estimated that the cost arising from antibiotic-resistant infections will

reach US$100 trillion worldwide by 2050, and will have implications on the economic growth while threatening to reverse the advancements made on antibacterial treatments within the last century [320, 321]. The increasing number of antibacterial-resistant organisms has complicated the ability to treat resulting infections, and if little is done to combat the overuse of antibiotics and the increasing number of antibiotic-resistant bacteria the effective use of antibiotics will come to an end. To alleviate such a crisis from occurring, we seek to find an alternative approach that will not increase the bacterial survival pressure which would reduce bacterial mutation rates [322]. By focusing on inhibiting the toxins that are secreted by the pathogenic bacteria, we could inhibit the virulence of the pathogenic bacteria without targeting the organisms directly.

Streptococci bacteria employ many virulence factors that are critical to their ability to fight off the host's immune system, bind to their target cell, and facilitate the process of lysing the cell [323-326]. Among them, PLO and SLO are key to a successful infection by the *Streptococcus* genus [327-331]. Both toxins can form pores in membranes containing Chol thus leading to inflammation and the death of the host's immune cells in the process [310, 332, 333]. Furthermore, it has been shown that by preventing such binding to the cell membrane, through mutations to the bacterium that prevent toxin secretion or to the primary structure of the toxin, the virulence of these bacteria was reduced in animal studies [332, 333]. This suggests that the development of novel therapeutics that target the toxin secreted can be a viable approach to treating these infections, which in turn would decrease the use of antibiotics and decrease the rate of evolution by antibiotic-resistant bacteria.

The main goal of this study was to explore a possible alternative treatment for bacterial infections. Previously we have demonstrated the ability of a Chol-binding

peptide, $CRAC^{WT}$, to inhibit the bacterial toxin LtxA of *A. actinomycetemcomitans*, which utilizes Chol in its mode of toxicity [17, 19]. Due to the requirement of Chol for the binding of SLO and PLO to cell membranes we investigated the ability of our peptide, $CRAC^{WT}$, to inhibit the cytotoxicity and hemolytic activity of these two toxins [19, 310]. We employed sheep erythrocytes and THP-1 cells to measure the inhibitory action of $CRAC^{WT}$ against the hemolytic and cytotoxic activities, respectively, of SLO and PLO.

Here, we provide evidence that $CRAC^{WT}$ has activity against SLO and PLO in a concentration-dependent manner. $CRAC^{WT}$ was successful in inhibiting both SLO and PLO toxins from killing THP-1 cells. The IC_{50} of $CRAC^{WT}$ for SLO was comparable to that of PLO, and because the affinity of SLO for Chol has not been reported, this could suggest that the affinity of SLO for Chol is similar to that of PLO. Furthermore, for our hemolysis assays with sheep erythrocytes, the IC_{50} of $CRAC^{WT}$ against PLO was much lower than what we found for THP-1 cells. This could be a result of lower total Chol concentration in the membranes of sheep erythrocytes versus THP-1 cells, thus requiring a lower amount of peptide for inhibition [334, 335]. Regarding the hemolytic activity of SLO, no activity was detected. A possible explanation for this occurrence is the inactivation of SLO, which is an oxygen-labile protein that is reduced in solution and inactivated in storage conditions between 2-8 °C [327, 336, 337].

Other groups have also investigated alternative antibacterial treatments. Three such compounds used as alternative therapeutics against SLO and PLO are allicin, a component of garlic, β-sitosterol which is a plant sterol, and cyclodextrins [316, 338-342]. *In vitro* studies of allicin have shown that it inhibits SLO and PLO toxicity by binding to the cysteine residue within a conserved amino acid sequence. This sequence is thought to play

a role in toxin binding to the membrane or affect the toxin's conformation needed for activity [343, 344]. Studies of β-sitosterol have shown it acts by binding directly to the toxin, more specifically the threonine and Leu residues required for Chol binding, thus inhibiting the toxin form binding to Chol within the cell membrane [135]. In the case of cyclodextrins, which have a strong affinity for Chol, they act by extracting Chol from the membrane and reducing the number of possible binding sites for such toxins [237, 345]. Although these compounds have presented a viable alternative in the treatment against the bacterial toxins SLO and PLO, they do come with limitations. Allicin's drawback lies in its instability in physiological fluids, which significantly impacts its ability to be used as a therapeutic [346]. β-sitosterol is unstable while bound to the toxin, and a correlation between increased plasma concentrations of β-sitosterol and an increase in the rate of heart disease in men has been found [338]. Lastly, the downside of cyclodextrins is that by removing membrane Chol they alter the cell's processes and reduce the cell's viability [235, 347].

In summary, we have demonstrated that $CRAC^{WT}$ possesses the capacity to inhibit SLO, PLO, and possibly other Chol-dependent cytolysins due to how structurally similar they are [314]. Previously, we have demonstrated that the $CRAC^{WT}$ peptide does not induce cytotoxicity in host cells, making it a viable therapeutic candidate [235]. The ability of $CRAC^{WT}$ to inhibit toxin activity by blocking the toxin's interaction with Chol in the cell membrane is a novel therapeutic concept that could have an impact in not only reducing the rise of antibiotic-resistant bacteria but could also be used in the treatment of other pathogens that utilize membrane Chol.

Chapter 8

Concluding Remarks

8.1 Project Outcomes

We found that LtxA requires Chol to be present in the membrane to induce toxicity, and this dependence on Chol enabled us to explore this interaction as a means of inhibiting the activity of the toxin. Initially, as a method of inhibition, we utilized Chol-containing liposomes as an alternative binding site of LtxA. This prevented the toxin from binding to the cell and opened the door to other novel therapeutic approaches including the use of a Chol-binding peptide ($CRAC^{WT}$) derived from LtxA's CRAC domain to inhibit LtxA cytotoxicity.

$CRAC^{WT}$ acts by binding to Chol-containing membranes with a strong affinity, as does our model toxin LtxA. Once incubated with THP-1 cells, $CRAC^{WT}$ binds to Chol within the cell's membrane and prevents subsequent LtxA from binding to the membrane and becoming internalized, this in turn renders the toxin ineffective. During this binding interaction with Chol, $CRAC^{WT}$ sits near the water-membrane interface suggesting that the inhibition of LtxA due to $CRAC^{WT}$ occurs through obstruction of potential Chol binding sites. This technique was the first time a peptide derived from a Chol-binding bacterial toxin was used therapeutically against the toxin that it was derived from.

In the interaction between membrane Chol and $CRAC^{WT}$, the structure of the Chol molecule plays a significant role. We demonstrated that the hydroxyl group of Chol is key in its successful binding with $CRAC^{WT}$ and in addition, the tail structure of Chol facilitates

binding of the peptide as well. This demonstrates key interactions between the CRAC domain and Chol occur at the hydroxyl and tail group of Chol.

The CRAC peptide's charge and sequence also influence its ability to bind to membrane Chol. We found that decreasing or increasing the net charge of a CRAC peptide relative to $CRAC^{WT}$ affected the peptide's affinity for Chol-containing membranes. A decrease in net charge resulted in the reduction of the peptide's affinity for Chol-containing membranes while an increase in net charge significantly reduced the peptide's affinity for Chol-containing membranes. This suggests that electrostatic interactions can influence the CRAC domain's interaction with Chol. Furthermore, we found that the most critical residues involved in the interaction between $CRAC^{WT}$ and Chol are the initial Leu, the central Tyr, and the final Arg. These results fulfill the CRAC defection outlined in the introduction of this work. In addition, our alanine mutant results described in Chapter 6 demonstrate that residues residing between the central Tyr and the initial and final residues of the CRAC domain can contribute to the peptide's affinity for Chol as well.

Lastly, we found that $CRAC^{WT}$ can be utilized to inhibit other Chol-binding bacterial toxins. The affinity of $CRAC^{WT}$ was strong enough to outcompete two Streptococcal toxins, SLO and PLO. This demonstrated the broad-spectrum applicability of $CRAC^{WT}$ as a potential therapeutic not only for Chol-binding bacterial toxins but for viruses which utilize Chol in their toxic mechanisms.

8.2 Contributions to the Field

Throughout this work contributions were made to four areas. 1) The interaction of LtxA to Chol-containing membranes and cells. 2) The interaction of a CRAC peptide to Chol-containing membranes and cells. 3) The significance of amino acid residues within

a CRAC domain pertaining to its ability to bind to Chol-containing membranes and cells. 4) The broad-spectrum applicability of a CRAC peptide in inhibiting Chol-utilizing toxins.

Utilizing an MβCD study we demonstrated that the binding of LtxA to THP-1 cells and model membranes is dependent on the presence of Chol. For this interaction we contributed thermodynamic information pertaining to the binding between LtxA and synthetic PC and PC/Chol membranes.

Through this work we introduced a novel therapeutic approach using a Chol-binding peptide derived from the CRAC domain of a bacterial toxin. We demonstrated that the CRAC domain of LtxA can be used to bind to Chol and prevent LtxA from binding to the cell membrane and subsequently becoming internalized, thus successfully inhibiting the toxin. We also demonstrated experimentally, for the first time, that the interaction between a CRAC peptide and Chol is dependent on the peptide's interaction with the hydroxyl group of Chol and the tail end of Chol.

The lack of affinity information for a CRAC peptide's interaction with PC and PC/Chol liposomes allowed us to contribute thermodynamic and kinetic information pertaining to these interactions with the aid of ITC and LSPR experiments respectively. In addition to previous experimental and *in silico* studies, we contributed secondary structure analysis pertaining to CRAC peptides in solution, while interacting with Chol-free membranes, and while interacting with Chol-containing membranes.

Varying the primary structure of the CRAC peptide allowed us to investigate the effects of single-residue substitution as well as the effects of net charge on the peptides ability to bind to Chol-containing membranes. We found that changes to the overall net charge of the peptide can affect its membrane-binding ability. In addition, we found that

each residue can also play a facilitating role in the peptide's ability to bind to Chol-containing membranes.

8.3 Conclusion

LtxA secreted by *A. actinomycetemcomitans* is chiefly dependent on the presence of Chol within the membrane for binding. Using Chol-binding peptides that inhibit LtxA's ability to bind to the membrane presented a novel alternative therapeutic approach to combating this bacterial toxin. The strong affinity of $CRAC^{WT}$ for Chol-containing membranes enabled $CRAC^{WT}$ to successfully prevent- LtxA-mediated cytotoxicity. Additionally, the inhibition of this interaction allowed us to explore the broad-spectrum applicability of $CRAC^{WT}$ and demonstrate that it can inhibit the cytotoxicity and hemolysis of other bacterial toxins as well.

Demonstrating the effectiveness of this Chol-binding peptide to inhibit the interaction between numerous virulence factor and Chol introduces a novel strategy. We gain the ability to attack any Chol-dependent illnesses, as there are currently no viable approaches to inhibit this interaction. More importantly, $CRAC^{WT}$ exhibits no long-term toxicity to white blood cells, further bolstering its potential as an alternative therapeutic. This strategy has enormous potential for the treatment of not just illnesses caused by bacteria, but also those caused by viruses that utilize Chol, including HIV, the influenza virus, and the herpes simplex virus. Furthermore, the use of these types of peptides has the potential to replace or supplement the use of antibiotics, leading to a decrease in the increasingly rising number of antibiotic resistant bacteria.

Bibliography

[1] C.L. Ventola, The antibiotic resistance crisis: part 1: causes and threats, P T, 40 (2015) 277-283.

[2] M.R. Gillings, H.W. Stokes, Are humans increasing bacterial evolvability?, Trends Ecol Evol, 27 (2012) 346-352.

[3] Antibiotic Resistance Threats in the United States, 2013, in, Centers for Disease Control and Prevention, U.S. Department of Health and Human Services, 2013, Atlanta, GA, 2013.

[4] L.K. Shewell, R.M. Harvey, M.A. Higgins, C.J. Day, L.E. Hartley-Tassell, A.Y. Chen, C.M. Gillen, D.B. James, F. Alonzo, 3rd, V.J. Torres, M.J. Walker, A.W. Paton, J.C. Paton, M.P. Jennings, The cholesterol-dependent cytolysins pneumolysin and streptolysin O require binding to red blood cell glycans for hemolytic activity, Proc Natl Acad Sci U S A, 111 (2014) E5312-5320.

[5] Antimicrobial resistance : global report on surveillance 2014, in, Geneva : World Health Organization, 2014, Switzerland, 2014.

[6] J.F. Barrett, Can biotech deliver new antibiotics?, Curr Opin Microbiol, 8 (2005) 498-503.

[7] K. Bush, Antibacterial drug discovery in the 21st century, Clin Microbiol Infect, 10 Suppl 4 (2004) 10-17.

[8] Antimicrobial resistance, in, World Health Organization, 2016.

[9] The State of the World's Antibiotics 2015, in, 2015.

[10] P.M. Hwang, H.J. Vogel, Structure-function relationships of antimicrobial peptides, Biochem Cell Biol, 76 (1998) 235-246.

[11] J.L. Fox, Anti-infective monoclonals step in where antimicrobials fail, Nat Biotechnol, 31 (2013) 952-954.

[12] S.C. Yang, C.H. Lin, C.T. Sung, J.Y. Fang, Antibacterial activities of bacteriocins: application in foods and pharmaceuticals, Front Microbiol, 5 (2014) 241.

[13] R.W. Titball, Vaccines against intracellular bacterial pathogens, Drug Discov Today, 13 (2008) 596-600.

[14] R. Eckert, F. Qi, D.K. Yarbrough, J. He, M.H. Anderson, W. Shi, Adding selectivity to antimicrobial peptides: rational design of a multidomain peptide against Pseudomonas spp, Antimicrob Agents Chemother, 50 (2006) 1480-1488.

[15] P.D. Cotter, R.P. Ross, C. Hill, Bacteriocins - a viable alternative to antibiotics?, Nat Rev Microbiol, 11 (2013) 95-105.

[16] R. Eckert, J. He, D.K. Yarbrough, F. Qi, M.H. Anderson, W. Shi, Targeted killing of Streptococcus mutans by a pheromone-guided "smart" antimicrobial peptide, Antimicrob Agents Chemother, 50 (2006) 3651-3657.

[17] A.C. Brown, E. Koufos, N.V. Balashova, K. Boesze-Battaglia, E.T. Lally, Inhibition of LtxA toxicity by blocking cholesterol binding with peptides, Mol. Oral Microbiol., 31 (2016) 94-105.

[18] J.L. Fox, Antimicrobial peptides stage a comeback, Nat Biotechnol, 31 (2013) 379-382.

[19] E. Koufos, E.H. Chang, E.S. Rasti, E. Krueger, A.C. Brown, Use of a Cholesterol Recognition Amino Acid Consensus Peptide To Inhibit Binding of a Bacterial Toxin to Cholesterol, Biochemistry, 55 (2016) 4787-4197.

[20] Peptide Therapeutics Market: Global Industry Analysis, Size, Share, Growth, Trends and Forecast 2012–2018, in, Transparency Market Research, 2012.

[21] M.S. Dryden, Complicated skin and soft tissue infection, J Antimicrob Chemother, 65 Suppl 3 (2010) iii35-44.

[22] P.D. Cotter, C. Hill, R.P. Ross, Bacteriocins: developing innate immunity for food, Nat Rev Microbiol, 3 (2005) 777-788.

[23] H. Ghodhbane, S. Elaidi, J.M. Sabatier, S. Achour, J. Benhmida, I. Regaya, Bacteriocins active against multi-resistant gram negative bacteria implicated in nosocomial infections, Infect Disord Drug Targets, 15 (2015) 2-12.

[24] P. Kosikowska, A. Lesner, Antimicrobial peptides (AMPs) as drug candidates: a patent review (2003-2015), Expert Opin Ther Pat, 26 (2016) 689-702.

[25] A.R. Koczulla, R. Bals, Antimicrobial peptides: current status and therapeutic potential, Drugs, 63 (2003) 389-406.

[26] B.C. Kirkup, Jr., Bacteriocins as oral and gastrointestinal antibiotics: theoretical considerations, applied research, and practical applications, Curr Med Chem, 13 (2006) 3335-3350.

[27] K. Fosgerau, T. Hoffmann, Peptide therapeutics: current status and future directions, Drug Discov Today, 20 (2015) 122-128.

[28] M.R. Yeaman, N.Y. Yount, Mechanisms of antimicrobial peptide action and resistance, Pharmacol Rev, 55 (2003) 27-55.

[29] Y.J. Gordon, E.G. Romanowski, A.M. McDermott, A review of antimicrobial peptides and their therapeutic potential as anti-infective drugs, Curr Eye Res, 30 (2005) 505-515.

[30] Y. Zhao, M. Zhang, S. Qiu, J. Wang, J. Peng, P. Zhao, R. Zhu, H. Wang, Y. Li, K. Wang, W. Yan, R. Wang, Antimicrobial activity and stability of the D-amino acid substituted derivatives of antimicrobial peptide polybia-MPI, AMB Express, 6 (2016) 122.

[31] J.B. McPhee, M.G. Scott, R.E. Hancock, Design of host defence peptides for antimicrobial and immunity enhancing activities, Comb Chem High Throughput Screen, 8 (2005) 257-272.

[32] H. John, E. Maronde, W.G. Forssmann, M. Meyer, K. Adermann, N-terminal acetylation protects glucagon-like peptide GLP-1-(7-34)-amide from DPP-IV-mediated degradation retaining cAMP- and insulin-releasing capacity, Eur J Med Res, 13 (2008) 73-78.

[33] L.D. Saravolatz, J. Pawlak, L. Johnson, H. Bonilla, L.D. Saravolatz, 2nd, M.G. Fakih, A. Fugelli, W.M. Olsen, In vitro activities of LTX-109, a synthetic antimicrobial peptide, against methicillin-resistant, vancomycin-intermediate, vancomycin-resistant, daptomycin-nonsusceptible, and linezolid-nonsusceptible Staphylococcus aureus, Antimicrob Agents Chemother, 56 (2012) 4478-4482.

[34] K.T. Cheng, C.L. Wu, B.S. Yip, H.Y. Yu, H.T. Cheng, Y.H. Chih, J.W. Cheng, High Level Expression and Purification of the Clinically Active Antimicrobial Peptide P-113 in Escherichia coli, Molecules, 23 (2018).

[35] A. Catania, P. Grieco, A. Randazzo, E. Novellino, S. Gatti, C. Rossi, G. Colombo, J.M. Lipton, Three-dimensional structure of the alpha-MSH-derived candidacidal peptide [Ac-CKPV]2, J Pept Res, 66 (2005) 19-26.

[36] W.J. Velden, T.M. van Iersel, N.M. Blijlevens, J.P. Donnelly, Safety and tolerability of the antimicrobial peptide human lactoferrin 1-11 (hLF1-11), BMC Med, 7 (2009) 44.

[37] E. Sparrow, M. Friede, M. Sheikh, S. Torvaldsen, Therapeutic antibodies for infectious diseases, Bull World Health Organ, 95 (2017) 235-237.

[38] Y. Song, M. Baer, R. Srinivasan, J. Lima, G. Yarranton, C. Bebbington, S.V. Lynch, PcrV antibody-antibiotic combination improves survival in Pseudomonas aeruginosa-infected mice, Eur J Clin Microbiol Infect Dis, 31 (2012) 1837-1845.

[39] L. Hua, J.J. Hilliard, Y. Shi, C. Tkaczyk, L.I. Cheng, X. Yu, V. Datta, S. Ren, H. Feng, R. Zinsou, A. Keller, T. O'Day, Q. Du, L. Cheng, M. Damschroder, G. Robbie, J. Suzich, C.K. Stover, B.R. Sellman, Assessment of an anti-alpha-toxin monoclonal antibody for prevention and treatment of Staphylococcus aureus-induced pneumonia, Antimicrob Agents Chemother, 58 (2014) 1108-1117.

[40] B. Kelley, Industrialization of mAb production technology: the bioprocessing industry at a crossroads, MAbs, 1 (2009) 443-452.

[41] L.M. Weiner, M. Holmes, A. Richeson, A. Godwin, G.P. Adams, S.T. Hsieh-Ma, D.B. Ring, R.K. Alpaugh, Binding and cytotoxicity characteristics of the bispecific murine monoclonal antibody 2B1, J Immunol, 151 (1993) 2877-2886.

[42] B. Francois, O. Barraud, H.S. Jafri, Antibody-based therapy to combat Staphylococcus aureus infections, Clin Microbiol Infect, 23 (2017) 219-221.

[43] S.X. Wang-Lin, J.P. Balthasar, Pharmacokinetic and Pharmacodynamic Considerations for the Use of Monoclonal Antibodies in the Treatment of Bacterial Infections, Antibodies, 7 (2018) 5-25.

[44] J.D. Berry, R.G. Gaudet, Antibodies in infectious diseases: polyclonals, monoclonals and niche biotechnology, N Biotechnol, 28 (2011) 489-501.

[45] A. DiGiandomenico, B.R. Sellman, Antibacterial monoclonal antibodies: the next generation?, Curr Opin Microbiol, 27 (2015) 78-85.

[46] M.B. Oleksiewicz, G. Nagy, E. Nagy, Anti-bacterial monoclonal antibodies: back to the future?, Arch Biochem Biophys, 526 (2012) 124-131.

[47] T.A. Russo, J.M. Beanan, R. Olson, U. MacDonald, J.J. Cope, Capsular polysaccharide and the O-specific antigen impede antibody binding: a potential obstacle for the successful development of an extraintestinal pathogenic Escherichia coli vaccine, Vaccine, 27 (2009) 388-395.

[48] P. van der Ley, O. Kuipers, J. Tommassen, B. Lugtenberg, O-antigenic chains of lipopolysaccharide prevent binding of antibody molecules to an outer membrane pore protein in Enterobacteriaceae, Microb Pathog, 1 (1986) 43-49.

[49] S.X. Wang-Lin, R. Olson, J.M. Beanan, U. MacDonald, J.P. Balthasar, T.A. Russo, The Capsular Polysaccharide of Acinetobacter baumannii Is an Obstacle for Therapeutic Passive Immunization Strategies, Infect Immun, 85 (2017).

[50] E.B. Hirsch, V.H. Tam, Impact of multidrug-resistant Pseudomonas aeruginosa infection on patient outcomes, Expert Rev Pharmacoecon Outcomes Res, 10 (2010) 441-451.

[51] K. Kingwell, Infectious diseases: Two-hit antibody tackles bacteria, Nat Rev Drug Discov, 14 (2015) 15.

[52] A. DiGiandomenico, A.E. Keller, C. Gao, G.J. Rainey, P. Warrener, M.M. Camara, J. Bonnell, R. Fleming, B. Bezabeh, N. Dimasi, B.R. Sellman, J. Hilliard, C.M. Guenther, V. Datta, W. Zhao, C. Gao, X.Q. Yu, J.A. Suzich, C.K. Stover, A multifunctional bispecific antibody protects against Pseudomonas aeruginosa, Sci Transl Med, 6 (2014) 262ra155.

[53] Zinplava, European Public Assessment Reports, European Medicines Agency, (2018).

[54] E. Pelfrene, M. Mura, A. Cavaleiro Sanches, M. Cavaleri, Monoclonal antibodies as anti-infective products: a promising future?, Clin Microbiol Infect, (2018).

[55] G.P. Carter, J.I. Rood, D. Lyras, The role of toxin A and toxin B in Clostridium difficile-associated disease: Past and present perspectives, Gut Microbes, 1 (2010) 58-64.

[56] M.S. Duthie, M.T. Pena, G.J. Ebenezer, T.P. Gillis, R. Sharma, K. Cunningham, M. Polydefkis, Y. Maeda, M. Makino, R.W. Truman, S.G. Reed, LepVax, a defined subunit vaccine that provides effective pre-exposure and post-exposure prophylaxis of M. leprae infection, NPJ Vaccines, 3 (2018) 12.

[57] E.D.G. McIntosh, Healthcare-associated infections: potential for prevention through vaccination, Therapeutic Advances in Vaccines and Immunotherapy, 6 (2018) 19-27.

[58] T.H. Casswall, B. Fischler, Vaccination of the immunocompromised child, Expert Rev Vaccines, 4 (2005) 725-738.

[59] K.E. Luthy, M.E. Tiedeman, R.L. Beckstrand, D.A. Mills, Safety of live-virus vaccines for children with immune deficiency, J Am Acad Nurse Pract, 18 (2006) 494-503.

[60] D.A. Skibinski, B.C. Baudner, M. Singh, D.T. O'Hagan, Combination vaccines, J Glob Infect Dis, 3 (2011) 63-72.

[61] C.T. Le, Combination vaccines: choices or chaos? A practitioner's perspective, Clin Infect Dis, 33 Suppl 4 (2001) S367-371.

[62] S. Ainsworth, P.M. Ketter, J.J. Yu, R.C. Grimm, H.C. May, A.P. Cap, J.P. Chambers, M.N. Guentzel, B.P. Arulanandam, Vaccination with a live attenuated Acinetobacter baumannii deficient in thioredoxin provides protection against systemic Acinetobacter infection, Vaccine, 35 (2017) 3387-3394.

[63] H. Petousis-Harris, J. Paynter, J. Morgan, P. Saxton, B. McArdle, F. Goodyear-Smith, S. Black, Effectiveness of a group B outer membrane vesicle meningococcal vaccine against gonorrhoea in New Zealand: a retrospective case-control study, Lancet, 390 (2017) 1603-1610.

[64] K.J. Sherman, J.R. Daling, N.S. Weiss, Sexually transmitted diseases and tubal infertility, Sex Transm Dis, 14 (1987) 12-16.

[65] M.P. Cabral, P. Garcia, A. Beceiro, C. Rumbo, A. Perez, M. Moscoso, G. Bou, Design of live attenuated bacterial vaccines based on D-glutamate auxotrophy, Nat Commun, 8 (2017) 15480.

[66] N. Bezay, A. Ayad, K. Dubischar, C. Firbas, R. Hochreiter, S. Kiermayr, I. Kiss, F. Pinl, B. Jilma, K. Westritschnig, Safety, immunogenicity and dose response of VLA84, a new vaccine candidate against Clostridium difficile, in healthy volunteers, Vaccine, 34 (2016) 2585-2592.

[67] R.J. Fair, Y. Tor, Antibiotics and bacterial resistance in the 21st century, Perspect Medicin Chem, 6 (2014) 25-64.

[68] B.K. Giersing, S.S. Dastgheyb, K. Modjarrad, V. Moorthy, Status of vaccine research and development of vaccines for Staphylococcus aureus, Vaccine, 34 (2016) 2962-2966.

[69] D.A. Rasko, V. Sperandio, Anti-virulence strategies to combat bacteria-mediated disease, Nat Rev Drug Discov, 9 (2010) 117-128.

[70] S. Muhlen, P. Dersch, Anti-virulence Strategies to Target Bacterial Infections, Curr Top Microbiol Immunol, 398 (2016) 147-183.

[71] J.W. Peterson, Bacterial Pathogenesis, in: th, S. Baron (Eds.) Medical Microbiology, Galveston (TX), 1996.

[72] K. Yannakopoulou, L. Jicsinszky, C. Aggelidou, N. Mourtzis, T.M. Robinson, A. Yohannes, E.M. Nestorovich, S.M. Bezrukov, V.A. Karginov, Symmetry requirements for effective blocking of pore-forming toxins: comparative study with alpha-, beta-, and gamma-cyclodextrin derivatives, Antimicrob Agents Chemother, 55 (2011) 3594-3597.

[73] S.M. Bezrukov, E.M. Nestorovich, Inhibiting bacterial toxins by channel blockage, Pathog Dis, 74 (2016).

[74] J.N. Webb, E. Koufos, A.C. Brown, Inhibition of Bacterial Toxin Activity by the Nuclear Stain, DRAQ5, J Membr Biol, (2016).

[75] T.R. Branson, W.B. Turnbull, Bacterial toxin inhibitors based on multivalent scaffolds, Chem Soc Rev, 42 (2013) 4613-4622.

[76] J.P. Caeiro, H.L. DuPont, Management of travellers' diarrhoea, Drugs, 56 (1998) 73-81.

[77] J.A. Adachi, Z.D. Jiang, J.J. Mathewson, M.P. Verenkar, S. Thompson, F. Martinez-Sandoval, R. Steffen, C.D. Ericsson, H.L. DuPont, Enteroaggregative Escherichia coli as a major etiologic agent in traveler's diarrhea in 3 regions of the world, Clin Infect Dis, 32 (2001) 1706-1709.

[78] M. Taylor, T. Banerjee, F. Navarro-Garcia, J. Huerta, S. Massey, M. Burlingame, A.H. Pande, S.A. Tatulian, K. Teter, A therapeutic chemical chaperone inhibits cholera intoxication and unfolding/translocation of the cholera toxin A1 subunit, PLoS One, 6 (2011) e18825.

[79] M. Taylor, F. Navarro-Garcia, J. Huerta, H. Burress, S. Massey, K. Ireton, K. Teter, Hsp90 is required for transfer of the cholera toxin A1 subunit from the endoplasmic reticulum to the cytosol, J Biol Chem, 285 (2010) 31261-31267.

[80] P. Cherubin, M.C. Garcia, D. Curtis, C.B. Britt, J.W. Craft, Jr., H. Burress, C. Berndt, S. Reddy, J. Guyette, T. Zheng, Q. Huo, B. Quinones, J.M. Briggs, K. Teter, Inhibition of Cholera Toxin and Other AB Toxins by Polyphenolic Compounds, PLoS One, 11 (2016) e0166477.

[81] I. Linhartova, L. Bumba, J. Masin, M. Basler, R. Osicka, J. Kamanova, K. Prochazkova, I. Adkins, J. Hejnova-Holubova, L. Sadilkova, J. Morova, P. Sebo, RTX proteins: a highly diverse family secreted by a common mechanism, FEMS Microbiol Rev, 34 (2010) 1076-1112.

[82] A. Yuan, P.C. Yang, L.N. Lee, D.B. Chang, S.H. Kuo, K.T. Luh, Actinobacillus actinomycetemcomitans pneumonia with chest wall involvement and rib destruction, Chest, 101 (1992) 1450-1452.

[83] J.J. Zambon, Actinobacillus actinomycetemcomitans in human periodontal disease, J Clin Periodontol, 12 (1985) 1-20.

[84] M. Sugai, T. Kawamoto, S.Y. Peres, Y. Ueno, H. Komatsuzawa, T. Fujiwara, H. Kurihara, H. Suginaka, E. Oswald, The cell cycle-specific growth-inhibitory factor produced by Actinobacillus actinomycetemcomitans is a cytolethal distending toxin, Infect Immun, 66 (1998) 5008-5019.

[85] E.T. Lally, I.R. Kieba, D.R. Demuth, J. Rosenbloom, E.E. Golub, N.S. Taichman, C.W. Gibson, Identification and expression of the Actinobacillus actinomycetemcomitans leukotoxin gene, Biochem Biophys Res Commun, 159 (1989) 256-262.

[86] D.H. Fine, J.B. Kaplan, S.C. Kachlany, H.C. Schreiner, How we got attached to Actinobacillus actinomycetemcomitans: A model for infectious diseases, Periodontol 2000, 42 (2006) 114-157.

[87] E.T. Lally, R.B. Hill, I.R. Kieba, J. Korostoff, The interaction between RTX toxins and target cells, Trends Microbiol, 7 (1999) 356-361.

[88] G.N. Belibasakis, A. Mattsson, Y. Wang, C. Chen, A. Johansson, Cell cycle arrest of human gingival fibroblasts and periodontal ligament cells by Actinobacillus actinomycetemcomitans: involvement of the cytolethal distending toxin, APMIS, 112 (2004) 674-685.

[89] A.C. Brown, K. Boesze-Battaglia, Y. Du, F.P. Stefano, I.R. Kieba, R.F. Epand, L. Kakalis, P.L. Yeagle, R.M. Epand, E.T. Lally, Aggregatibacter actinomycetemcomitans leukotoxin cytotoxicity occurs through bilayer destabilization, Cell Microbiol, 14 (2012) 869-881.

[90] B. Henderson, J.M. Ward, D. Ready, Aggregatibacter (Actinobacillus) actinomycetemcomitans: a triple A* periodontopathogen?, Periodontol 2000, 54 (2010) 78-105.

[91] V.I. Haraszthy, G. Hariharan, E.M. Tinoco, J.R. Cortelli, E.T. Lally, E. Davis, J.J. Zambon, Evidence for the role of highly leukotoxic Actinobacillus actinomycetemcomitans in the pathogenesis of localized juvenile and other forms of early-onset periodontitis, J Periodontol, 71 (2000) 912-922.

[92] J.J. Zambon, V.I. Haraszthy, G. Hariharan, E.T. Lally, D.R. Demuth, The Microbiology of Early-Onset Periodontitis: Association of Highly Toxic Actinobacillus actinomycetemcomitans Strains With Localized Juvenile Periodontitis, J Periodontol, 67 Suppl 3S (1996) 282-290.

[93] J.M. DiRienzo, J. Slots, M. Sixou, M.A. Sol, R. Harmon, T.L. McKay, Specific genetic variants of Actinobacillus actinomycetemcomitans correlate with disease and

health in a regional population of families with localized juvenile periodontitis, Infect Immun, 62 (1994) 3058-3065.

[94] C.C. Tsai, Y.P. Ho, Y.S. Chou, K.Y. Ho, Y.M. Wu, Y.C. Lin, Aggregatibacter (Actinobacillus) actimycetemcomitans leukotoxin and human periodontitis - A historic review with emphasis on JP2, Kaohsiung J Med Sci, 34 (2018) 186-193.

[95] D. Haubek, O.K. Ennibi, K. Poulsen, M. Vaeth, S. Poulsen, M. Kilian, Risk of aggressive periodontitis in adolescent carriers of the JP2 clone of Aggregatibacter (Actinobacillus) actinomycetemcomitans in Morocco: a prospective longitudinal cohort study, Lancet, 371 (2008) 237-242.

[96] J.M. Brogan, E.T. Lally, K. Poulsen, M. Kilian, D.R. Demuth, Regulation of Actinobacillus actinomycetemcomitans leukotoxin expression: analysis of the promoter regions of leukotoxic and minimally leukotoxic strains, Infect Immun, 62 (1994) 501-508.

[97] N.S. Taichman, R.T. Dean, C.J. Sanderson, Biochemical and morphological characterization of the killing of human monocytes by a leukotoxin derived from *Actinobacillus actinomycetemcomitans*, Infect Immun, 28 (1980) 258-268.

[98] R.A. Welch, Pore-forming cytolysins of gram-negative bacteria, Mol Microbiol, 5 (1991) 521-528.

[99] N.S. Taichman, B.J. Shenker, C.C. Tsai, L.T. Glickman, P.C. Baehni, R. Stevens, B.F. Hammond, Cytopathic effects of *Actinobacillus actinomycetemcomitans* on monkey blood leukocytes, J. Periodontal Res., 19 (1984) 133-145.

[100] N.S. Taichman, D.L. Simpson, S. Sakurada, M. Cranfield, J. DiRienzo, J. Slots, Comparative studies on the biology of *Actinobacillus actinomycetemcomitans* leukotoxin in primates, Oral Microbiol Immunol, 2 (1987) 97-104.

[101] E.T. Lally, I.R. Kieba, A. Sato, C.L. Green, J. Rosenbloom, J. Korostoff, J.F. Wang, B.J. Shenker, S. Ortlepp, M.K. Robinson, P.C. Billings, RTX toxins recognize a beta2 integrin on the surface of human target cells, J Biol Chem, 272 (1997) 30463-30469.

[102] A.C. Brown, N.V. Balashova, R.M. Epand, R.F. Epand, A. Bragin, S.C. Kachlany, M.J. Walters, Y. Du, K. Boesze-Battaglia, E.T. Lally, Aggregatibacter actinomycetemcomitans leukotoxin utilizes a cholesterol recognition/amino acid consensus site for membrane association, J Biol Chem, 288 (2013) 23607-23621.

[103] N. Sato, K. Takahashi, H. Ohta, H. Kurihara, K. Fukui, Y. Murayama, S. Taniguchi, Effect of Ca2+ on the binding of Actinobacillus actinomycetemcomitans leukotoxin and the cytotoxicity to promyelocytic leukemia HL-60 cells, Biochem Mol Biol Int, 29 (1993) 899-905.

[104] J.F. Wang, I.R. Kieba, J. Korostoff, T.L. Guo, N. Yamaguchi, H. Rozmiarek, P.C. Billings, B.J. Shenker, E.T. Lally, Molecular and biochemical mechanisms of Pasteurella haemolytica leukotoxin-induced cell death, Microb Pathog, 25 (1998) 317-331.

[105] E.T. Lally, I.R. Kieba, E.E. Golub, J.D. Lear, J.C. Tanaka, Structure/Function Aspects of Actinobacillus actinomycetemcomitans Leukotoxin, J Periodontol, 67 Suppl 3S (1996) 298-308.

[106] E.T. Lally, E.E. Golub, I.R. Kieba, N.S. Taichman, J. Rosenbloom, J.C. Rosenbloom, C.W. Gibson, D.R. Demuth, Analysis of the Actinobacillus actinomycetemcomitans leukotoxin gene. Delineation of unique features and comparison to homologous toxins, J Biol Chem, 264 (1989) 15451-15456.

[107] N.V. Balashova, C. Shah, J.K. Patel, S. Megalla, S.C. Kachlany, Aggregatibacter actinomycetemcomitans LtxC is required for leukotoxin activity and initial interaction between toxin and host cells, Gene, 443 (2009) 42-47.

[108] E.T. Lally, E.E. Golub, I.R. Kieba, Identification and immunological characterization of the domain of Actinobacillus actinomycetemcomitans leukotoxin that determines its specificity for human target cells, J Biol Chem, 269 (1994) 31289-31295.

[109] R.A. Welch, RTX toxin structure and function: a story of numerous anomalies and few analogies in toxin biology, Curr Top Microbiol Immunol, 257 (2001) 85-111.

[110] C.M. Ardila, M.A. Lopez, I.C. Guzman, High resistance against clindamycin, metronidazole and amoxicillin in Porphyromonas gingivalis and Aggregatibacter actinomycetemcomitans isolates of periodontal disease, Med Oral Patol Oral Cir Bucal, 15 (2010) e947-951.

[111] J. Slots, M. Ting, Systemic antibiotics in the treatment of periodontal disease, Periodontol 2000, 28 (2002) 106-176.

[112] C. Akrivopoulou, I.M. Green, N. Donos, S.P. Nair, D. Ready, Aggregatibacter actinomycetemcomitans serotype prevalence and antibiotic resistance in a UK population with periodontitis, J Glob Antimicrob Resist, 10 (2017) 54-58.

[113] I.A. Reis, S.B. Santos, L.A. Santos, N. Oliveira, M.G. Freire, J.F. Pereira, S.P. Ventura, J.A. Coutinho, C.M. Soares, A.S. Lima, Increased significance of food wastes: selective recovery of added-value compounds, Food Chem, 135 (2012) 2453-2461.

[114] W. Teughels, R. Dhondt, C. Dekeyser, M. Quirynen, Treatment of aggressive periodontitis, Periodontol 2000, 65 (2014) 107-133.

[115] A. Johansson, Aggregatibacter actinomycetemcomitans leukotoxin: a powerful tool with capacity to cause imbalance in the host inflammatory response, Toxins (Basel), 3 (2011) 242-259.

[116] M. Edidin, Lipids on the frontier: a century of cell-membrane bilayers, Nat Rev Mol Cell Biol, 4 (2003) 414-418.

[117] P. Goluszko, B. Nowicki, Membrane cholesterol: a crucial molecule affecting interactions of microbial pathogens with mammalian cells, Infect Immun, 73 (2005) 7791-7796.

[118] D.J. Hawkes, J. Mak, Lipid membrane; a novel target for viral and bacterial pathogens, Curr Drug Targets, 7 (2006) 1615-1621.

[119] G.A. Kumar, M. Jafurulla, A. Chattopadhyay, The membrane as the gatekeeper of infection: Cholesterol in host-pathogen interaction, Chem Phys Lipids, 199 (2016) 179-185.

[120] F.R. Maxfield, I. Tabas, Role of cholesterol and lipid organization in disease, Nature, 438 (2005) 612-621.

[121] G. Gimpl, Interaction of G protein coupled receptors and cholesterol, Chem Phys Lipids, 199 (2016) 61-73.

[122] M. Jafurulla, A. Chattopadhyay, Membrane lipids in the function of serotonin and adrenergic receptors, Curr Med Chem, 20 (2013) 47-55.

[123] Y.D. Paila, A. Chattopadhyay, Membrane cholesterol in the function and organization of G-protein coupled receptors, Subcell Biochem, 51 (2010) 439-466.

[124] P.L. Yeagle, Modulation of membrane function by cholesterol, Biochimie, 73 (1991) 1303-1310.

[125] S. Manes, G. del Real, A.C. Martinez, Pathogens: raft hijackers, Nat Rev Immunol, 3 (2003) 557-568.

[126] C.M. Rosenberger, J.H. Brumell, B.B. Finlay, Microbial pathogenesis: lipid rafts as pathogen portals, Curr Biol, 10 (2000) R823-R825.

[127] F.G. van der Goot, T. Harder, Raft membrane domains: from a liquid-ordered membrane phase to a site of pathogen attack, Semin Immunol, 13 (2001) 89-97.

[128] O.G. Mouritsen, M.J. Zuckermann, What's so special about cholesterol?, Lipids, 39 (2004) 1101-1113.

[129] D.A. Brown, E. London, Functions of lipid rafts in biological membranes, Annu Rev Cell Dev Biol, 14 (1998) 111-136.

[130] A.I. Greenwood, J. Pan, T.T. Mills, J.F. Nagle, R.M. Epand, S. Tristram-Nagle, CRAC motif peptide of the HIV-1 gp41 protein thins SOPC membranes and interacts with cholesterol, Biochim Biophys Acta, 1778 (2008) 1120-1130.

[131] H. Li, V. Papadopoulos, Peripheral-type benzodiazepine receptor function in cholesterol transport. Identification of a putative cholesterol recognition/interaction amino acid sequence and consensus pattern, Endocrinology, 139 (1998) 4991-4997.

[132] B. Thaa, I. Levental, A. Herrmann, M. Veit, Intrinsic membrane association of the cytoplasmic tail of influenza virus M2 protein and lateral membrane sorting regulated by cholesterol binding and palmitoylation, Biochem J, 437 (2011) 389-397.

[133] G. Polekhina, K.S. Giddings, R.K. Tweten, M.W. Parker, Insights into the action of the superfamily of cholesterol-dependent cytolysins from studies of intermedilysin, Proc Natl Acad Sci U S A, 102 (2005) 600-605.

[134] P.E. Kuwabara, M. Labouesse, The sterol-sensing domain: multiple families, a unique role?, Trends Genet, 18 (2002) 193-201.

[135] A.J. Farrand, S. LaChapelle, E.M. Hotze, A.E. Johnson, R.K. Tweten, Only two amino acids are essential for cytolytic toxin recognition of cholesterol at the membrane surface, Proc Natl Acad Sci U S A, 107 (2010) 4341-4346.

[136] Y. Tang, I.C. Leao, E.M. Coleman, R.S. Broughton, J.E. Hildreth, Deficiency of niemann-pick type C-1 protein impairs release of human immunodeficiency virus type 1 and results in Gag accumulation in late endosomal/lysosomal compartments, J Virol, 83 (2009) 7982-7995.

[137] J.E. Carette, M. Raaben, A.C. Wong, A.S. Herbert, G. Obernosterer, N. Mulherkar, A.I. Kuehne, P.J. Kranzusch, A.M. Griffin, G. Ruthel, P. Dal Cin, J.M. Dye, S.P. Whelan, K. Chandran, T.R. Brummelkamp, Ebola virus entry requires the cholesterol transporter Niemann-Pick C1, Nature, 477 (2011) 340-343.

[138] K. Boesze-Battaglia, A. Brown, L. Walker, D. Besack, A. Zekavat, S. Wrenn, C. Krummenacher, B.J. Shenker, Cytolethal distending toxin-induced cell cycle arrest of lymphocytes is dependent upon recognition and binding to cholesterol, J Biol Chem, 284 (2009) 10650-10658.

[139] C.J. Baier, J. Fantini, F.J. Barrantes, Disclosure of cholesterol recognition motifs in transmembrane domains of the human nicotinic acetylcholine receptor, Sci Rep, 1 (2011) 69.

[140] J. Fantini, F.J. Barrantes, How cholesterol interacts with membrane proteins: an exploration of cholesterol-binding sites including CRAC, CARC, and tilted domains, Frontiers in physiology, 4 (2013) 31.

[141] J. Fantini, C. Di Scala, L.S. Evans, P.T. Williamson, F.J. Barrantes, A mirror code for protein-cholesterol interactions in the two leaflets of biological membranes, Sci Rep, 6 (2016) 21907.

[142] N. Jamin, J.M. Neumann, M.A. Ostuni, T.K. Vu, Z.X. Yao, S. Murail, J.C. Robert, C. Giatzakis, V. Papadopoulos, J.J. Lacapere, Characterization of the cholesterol recognition amino acid consensus sequence of the peripheral-type benzodiazepine receptor, Mol Endocrinol, 19 (2005) 588-594.

[143] R.F. Epand, A. Thomas, R. Brasseur, S.A. Vishwanathan, E. Hunter, R.M. Epand, Juxtamembrane protein segments that contribute to recruitment of cholesterol into domains, Biochemistry, 45 (2006) 6105-6114.

[144] I.A. Pikuleva, R.L. Mackman, N. Kagawa, M.R. Waterman, P.R. Ortiz de Montellano, Active-site topology of bovine cholesterol side-chain cleavage cytochrome P450 (P450scc) and evidence for interaction of tyrosine 94 with the side chain of cholesterol, Arch Biochem Biophys, 322 (1995) 189-197.

[145] R.M. Epand, Cholesterol and the interaction of proteins with membrane domains, Prog Lipid Res, 45 (2006) 279-294.

[146] F. Li, Y. Xia, J. Meiler, S. Ferguson-Miller, Characterization and modeling of the oligomeric state and ligand binding behavior of purified translocator protein 18 kDa from Rhodobacter sphaeroides, Biochemistry, 52 (2013) 5884-5899.

[147] M.A. Listowski, J. Leluk, S. Kraszewski, A.F. Sikorski, Cholesterol Interaction with the MAGUK Protein Family Member, MPP1, via CRAC and CRAC-Like Motifs: An In Silico Docking Analysis, PLoS One, 10 (2015) e0133141.

[148] A.D. Dergunov, Mutation mapping of apolipoprotein A-I structure assisted with the putative cholesterol recognition regions, Biochim Biophys Acta, 1834 (2013) 2030-2035.

[149] M.R. Elkins, J.K. Williams, M.D. Gelenter, P. Dai, B. Kwon, I.V. Sergeyev, B.L. Pentelute, M. Hong, Cholesterol-binding site of the influenza M2 protein in lipid bilayers from solid-state NMR, Proc Natl Acad Sci U S A, 114 (2017) 12946-12951.

[150] M. Palmer, Cholesterol and the activity of bacterial toxins, FEMS Microbiol Lett, 238 (2004) 281-289.

[151] S. Scolari, K. Muller, R. Bittman, A. Herrmann, P. Muller, Interaction of mammalian seminal plasma protein PDC-109 with cholesterol: implications for a putative CRAC domain, Biochemistry, 49 (2010) 9027-9031.

[152] S.P. Pydi, M. Jafurulla, L. Wai, R.P. Bhullar, P. Chelikani, A. Chattopadhyay, Cholesterol modulates bitter taste receptor function, Biochim Biophys Acta, 1858 (2016) 2081-2087.

[153] K. Salzwedel, J.T. West, E. Hunter, A conserved tryptophan-rich motif in the membrane-proximal region of the human immunodeficiency virus type 1 gp41 ectodomain is important for Env-mediated fusion and virus infectivity, J Virol, 73 (1999) 2469-2480.

[154] L.M. Molinos-Albert, E. Bilbao, L. Agullo, S. Marfil, E. Garcia, M.L. Rodriguez de la Concepcion, N. Izquierdo-Useros, C. Vilaplana, J.A. Nieto-Garai, F.X. Contreras, M. Floor, P.J. Cardona, J. Martinez-Picado, B. Clotet, J. Villa-Freixa, M. Lorizate, J. Carrillo, J. Blanco, Proteoliposomal formulations of an HIV-1 gp41-based miniprotein elicit a lipid-dependent immunodominant response overlapping the 2F5 binding motif, Sci Rep, 7 (2017) 40800.

[155] A. Saez-Cirion, S. Nir, M. Lorizate, A. Agirre, A. Cruz, J. Perez-Gil, J.L. Nieva, Sphingomyelin and cholesterol promote HIV-1 gp41 pretransmembrane sequence surface aggregation and membrane restructuring, J Biol Chem, 277 (2002) 21776-21785.

[156] C. Schroeder, H. Heider, E. Moncke-Buchner, T.I. Lin, The influenza virus ion channel and maturation cofactor M2 is a cholesterol-binding protein, Eur Biophys J, 34 (2005) 52-66.

[157] A. Luz-Madrigal, A. Asanov, A.R. Camacho-Zarco, A. Sampieri, L. Vaca, A cholesterol recognition amino acid consensus domain in GP64 fusion protein facilitates anchoring of baculovirus to mammalian cells, J Virol, 87 (2013) 11894-11907.

[158] S.A. Connolly, R. Longnecker, Residues within the C-terminal arm of the herpes simplex virus 1 glycoprotein B ectodomain contribute to its refolding during the fusion step of virus entry, J Virol, 86 (2012) 6386-6393.

[159] M. Jafurulla, S. Tiwari, A. Chattopadhyay, Identification of cholesterol recognition amino acid consensus (CRAC) motif in G-protein coupled receptors, Biochem Biophys Res Commun, 404 (2011) 569-573.

[160] R.A. Hall, R.T. Premont, C.W. Chow, J.T. Blitzer, J.A. Pitcher, A. Claing, R.H. Stoffel, L.S. Barak, S. Shenolikar, E.J. Weinman, S. Grinstein, R.J. Lefkowitz, The beta2-adrenergic receptor interacts with the Na+/H+-exchanger regulatory factor to control Na+/H+ exchange, Nature, 392 (1998) 626-630.

[161] K. Palczewski, C.L. Verlinde, F. Haeseleer, Molecular mechanism of visual transduction, Novartis Found Symp, 224 (1999) 191-204; discussion 204-197.

[162] A.L. Garcia-Garcia, A. Newman-Tancredi, E.D. Leonardo, 5-HT(1A) [corrected] receptors in mood and anxiety: recent insights into autoreceptor versus heteroreceptor function, Psychopharmacology (Berl), 231 (2014) 623-636.

[163] E. Lyman, C. Higgs, B. Kim, D. Lupyan, J.C. Shelley, R. Farid, G.A. Voth, A role for a specific cholesterol interaction in stabilizing the Apo configuration of the human A(2A) adenosine receptor, Structure, 17 (2009) 1660-1668.

[164] K. Burger, G. Gimpl, F. Fahrenholz, Regulation of receptor function by cholesterol, Cell Mol Life Sci, 57 (2000) 1577-1592.

[165] G. Khelashvili, A. Grossfield, S.E. Feller, M.C. Pitman, H. Weinstein, Structural and dynamic effects of cholesterol at preferred sites of interaction with rhodopsin identified from microsecond length molecular dynamics simulations, Proteins, 76 (2009) 403-417.

[166] G. Gimpl, K. Burger, F. Fahrenholz, A closer look at the cholesterol sensor, Trends Biochem Sci, 27 (2002) 596-599.

[167] H. Ohvo-Rekila, B. Ramstedt, P. Leppimaki, J.P. Slotte, Cholesterol interactions with phospholipids in membranes, Prog Lipid Res, 41 (2002) 66-97.

[168] A.G. Lee, How lipids affect the activities of integral membrane proteins, Biochim Biophys Acta, 1666 (2004) 62-87.

[169] Y.D. Paila, A. Chattopadhyay, The function of G-protein coupled receptors and membrane cholesterol: specific or general interaction?, Glycoconj J, 26 (2009) 711-720.

[170] T.J. Pucadyil, A. Chattopadhyay, Role of cholesterol in the function and organization of G-protein coupled receptors, Prog Lipid Res, 45 (2006) 295-333.

[171] D. Sengupta, A. Chattopadhyay, Molecular dynamics simulations of GPCR-cholesterol interaction: An emerging paradigm, Biochim Biophys Acta, 1848 (2015) 1775-1782.

[172] S.A. Vishwanathan, A. Thomas, R. Brasseur, R.F. Epand, E. Hunter, R.M. Epand, Hydrophobic substitutions in the first residue of the CRAC segment of the gp41 protein of HIV, Biochemistry, 47 (2008) 124-130.

[173] S.A. Vishwanathan, A. Thomas, R. Brasseur, R.F. Epand, E. Hunter, R.M. Epand, Large changes in the CRAC segment of gp41 of HIV do not destroy fusion activity if the segment interacts with cholesterol, Biochemistry, 47 (2008) 11869-11876.

[174] H. Li, Z. Yao, B. Degenhardt, G. Teper, V. Papadopoulos, Cholesterol binding at the cholesterol recognition/ interaction amino acid consensus (CRAC) of the peripheral-type benzodiazepine receptor and inhibition of steroidogenesis by an HIV TAT-CRAC peptide, Proc Natl Acad Sci U S A, 98 (2001) 1267-1272.

[175] T. Tsfasman, V. Kost, S. Markushin, V. Lotte, I. Koptiaeva, E. Bogacheva, L. Baratova, V. Radyukhin, Amphipathic alpha-helices and putative cholesterol binding domains of the influenza virus matrix M1 protein are crucial for virion structure organisation, Virus Res, 210 (2015) 114-118.

[176] S. Oddi, E. Dainese, F. Fezza, M. Lanuti, D. Barcaroli, V. De Laurenzi, D. Centonze, M. Maccarrone, Functional characterization of putative cholesterol binding sequence (CRAC) in human type-1 cannabinoid receptor, J Neurochem, 116 (2011) 858-865.

[177] L.J. Sharpe, G. Rao, P.M. Jones, E. Glancey, S.M. Aleidi, A.M. George, A.J. Brown, I.C. Gelissen, Cholesterol sensing by the ABCG1 lipid transporter: Requirement of a

CRAC motif in the final transmembrane domain, Biochim Biophys Acta, 1851 (2015) 956-964.

[178] Z. Gal, C. Hegedus, G. Szakacs, A. Varadi, B. Sarkadi, C. Ozvegy-Laczka, Mutations of the central tyrosines of putative cholesterol recognition amino acid consensus (CRAC) sequences modify folding, activity, and sterol-sensing of the human ABCG2 multidrug transporter, Biochim Biophys Acta, 1848 (2015) 477-487.

[179] A.K. Singh, J. McMillan, A.N. Bukiya, B. Burton, A.L. Parrill, A.M. Dopico, Multiple cholesterol recognition/interaction amino acid consensus (CRAC) motifs in cytosolic C tail of Slo1 subunit determine cholesterol sensitivity of Ca2+- and voltage-gated K+ (BK) channels, J Biol Chem, 287 (2012) 20509-20521.

[180] J. Fantini, F.J. Barrantes, Sphingolipid/cholesterol regulation of neurotransmitter receptor conformation and function, Biochim Biophys Acta, 1788 (2009) 2345-2361.

[181] M.A. Hanson, V. Cherezov, M.T. Griffith, C.B. Roth, V.P. Jaakola, E.Y. Chien, J. Velasquez, P. Kuhn, R.C. Stevens, A specific cholesterol binding site is established by the 2.8 A structure of the human beta2-adrenergic receptor, Structure, 16 (2008) 897-905.

[182] C.M. Miller, A.C. Brown, J. Mittal, Disorder in cholesterol-binding functionality of CRAC peptides: a molecular dynamics study, J. Phys. Chem. B, 118 (2014) 13169-13174.

[183] E. Strandberg, J.A. Killian, Snorkeling of lysine side chains in transmembrane helices: how easy can it get?, FEBS Lett, 544 (2003) 69-73.

[184] A.C. Johansson, E. Lindahl, Amino-acid solvation structure in transmembrane helices from molecular dynamics simulations, Biophys J, 91 (2006) 4450-4463.

[185] A.C. Johansson, E. Lindahl, The role of lipid composition for insertion and stabilization of amino acids in membranes, J Chem Phys, 130 (2009) 185101.

[186] J.P. Ulmschneider, M. Andersson, M.B. Ulmschneider, Determining peptide partitioning properties via computer simulation, J Membr Biol, 239 (2011) 15-26.

[187] R.F. Epand, B.G. Sayer, R.M. Epand, The tryptophan-rich region of HIV gp41 and the promotion of cholesterol-rich domains, Biochemistry, 44 (2005) 5525-5531.

[188] Z. Liao, L.M. Cimakasky, R. Hampton, D.H. Nguyen, J.E. Hildreth, Lipid rafts and HIV pathogenesis: host membrane cholesterol is required for infection by HIV type 1, AIDS Res Hum Retroviruses, 17 (2001) 1009-1019.

[189] P. Scheiffele, M.G. Roth, K. Simons, Interaction of influenza virus haemagglutinin with sphingolipid-cholesterol membrane domains via its transmembrane domain, EMBO J, 16 (1997) 5501-5508.

[190] D.H. Fine, D. Furgang, H.C. Schreiner, P. Goncharoff, J. Charlesworth, G. Ghazwan, P. Fitzgerald-Bocarsly, D.H. Figurski, Phenotypic variation in Actinobacillus actinomycetemcomitans during laboratory growth: implications for virulence, Microbiology, 145 (Pt 6) (1999) 1335-1347.

[191] S.C. Kachlany, D.H. Fine, D.H. Figurski, Purification of secreted leukotoxin (LtxA) from Actinobacillus actinomycetemcomitans, Protein Expr Purif, 25 (2002) 465-471.

[192] A.D. Bangham, R.W. Horne, Negative Staining of Phospholipids and Their Structural Modification by Surface-Active Agents as Observed in the Electron Microscope, J Mol Biol, 8 (1964) 660-668.

[193] R.C. MacDonald, R.I. MacDonald, B.P. Menco, K. Takeshita, N.K. Subbarao, L.R. Hu, Small-volume extrusion apparatus for preparation of large, unilamellar vesicles, Biochim Biophys Acta, 1061 (1991) 297-303.

[194] J.T. Buboltz, G.W. Feigenson, A novel strategy for the preparation of liposomes: rapid solvent exchange, Biochim Biophys Acta, 1417 (1999) 232-245.

[195] D.J. Estes, M. Mayer, Electroformation of giant liposomes from spin-coated films of lipids, Colloids Surf B Biointerfaces, 42 (2005) 115-123.

[196] M.I. Angelova, S. Soléau, P. Méléard, F. Faucon, P. Bothorel, Preparation of giant vesicles by external AC electric fields. Kinetics and applications, Trends in Colloid and Interface Science VI, 89 (1992) 127-131.

[197] J.A. Sophianopoulos, S.J. Durham, A.J. Sophianopoulos, H.L. Ragsdale, W.P. Cropper, Jr., Ultrafiltration is theoretically equivalent to equilibrium dialysis but much simpler to carry out, Arch. Biochem. Biophys., 187 (1978) 132-137.

[198] L. Voglino, T.J. McIntosh, S.A. Simon, Modulation of the binding of signal peptides to lipid bilayers by dipoles near the hydrocarbon-water interface, Biochemistry, 37 (1998) 12241-12252.

[199] L. Voglino, S.A. Simon, T.J. McIntosh, Orientation of LamB signal peptides in bilayers: influence of lipid probes on peptide binding and interpretation of fluorescence quenching data, Biochemistry, 38 (1999) 7509-7516.

[200] E. Freire, O.L. Mayorga, M. Straume, Isothermal Titration Calorimetry, Analytical Chemistry, 62 (1990) A950-A959.

[201] L. Whitmore, B.A. Wallace, DICHROWEB, an online server for protein secondary structure analyses from circular dichroism spectroscopic data, Nucleic Acids Res, 32 (2004) W668-W673.

[202] L. Whitmore, B.A. Wallace, Protein secondary structure analyses from circular dichroism spectroscopy: methods and reference databases, Biopolymers, 89 (2008) 392-400.

[203] J.G. Lees, A.J. Miles, F. Wien, B.A. Wallace, A reference database for circular dichroism spectroscopy covering fold and secondary structure space, Bioinformatics, 22 (2006) 1955-1962.

[204] A. Abdul-Gader, A.J. Miles, B.A. Wallace, A reference dataset for the analyses of membrane protein secondary structures and transmembrane residues using circular dichroism spectroscopy, Bioinformatics, 27 (2011) 1630-1636.

[205] S.W. Provencher, J. Glockner, Estimation of globular protein secondary structure from circular dichroism, Biochemistry, 20 (1981) 33-37.

[206] I.H. van Stokkum, H.J. Spoelder, M. Bloemendal, R. van Grondelle, F.C. Groen, Estimation of protein secondary structure and error analysis from circular dichroism spectra, Anal Biochem, 191 (1990) 110-118.

[207] J. Schindelin, I. Arganda-Carreras, E. Frise, V. Kaynig, M. Longair, T. Pietzsch, S. Preibisch, C. Rueden, S. Saalfeld, B. Schmid, J.Y. Tinevez, D.J. White, V. Hartenstein, K. Eliceiri, P. Tomancak, A. Cardona, Fiji: an open-source platform for biological-image analysis, Nat Methods, 9 (2012) 676-682.

[208] Handbook of Surface Plasmon Resonance, 2 ed., Royal Society of Chemistry, 2017.

[209] M.F. Harris, Logan, J.L., Determination of log Kow Values for Four Drugs, Journal of Chemical Education, 91 (2014) 915-918.

[210] Product Properties Test Guidelines: OPPTS 830.7550 Partition Coefficient (n-Octanol/Water), Shake Flask Method, in, United States Environmental Protection Agency, 1996.

[211] A. Magarkar, V. Dhawan, P. Kallinteri, T. Viitala, M. Elmowafy, T. Rog, A. Bunker, Cholesterol level affects surface charge of lipid membranes in saline solution, Sci Rep, 4 (2014) 5005.

[212] B.C. Evans, C.E. Nelson, S.S. Yu, K.R. Beavers, A.J. Kim, H. Li, H.M. Nelson, T.D. Giorgio, C.L. Duvall, Ex vivo red blood cell hemolysis assay for the evaluation of pH-responsive endosomolytic agents for cytosolic delivery of biomacromolecular drugs, J Vis Exp, (2013) e50166.

[213] P.M. Fives-Taylor, D.H. Meyer, K.P. Mintz, C. Brissette, Virulence factors of Actinobacillus actinomycetemcomitans, Periodontol 2000, 20 (1999) 136-167.

[214] E. London, Diphtheria toxin: membrane interaction and membrane translocation, Biochim Biophys Acta, 1113 (1992) 25-51.

[215] R.R. Isberg, G. Tran Van Nhieu, Binding and internalization of microorganisms by integrin receptors, Trends Microbiol, 2 (1994) 10-14.

[216] E.A. Merritt, W.G. Hol, AB5 toxins, Curr Opin Struct Biol, 5 (1995) 165-171.

[217] M.W. Parker, A.D. Tucker, D. Tsernoglou, F. Pattus, Insights into membrane insertion based on studies of colicins, Trends Biochem Sci, 15 (1990) 126-129.

[218] J. Van Rie, S. Jansens, H. Hofte, D. Degheele, H. Van Mellaert, Specificity of Bacillus thuringiensis delta-endotoxins. Importance of specific receptors on the brush border membrane of the mid-gut of target insects, Eur J Biochem, 186 (1989) 239-247.

[219] I. Barcena-Uribarri, R. Benz, M. Winterhalter, E. Zakharian, N. Balashova, Pore forming activity of the potent RTX-toxin produced by pediatric pathogen Kingella kingae: Characterization and comparison to other RTX-family members, Biochim Biophys Acta, 1848 (2015) 1536-1544.

[220] C. Martin, M.A. Requero, J. Masin, I. Konopasek, F.M. Goni, P. Sebo, H. Ostolaza, Membrane restructuring by Bordetella pertussis adenylate cyclase toxin, a member of the RTX toxin family, J Bacteriol, 186 (2004) 3760-3765.

[221] K.P. Fong, C.M. Pacheco, L.L. Otis, S. Baranwal, I.R. Kieba, G. Harrison, E.V. Hersh, K. Boesze-Battaglia, E.T. Lally, *Actinobacillus actinomycetemcomitans* leukotoxin requires lipid microdomains for target cell cytotoxicity, Cell Microbiol, 8 (2006) 1753-1767.

[222] L. Bumba, J. Masin, R. Fiser, P. Sebo, Bordetella adenylate cyclase toxin mobilizes its beta2 integrin receptor into lipid rafts to accomplish translocation across target cell membrane in two steps, PLoS Pathog, 6 (2010) e1000901.

[223] D.N. Atapattu, C.J. Czuprynski, Mannheimia haemolytica leukotoxin binds to lipid rafts in bovine lymphoblastoid cells and is internalized in a dynamin-2- and clathrin-dependent manner, Infect Immun, 75 (2007) 4719-4727.

[224] A. Arora, H. Raghuraman, A. Chattopadhyay, Influence of cholesterol and ergosterol on membrane dynamics: a fluorescence approach, Biochem Biophys Res Commun, 318 (2004) 920-926.

[225] E. Endress, H. Heller, H. Casalta, M.F. Brown, T.M. Bayerl, Anisotropic motion and molecular dynamics of cholesterol, lanosterol, and ergosterol in lecithin bilayers studied by quasi-elastic neutron scattering, Biochemistry, 41 (2002) 13078-13086.

[226] R. Krivanek, L. Okoro, R. Winter, Effect of cholesterol and ergosterol on the compressibility and volume fluctuations of phospholipid-sterol bilayers in the critical point region: a molecular acoustic and calorimetric study, Biophys J, 94 (2008) 3538-3548.

[227] J.A. Urbina, S. Pekerar, H.B. Le, J. Patterson, B. Montez, E. Oldfield, Molecular order and dynamics of phosphatidylcholine bilayer membranes in the presence of cholesterol, ergosterol and lanosterol: a comparative study using 2H-, 13C- and 31P-NMR spectroscopy, Biochim Biophys Acta, 1238 (1995) 163-176.

[228] G. van Meer, D.R. Voelker, G.W. Feigenson, Membrane lipids: where they are and how they behave, Nat Rev Mol Cell Biol, 9 (2008) 112-124.

[229] K. Simons, E. Ikonen, Functional rafts in cell membranes, Nature, 387 (1997) 569-572.

[230] K. Simons, D. Toomre, Lipid rafts and signal transduction, Nat Rev Mol Cell Biol, 1 (2000) 31-39.

[231] R. Varma, S. Mayor, GPI-anchored proteins are organized in submicron domains at the cell surface, Nature, 394 (1998) 798-801.

[232] B. Chini, M. Parenti, G-protein coupled receptors in lipid rafts and caveolae: how, when and why do they go there?, J Mol Endocrinol, 32 (2004) 325-338.

[233] X. Liang, A. Nazarian, H. Erdjument-Bromage, W. Bornmann, P. Tempst, M.D. Resh, Heterogeneous fatty acylation of Src family kinases with polyunsaturated fatty acids regulates raft localization and signal transduction, J Biol Chem, 276 (2001) 30987-30994.

[234] J. Gatfield, J. Pieters, Essential role for cholesterol in entry of mycobacteria into macrophages, Science, 288 (2000) 1647-1650.

[235] T.J. Pucadyil, A. Chattopadhyay, Cholesterol: a potential therapeutic target in *Leishmania* infection?, Trends Parasitol, 23 (2007) 49-53.

[236] J. Pieters, J. Gatfield, Hijacking the host: survival of pathogenic mycobacteria inside macrophages, Trends Microbiol, 10 (2002) 142-146.

[237] K. Boesze-Battaglia, D. Besack, T. McKay, A. Zekavat, L. Otis, K. Jordan-Sciutto, B.J. Shenker, Cholesterol-rich membrane microdomains mediate cell cycle arrest induced by Actinobacillus actinomycetemcomitans cytolethal-distending toxin, Cell Microbiol, 8 (2006) 823-836.

[238] K.S. Giddings, J. Zhao, P.J. Sims, R.K. Tweten, Human CD59 is a receptor for the cholesterol-dependent cytolysin intermedilysin, Nat Struct Mol Biol, 11 (2004) 1173-1178.

[239] C.H. Lai, C.K. Lai, Y.J. Lin, C.L. Hung, C.H. Chu, C.L. Feng, C.S. Chang, H.L. Su, Characterization of putative cholesterol recognition/interaction amino acid consensus-like motif of Campylobacter jejuni cytolethal distending toxin C, PLoS One, 8 (2013) e66202.

[240] P.A. Orlandi, P.H. Fishman, Filipin-dependent inhibition of cholera toxin: evidence for toxin internalization and activation through caveolae-like domains, J Cell Biol, 141 (1998) 905-915.

[241] H.K. Patel, D.C. Willhite, R.M. Patel, D. Ye, C.L. Williams, E.M. Torres, K.B. Marty, R.A. MacDonald, S.R. Blanke, Plasma membrane cholesterol modulates cellular vacuolation induced by the Helicobacter pylori vacuolating cytotoxin, Infect Immun, 70 (2002) 4112-4123.

[242] W. Schraw, Y. Li, M.S. McClain, F.G. van der Goot, T.L. Cover, Association of Helicobacter pylori vacuolating toxin (VacA) with lipid rafts, J Biol Chem, 277 (2002) 34642-34650.

[243] M. Zhou, Q. Zhang, J. Zhao, M. Jin, Haemophilus parasuis encodes two functional cytolethal distending toxins: CdtC contains an atypical cholesterol recognition/interaction region, PLoS One, 7 (2012) e32580.

[244] X. Sun, G.R. Whittaker, Role for influenza virus envelope cholesterol in virus entry and infection, J Virol, 77 (2003) 12543-12551.

[245] M. Guyader, E. Kiyokawa, L. Abrami, P. Turelli, D. Trono, Role for human immunodeficiency virus type 1 membrane cholesterol in viral internalization, J Virol, 76 (2002) 10356-10364.

[246] S. Bavari, C.M. Bosio, E. Wiegand, G. Ruthel, A.B. Will, T.W. Geisbert, M. Hevey, C. Schmaljohn, A. Schmaljohn, M.J. Aman, Lipid raft microdomains: a gateway for compartmentalized trafficking of Ebola and Marburg viruses, J Exp Med, 195 (2002) 593-602.

[247] K.M. DiFranco, A. Gupta, L.E. Galusha, J. Perez, T.V. Nguyen, C.D. Fineza, S.C. Kachlany, Leukotoxin (Leukothera(R)) targets active leukocyte function antigen-1 (LFA-1) protein and triggers a lysosomal mediated cell death pathway, J Biol Chem, 287 (2012) 17618-17627.

[248] S.C. Kachlany, A.B. Schwartz, N.V. Balashova, C.E. Hioe, M. Tuen, A. Le, M. Kaur, Y. Mei, J. Rao, Anti-leukemia activity of a bacterial toxin with natural specificity for LFA-1 on white blood cells, Leuk Res, 34 (2010) 777-785.

[249] I.R. Kieba, K.P. Fong, H.Y. Tang, K.E. Hoffman, D.W. Speicher, L.B. Klickstein, E.T. Lally, Aggregatibacter actinomycetemcomitans leukotoxin requires beta-sheets 1 and 2 of the human CD11a beta-propeller for cytotoxicity, Cell Microbiol, 9 (2007) 2689-2699.

[250] M.J. Walters, A.C. Brown, T.C. Edrington, S. Baranwal, Y. Du, E.T. Lally, K. Boesze-Battaglia, Membrane association and destabilization by Aggregatibacter actinomycetemcomitans leukotoxin requires changes in secondary structures, Mol Oral Microbiol, 28 (2013) 342-353.

[251] J.D. Lear, D. Karakelian, U. Furblur, E.T. Lally, J.C. Tanaka, Conformational studies of Actinobacillus actinomycetemcomitans leukotoxin: partial denaturation enhances toxicity, Biochim Biophys Acta, 1476 (2000) 350-362.

[252] J. Oates, B. Faust, H. Attrill, P. Harding, M. Orwick, A. Watts, The role of cholesterol on the activity and stability of neurotensin receptor 1, Biochim Biophys Acta, 1818 (2012) 2228-2233.

[253] C.D. Lin, C.K. Lai, Y.H. Lin, J.T. Hsieh, Y.T. Sing, Y.C. Chang, K.C. Chen, W.C. Wang, H.L. Su, C.H. Lai, Cholesterol depletion reduces entry of Campylobacter jejuni cytolethal distending toxin and attenuates intoxication of host cells, Infect Immun, 79 (2011) 3563-3575.

[254] P. Danthi, M. Chow, Cholesterol removal by methyl-beta-cyclodextrin inhibits poliovirus entry, J Virol, 78 (2004) 33-41.

[255] A.A. Waheed, Y. Shimada, H.F. Heijnen, M. Nakamura, M. Inomata, M. Hayashi, S. Iwashita, J.W. Slot, Y. Ohno-Iwashita, Selective binding of perfringolysin O derivative to cholesterol-rich membrane microdomains (rafts), Proc Natl Acad Sci U S A, 98 (2001) 4926-4931.

[256] T.M. Allen, P.R. Cullis, Liposomal drug delivery systems: from concept to clinical applications, Adv Drug Deliv Rev, 65 (2013) 36-48.

[257] G.T. Noble, J.F. Stefanick, J.D. Ashley, T. Kiziltepe, B. Bilgicer, Ligand-targeted liposome design: challenges and fundamental considerations, Trends Biotechnol, 32 (2014) 32-45.

[258] M. Alavi, N. Karimi, M. Safaei, Application of Various Types of Liposomes in Drug Delivery Systems, Adv Pharm Bull, 7 (2017) 3-9.

[259] B.D. Henry, D.R. Neill, K.A. Becker, S. Gore, L. Bricio-Moreno, R. Ziobro, M.J. Edwards, K. Muhlemann, J. Steinmann, B. Kleuser, L. Japtok, M. Luginbuhl, H. Wolfmeier, A. Scherag, E. Gulbins, A. Kadioglu, A. Draeger, E.B. Babiychuk, Engineered liposomes sequester bacterial exotoxins and protect from severe invasive infections in mice, Nat Biotechnol, 33 (2015) 81-88.

[260] A. Pokorny, L.E. Yandek, A.I. Elegbede, A. Hinderliter, P.F. Almeida, Temperature and composition dependence of the interaction of delta-lysin with ternary mixtures of sphingomyelin/cholesterol/POPC, Biophys J, 91 (2006) 2184-2197.

[261] S.L. Veatch, S.L. Keller, Miscibility phase diagrams of giant vesicles containing sphingomyelin, Phys Rev Lett, 94 (2005) 148101.

[262] A.C. Brown, K.B. Towles, S.P. Wrenn, Measuring raft size as a function of membrane composition in PC-based systems: Part II--ternary systems, Langmuir, 23 (2007) 11188-11196.

[263] J. Seelig, P. Ganz, Nonclassical hydrophobic effect in membrane binding equilibria, Biochemistry, 30 (1991) 9354-9359.

[264] A.K. Bronowska, Thermodynamics of Ligand-Protein Interactions: Implications for Molecular Design, in: Thermodynamics - Interaction Studies - Solids, Liquids and Gases, InTech, 2011, pp. 1-49.

[265] I. Luque, E. Freire, Structure-based prediction of binding affinities and molecular design of peptide ligands, Methods Enzymol, 295 (1998) 100-127.

[266] J.E. Ladbury, G. Klebe, E. Freire, Adding calorimetric data to decision making in lead discovery: a hot tip, Nat Rev Drug Discov, 9 (2010) 23-27.

[267] S. Nunez, J. Venhorst, C.G. Kruse, Target-drug interactions: first principles and their application to drug discovery, Drug Discov Today, 17 (2012) 10-22.

[268] M.E. Schroeder, H.a. Hostetler, F. Schroeder, J.M. Ball, Elucidation of the Rotavirus NSP4-Caveolin-1 and -Cholesterol Interactions Using Synthetic Peptides., Journal of amino acids, 12 (2012) 16.

[269] T. Parasassi, G. De Stasio, A. d'Ubaldo, E. Gratton, Phase fluctuation in phospholipid membranes revealed by Laurdan fluorescence, Biophys J, 57 (1990) 1179-1186.

[270] T. Dileepan, S.C. Kachlany, N.V. Balashova, J. Patel, S.K. Maheswaran, Human CD18 is the functional receptor for Aggregatibacter actinomycetemcomitans leukotoxin, Infect Immun, 75 (2007) 4851-4856.

[271] M. Mukai, M.R. Krause, S.L. Regen, Peptide Recognition of Cholesterol in Fluid Phospholipid Bilayers, J Am Chem Soc, 137 (2015) 12518-12520.

[272] R.M. Epand, B.G. Sayer, R.F. Epand, Peptide-induced formation of cholesterol-rich domains, Biochemistry, 42 (2003) 14677-14689.

[273] M. Nollmann, R. Gilbert, T. Mitchell, M. Sferrazza, O. Byron, The role of cholesterol in the activity of pneumolysin, a bacterial protein toxin, Biophys J, 86 (2004) 3141-3151.

[274] K. Boesze-Battaglia, L.P. Walker, A. Zekavat, M. Dlakic, M.D. Scuron, P. Nygren, B.J. Shenker, The Aggregatibacter actinomycetemcomitans Cytolethal Distending Toxin

Active Subunit CdtB Contains a Cholesterol Recognition Sequence Required for Toxin Binding and Subunit Internalization, Infect Immun, 83 (2015) 4042-4055.

[275] R.F. Vazquez, S.M. Mate, L.S. Bakas, M.M. Fernandez, E.L. Malchiodi, V.S. Herlax, Novel evidence for the specific interaction between cholesterol and alpha-haemolysin of Escherichia coli, Biochem J, 458 (2014) 481-489.

[276] R.D. Hayward, R.J. Cain, E.J. McGhie, N. Phillips, M.J. Garner, V. Koronakis, Cholesterol binding by the bacterial type III translocon is essential for virulence effector delivery into mammalian cells, Mol Microbiol, 56 (2005) 590-603.

[277] J. Szejtli, Introduction and General Overview of Cyclodextrin Chemistry, Chem. Rev., 98 (1998) 1743-1754.

[278] D.R. Graham, E. Chertova, J.M. Hilburn, L.O. Arthur, J.E. Hildreth, Cholesterol depletion of human immunodeficiency virus type 1 and simian immunodeficiency virus with beta-cyclodextrin inactivates and permeabilizes the virions: evidence for virion-associated lipid rafts, J Virol, 77 (2003) 8237-8248.

[279] J.P. Hennessey, Jr., W.C. Johnson, Jr., Information content in the circular dichroism of proteins, Biochemistry, 20 (1981) 1085-1094.

[280] R.K. Das, R.V. Pappu, Conformations of intrinsically disordered proteins are influenced by linear sequence distributions of oppositely charged residues, Proc Natl Acad Sci U S A, 110 (2013) 13392-13397.

[281] M. Dathe, M. Schumann, T. Wieprecht, A. Winkler, M. Beyermann, E. Krause, K. Matsuzaki, O. Murase, M. Bienert, Peptide helicity and membrane surface charge modulate the balance of electrostatic and hydrophobic interactions with lipid bilayers and biological membranes, Biochemistry, 35 (1996) 12612-12622.

[282] C. Hansch, T. Fujita, p-σ-π Analysis. A Method for the Correlation of Biological Activity and Chemical Structure, J. Am. Chem. Soc., 86 (1964) 1616-1626.

[283] A. Leo, C. Hansch, D. Elkins, Partition coefficients and their uses, Chem. Rev., 71 (1971) 526-616.

[284] G. Datta, R.F. Epand, R.M. Epand, M. Chaddha, M.A. Kirksey, D.W. Garber, S. Lund-Katz, M.C. Phillips, S. Hama, M. Navab, A.M. Fogelman, M.N. Palgunachari, J.P. Segrest, G.M. Anantharamaiah, Aromatic residue position on the nonpolar face of class a amphipathic helical peptides determines biological activity, J Biol Chem, 279 (2004) 26509-26517.

[285] A. Keskin, E. Akdogan, C.D. Dunn, Evidence for Amino Acid Snorkeling from a High-Resolution, In Vivo Analysis of Fis1 Tail-Anchor Insertion at the Mitochondrial Outer Membrane, Genetics, 205 (2017) 691-705.

[286] L. Li, I. Vorobyov, T.W. Allen, The different interactions of lysine and arginine side chains with lipid membranes, J Phys Chem B, 117 (2013) 11906-11920.

[287] S. Shrivastava, A. Chattopadhyay, Influence of cholesterol and ergosterol on membrane dynamics using different fluorescent reporter probes, Biochem Biophys Res Commun, 356 (2007) 705-710.

[288] E.J. Dufourc, Sterols and membrane dynamics, J Chem Biol, 1 (2008) 63-77.

[289] A. B., A. Johnson, J. Lewis, M. Raff, K. Roberts, P. Walter, Molecular Biology of the Cell, 4th ed., Garland Science, 2004.

[290] J.L. MacCallum, W.F. Bennett, D.P. Tieleman, Distribution of amino acids in a lipid bilayer from computer simulations, Biophys J, 94 (2008) 3393-3404.

[291] G.A. Weiss, C.K. Watanabe, A. Zhong, A. Goddard, S.S. Sidhu, Rapid mapping of protein functional epitopes by combinatorial alanine scanning, Proc Natl Acad Sci U S A, 97 (2000) 8950-8954.

[292] K.L. Morrison, G.A. Weiss, Combinatorial alanine-scanning, Curr Opin Chem Biol, 5 (2001) 302-307.

[293] T. Hessa, H. Kim, K. Bihlmaier, C. Lundin, J. Boekel, H. Andersson, I. Nilsson, S.H. White, G. von Heijne, Recognition of transmembrane helices by the endoplasmic reticulum translocon, Nature, 433 (2005) 377-381.

[294] J. Kyte, R.F. Doolittle, A simple method for displaying the hydropathic character of a protein, J Mol Biol, 157 (1982) 105-132.

[295] S.M. Simonsen, L. Sando, K.J. Rosengren, C.K. Wang, M.L. Colgrave, N.L. Daly, D.J. Craik, Alanine scanning mutagenesis of the prototypic cyclotide reveals a cluster of residues essential for bioactivity, J Biol Chem, 283 (2008) 9805-9813.

[296] T. Kortemme, D.E. Kim, D. Baker, Computational alanine scanning of protein-protein interfaces, Sci STKE, 2004 (2004) pl2.

[297] I. Massova, P.A. Kollman, Computational Alanine Scanning To Probe Protein−Protein Interactions: A Novel Approach To Evaluate Binding Free Energies, J. Am. Chem. Soc., 121 (1999) 8133-8143.

[298] B.S. Zerbe, D.R. Hall, S. Vajda, A. Whitty, D. Kozakov, Relationship between hot spot residues and ligand binding hot spots in protein-protein interfaces, J Chem Inf Model, 52 (2012) 2236-2244.

[299] O. Keskin, B. Ma, R. Nussinov, Hot regions in protein--protein interactions: the organization and contribution of structurally conserved hot spot residues, J Mol Biol, 345 (2005) 1281-1294.

[300] W. Li, S.J. Hamill, A.M. Hemmings, G.R. Moore, R. James, C. Kleanthous, Dual recognition and the role of specificity-determining residues in colicin E9 DNase-immunity protein interactions, Biochemistry, 37 (1998) 11771-11779.

[301] Z. Hu, B. Ma, H. Wolfson, R. Nussinov, Conservation of polar residues as hot spots at protein interfaces, Proteins, 39 (2000) 331-342.

[302] O. Lichtarge, M.E. Sowa, Evolutionary predictions of binding surfaces and interactions, Curr Opin Struct Biol, 12 (2002) 21-27.

[303] I.S. Moreira, P.A. Fernandes, M.J. Ramos, Hot spots--a review of the protein-protein interface determinant amino-acid residues, Proteins, 68 (2007) 803-812.

[304] A.A. Bogan, K.S. Thorn, Anatomy of hot spots in protein interfaces, J Mol Biol, 280 (1998) 1-9.

[305] C.J. Tsai, S.L. Lin, H.J. Wolfson, R. Nussinov, Studies of protein-protein interfaces: a statistical analysis of the hydrophobic effect, Protein Sci, 6 (1997) 53-64.

[306] N. Ahmed, D. Dobler, M. Dean, P.J. Thornalley, Peptide mapping identifies hotspot site of modification in human serum albumin by methylglyoxal involved in ligand binding and esterase activity, J Biol Chem, 280 (2005) 5724-5732.

[307] M.J. Harms, J.L. Schlessman, G.R. Sue, B. Garcia-Moreno, Arginine residues at internal positions in a protein are always charged, Proc Natl Acad Sci U S A, 108 (2011) 18954-18959.

[308] J.B. Mitchell, C.L. Nandi, I.K. McDonald, J.M. Thornton, S.L. Price, Amino/aromatic interactions in proteins: is the evidence stacked against hydrogen bonding?, J Mol Biol, 239 (1994) 315-331.

[309] A.G. Jamieson, N. Boutard, D. Sabatino, W.D. Lubell, Peptide scanning for studying structure-activity relationships in drug discovery, Chem Biol Drug Des, 81 (2013) 148-165.

[310] R.K. Tweten, Cholesterol-dependent cytolysins, a family of versatile pore-forming toxins, Infect Immun, 73 (2005) 6199-6209.

[311] J.R. Harris, S. Bhakdi, U. Meissner, D. Scheffler, R. Bittman, G. Li, A. Zitzer, M. Palmer, Interaction of the Vibrio cholerae cytolysin (VCC) with cholesterol, some cholesterol esters, and cholesterol derivatives: a TEM study, J Struct Biol, 139 (2002) 122-135.

[312] T. Jank, K. Aktories, Structure and mode of action of clostridial glucosylating toxins: the ABCD model, Trends Microbiol, 16 (2008) 222-229.

[313] M.K. Johnson, D. Boese-Marrazzo, W.A. Pierce, Jr., Effects of pneumolysin on human polymorphonuclear leukocytes and platelets, Infect Immun, 34 (1981) 171-176.

[314] X. Zhao, H. Li, J. Wang, Y. Guo, B. Liu, X. Deng, X. Niu, Verbascoside Alleviates Pneumococcal Pneumonia by Reducing Pneumolysin Oligomers, Mol. Pharmacol., 89 (2016) 376-387.

[315] C.C. Mozola, N. Magassa, M.G. Caparon, A novel cholesterol-insensitive mode of membrane binding promotes cytolysin-mediated translocation by Streptolysin O, Mol Microbiol, 94 (2014) 675-687.

[316] G. Sierig, C. Cywes, M.R. Wessels, C.D. Ashbaugh, Cytotoxic effects of streptolysin o and streptolysin s enhance the virulence of poorly encapsulated group a streptococci, Infect Immun, 71 (2003) 446-455.

[317] S. Brunton, M. Pichichero, Considerations in the use of antibiotics for streptococcal pharyngitis, J Fam Pract, Suppl (2006) S9-16.

[318] E.J. Rosi-Marshall, J.J. Kelly, Antibiotic stewardship should consider environmental fate of antibiotics, Environ Sci Technol, 49 (2015) 5257-5258.

[319] G. Werner, B. Strommenger, W. Witte, Acquired vancomycin resistance in clinically relevant pathogens, Future Microbiol, 3 (2008) 547-562.

[320] J. O'Neill, Review on Antimicrobial Resistance, in, 2014.

[321] Health in 2015: from MDGs to SDGs, in: World Health Organization, 2015, pp. 204.

[322] T. Escajadillo, J. Olson, B.T. Luk, L. Zhang, V. Nizet, A Red Blood Cell Membrane-Camouflaged Nanoparticle Counteracts Streptolysin O-Mediated Virulence Phenotypes of Invasive Group A Streptococcus, Front Pharmacol, 8 (2017) 477.

[323] A. Kadioglu, J.N. Weiser, J.C. Paton, P.W. Andrew, The role of Streptococcus pneumoniae virulence factors in host respiratory colonization and disease, Nat Rev Microbiol, 6 (2008) 288-301.

[324] E. AlonsoDeVelasco, A.F. Verheul, J. Verhoef, H. Snippe, Streptococcus pneumoniae: virulence factors, pathogenesis, and vaccines, Microbiol Rev, 59 (1995) 591-603.

[325] N. Fittipaldi, M. Segura, D. Grenier, M. Gottschalk, Virulence factors involved in the pathogenesis of the infection caused by the swine pathogen and zoonotic agent Streptococcus suis, Future Microbiol, 7 (2012) 259-279.

[326] D.L. Stevens, A.E. Bryant, Severe Group A Streptococcal Infections, in: J.J. Ferretti, D.L. Stevens, V.A. Fischetti (Eds.) Streptococcus pyogenes : Basic Biology to Clinical Manifestations, Oklahoma City (OK), 2016.

[327] J.E. Alouf, Streptococcal toxins (streptolysin O, streptolysin S, erythrogenic toxin), Pharmacol Ther, 11 (1980) 661-717.

[328] B. Limbago, V. Penumalli, B. Weinrick, J.R. Scott, Role of streptolysin O in a mouse model of invasive group A streptococcal disease, Infect Immun, 68 (2000) 6384-6390.

[329] H. Baba, I. Kawamura, C. Kohda, T. Nomura, Y. Ito, T. Kimoto, I. Watanabe, S. Ichiyama, M. Mitsuyama, Essential role of domain 4 of pneumolysin from Streptococcus pneumoniae in cytolytic activity as determined by truncated proteins, Biochem Biophys Res Commun, 281 (2001) 37-44.

[330] J.B. Rubins, A.H. Paddock, D. Charboneau, A.M. Berry, J.C. Paton, E.N. Janoff, Pneumolysin in pneumococcal adherence and colonization, Microb Pathog, 25 (1998) 337-342.

[331] R. Cockeran, R. Anderson, C. Feldman, The role of pneumolysin in the pathogenesis of Streptococcus pneumoniae infection, Curr Opin Infect Dis, 15 (2002) 235-239.

[332] E. Chiarot, C. Faralla, N. Chiappini, G. Tuscano, F. Falugi, G. Gambellini, A. Taddei, S. Capo, E. Cartocci, D. Veggi, A. Corrado, S. Mangiavacchi, S. Tavarini, M. Scarselli, R. Janulczyk, G. Grandi, I. Margarit, G. Bensi, Targeted amino acid substitutions impair

streptolysin O toxicity and group A Streptococcus virulence, MBio, 4 (2013) e00387-00312.

[333] M. Song, L. Li, M. Li, Y. Cha, X. Deng, J. Wang, Apigenin protects mice from pneumococcal pneumonia by inhibiting the cytolytic activity of pneumolysin, Fitoterapia, 115 (2016) 31-36.

[334] K. Gaus, M. Rodriguez, K.R. Ruberu, I. Gelissen, T.M. Sloane, L. Kritharides, W. Jessup, Domain-specific lipid distribution in macrophage plasma membranes, J Lipid Res, 46 (2005) 1526-1538.

[335] G.J. Nelson, Composition of neutral lipids from erythrocytes of common mammals, J Lipid Res, 8 (1967) 374-379.

[336] J.E. Alouf, C. Geoffroy, Production, purification, and assay of streptolysin O, Methods Enzymol, 165 (1988) 52-59.

[337] Product Information Streptolysin O from Streptococcus pyogenes, in, vol. 2018, Sigma-Aldrich.

[338] H. Li, X. Zhao, J. Wang, Y. Dong, S. Meng, R. Li, X. Niu, X. Deng, beta-sitosterol interacts with pneumolysin to prevent Streptococcus pneumoniae infection, Sci Rep, 5 (2015) 17668.

[339] M. Yamaguchi, Y. Terao, Y. Mori-Yamaguchi, H. Domon, Y. Sakaue, T. Yagi, K. Nishino, A. Yamaguchi, V. Nizet, S. Kawabata, Streptococcus pneumoniae invades erythrocytes and utilizes them to evade human innate immunity, PLoS One, 8 (2013) e77282.

[340] M. Arzanlou, S. Bohlooli, Inhibition of streptolysin O by allicin - an active component of garlic, J Med Microbiol, 59 (2010) 1044-1049.

[341] M. Arzanlou, S. Bohlooli, E. Jannati, H. Mirzanejad-Asl, Allicin from garlic neutralizes the hemolytic activity of intra- and extra-cellular pneumolysin O in vitro, Toxicon, 57 (2011) 540-545.

[342] A.I. Iliev, J.R. Djannatian, R. Nau, T.J. Mitchell, F.S. Wouters, Cholesterol-dependent actin remodeling via RhoA and Rac1 activation by the Streptococcus pneumoniae toxin pneumolysin, Proc Natl Acad Sci U S A, 104 (2007) 2897-2902.

[343] M.A. Kehoe, L. Miller, J.A. Walker, G.J. Boulnois, Nucleotide sequence of the streptolysin O (SLO) gene: structural homologies between SLO and other membrane-damaging, thiol-activated toxins, Infect Immun, 55 (1987) 3228-3232.

[344] S. Bhakdi, J. Tranum-Jensen, A. Sziegoleit, Mechanism of membrane damage by streptolysin-O, Infect Immun, 47 (1985) 52-60.

[345] M.R. Amos, G.D. Healey, R.J. Goldstone, S.M. Mahan, A. Duvel, H.J. Schuberth, O. Sandra, P. Zieger, I. Dieuzy-Labaye, D.G. Smith, I.M. Sheldon, Differential endometrial cell sensitivity to a cholesterol-dependent cytolysin links Trueperella pyogenes to uterine disease in cattle, Biol Reprod, 90 (2014) 54.

[346] F. Freeman, Y. Kodera, Garlic chemistry: stability of S-(2- propenyl) 2-propene-1-sulfinothioate (allicin) in blood, solvents, and simulated physiological fluids, J. Agric. Food Chem., 43 (1995) 2332-2338.

[347] G. Assmann, P. Cullen, J. Erbey, D.R. Ramey, F. Kannenberg, H. Schulte, Plasma sitosterol elevations are associated with an increased incidence of coronary events in men: results of a nested case-control analysis of the Prospective Cardiovascular Munster (PROCAM) study, Nutr Metab Cardiovasc Dis, 16 (2006) 13-21.

Vita

Evan Koufos was born on October 7, 1989, in Point Pleasant, NJ, to Nikolaos (Nick) and Soteroulla (Terry) Koufos, and was raised in Toms River, NJ. He is the elder of their two children. Upon graduation from Toms River High School North, Toms River, NJ, in 2008, Evan attended Rutgers University and subsequently received a Bachelor of Science degree in chemical engineering and biomathematics in 2013. During his time at Rutgers, Evan was an active participant and elected treasurer of the Rutgers University Bioengineering Society. In his final year he was inducted into Tau Beta Pi: The National Engineering Honor Society, Sigma Xi: The Scientific Research Honor Society, and had the opportunity to become a James J. Slade Scholar under the supervision of Dr. Meenakshi Dutt, where he completed his undergraduate thesis on the mechanical properties of lipid bilayers utilizing dissipative particle dynamics. Upon graduating from Rutgers University, Evan continued on to pursue a Doctor of Philosophy degree in chemical and biomolecular engineering under the supervision of Dr. Angela C. Brown. While at Lehigh University, Evan had the opportunity to mentor five undergraduate research students and serve as the teaching assistant for Chemical Engineering Heat Transfer on two separate occasions. After graduation Evan will start the next chapter of his career as a Senior Scientist for Roche Diagnostics in Santa Clara, California.

Publications

Nice J, Krueger E, **Koufos E**, Brown AC, Outer Membrane Vesicle-Mediated Delivery of *Aggregatibacter actinomycetemcomitans* Leukotoxin to THP-1 Cells, *Mol Oral Microbiol*, submitted.

Balashova N, Giannakakis A, Brown AC, **Koufos E**, Arakawa T, Tang H, Lally ET, Generation of a recombinant *Aggregatibacter actinomycetemcomitans* RTX toxin in Escherichia coli, *GENE*, **672,** 106-114 (2018).

Koufos E, Chang EH, Boroujeni ER, Krueger E, Brown AC, Use of a CRAC Peptide to Inhibit Binding to Cholesterol by a Bacterial Toxin, *Biochemistry*, **55,** 4787-4797 (2016).
Webb JN, **Koufos E**, Brown AC, Inhibition of Bacterial Toxin Activity by the Nuclear Stain DRAQ5, *Membrane Biol*, **249,** 503-511 (2016).

Brown AC†, **Koufos E†**, Balashova NV, Boesze-Battaglia K, Lally ET, Inhibition of LtxA Toxicity by Blocking Cholesterol Binding with Peptides, *Mol Oral Microbiol*, **31,** 94-105 (2015).
†-These two authors contributed equally.

Koufos E, Mualidharan B, Dutt M, Computational Design of Multi-Component Bio-Inspired Bilayer Membranes, *AIMS Mater Sci***, 1,** 103–120 (2014).

Koufos E, Dutt M, Designing Nanostructured Hybrid Inorganic-biological Materials via the Self- assembly, *MRS Proc*, **1569,** mrss13–1569–ll02–03 (2013).

Presentations

Oral Conference Presentations

Koufos E, Brown AC, Design of a Cholesterol-Binding Peptide to Inhibit Bacterial Toxin Activity, 2017 American Institute of Chemical Engineers Annual Meeting, Minneapolis, Minnesota, November 1, 2017.

Koufos E, Brown AC, Inhibiting Bacterial Toxin Activity utilizing Toxin-Derived Cholesterol-Binding Peptides, 3rd Annual Chemical & Biomolecular Engineering Graduate Student Symposium, Bethlehem, Pennsylvania, September 29, 2017.

Koufos E, Brown AC, Assessing the Mechanism by which a Cholesterol Recognition Amino Acid Consensus (CRAC) Motif Recognizes Membrane Cholesterol, Biophysical Society 60th Annual Meeting, Los Angeles, California, March 1, 2016.

Koufos E, Brown AC, Designing and Characterizing Cholesterol-Binding Peptide Therapeutics from Bacterial Toxins, 2014 American Institute of Chemical Engineers Annual Meeting, Atlanta, Georgia, November 20, 2014.

Koufos E, Dutt M, Computational Investigations on the Role of Molecular Architecture on the Morphology and Properties of Bio-inspired Soft Materials, 2013 MRS Fall Meeting and Exhibit, Boston, Massachusetts, December 2, 2013.

Koufos E, Dutt M, Effect of Molecular Architecture on the Morphology and Properties of Bio-Nanostructured Soft Materials, 2013 AIChE Annual Meeting, San Francisco, California, November 5, 2013.

Poster Presentations

Koufos E, Sinani A, Huang J, DiMartino M, Brown AC, *Characterizing a Peptide Therapeutic Derived from the Cholesterol Recognition Amino Acid Consensus (CRAC) Motif of a Bacterial Toxin*, The Protein Society's 31st Annual Symposium, Montreal, Canada, July 25, 2017.

Koufos E, Sinani A, Huang J, Brown AC, *Determining How Key Amino Acid Substitutions Affect the Affinity of a Cholesterol Recognition Amino Acid Consensus (CRAC) Peptide to Cholesterol*, 2017 Delaware Membrane Protein Symposium, Newark, Delaware, May 22, 2017.

Koufos E, Sinani A, Brown AC, *How Changes to Net Charge and Hydrophobicity Affect the Affinity of a Cholesterol Recognition Amino Acid Consensus (CRAC) Peptide for Membrane Cholesterol*, 2nd Annual Lehigh University Chemical & Biomolecular Engineering Graduate Student Symposium, Bethlehem, Pennsylvania, February 3, 2017.

Koufos E, Sinani A, Brown AC, *Improving upon the Affinity of a Cholesterol Recognition Amino Acid Consensus (CRAC) Peptide for Membrane Cholesterol through Variations to its Primary Structure*, 4th Annual Biophysical Society Pennsylvania Network Meeting, Bethlehem, Pennsylvania, October 14, 2016.

Koufos E, Brown AC, *Characterizing the Primary Structure and Conformational Features of a Cholesterol Recognition Amino Acid Consensus (CRAC) Motif Required for Cholesterol Binding,* 252nd American Chemical Society National Meeting & Exhibition, Philadelphia, Pennsylvania, August 23, 2016.

Koufos E, Brown AC, *Inhibiting White Blood Cell Death by a Bacterial Toxin Utilizing Synthetic Peptides,* 1st Annual Lehigh University Chemical & Biomolecular Engineering Graduate Student Symposium, Bethlehem, Pennsylvania, April 22, 2016.

Koufos E, Brown AC, *Targeting Membrane Cholesterol: A Potential Avenue for Developing Novel Antimicrobial Therapeutics,* 2016 Delaware Membrane Protein Symposium, Newark, Delaware, April 18, 2016.

Koufos E, Brown AC, *Investigating the Mechanisms behind LtxA Cytotoxicity utilizing CRAC Peptides,* Biotechnology Regional Meeting of the American Chemical Society, Villanova, Pennsylvania, September 17, 2015.

Koufos E, Brown AC, *Investigating the Structure-Function Relationship of CRAC Peptides with Model Membranes,* 2015 Delaware Membrane Protein Symposium, Newark, Delaware, May 4, 2015

Koufos E, Brown AC, *Engineering Toxin-derived Cholesterol-binding Peptides to Prevent Bacterial Pathogenesis,* 2014 Delaware Membrane Protein Symposium, Newark, Delaware, May 12, 2014.

Koufos E, Dutt M, *Effect of Lipid Chain Length and Head Architecture on Mechanical Properties of Lipid Bilayers*, Rutgers University Department of Chemical & Biochemical Engineering Undergraduate Poster Session, Piscataway, New Jersey, March 11, 2013.